AD

409869

61

NAVWEPS REPORT 8099
NOTS TP 3157
COPY 90

SPECTROSCOPIC STUDIES USING FOURIER TRANSFORMATIONS

by

Mme. Janine Connes
Laboratorie Aimé Cotton, Bellevue

translated by

Czerna A. Flanagan
Research Department

ABSTRACT. This is a translation from the French of "Recherches sur la Spectroscopie par Transformation de Fourier" by Mme. Janine Connes, which appeared in 1961 in Revue d'Optique, Volume 40, pages 45-78, 116-140, 171-190, and 231-265. The article considers the use of the Michelson interferometer for spectroscopy in the infrared and treats the following: Fourier analysis of the interferogram using high-speed digital computers and analog methods, instrumental errors, analysis of noise and procedures for attaining maximum s/n ratios, specific applications to night sky spectrometry in the 1μ to 1.6μ region as well as to the re-emission spectrum of germanium, and comparison of this method with those using classical spectroscopic instruments.

U.S. NAVAL ORDNANCE TEST STATION

China Lake, California

January 1963

U. S. NAVAL ORDNANCE TEST STATION

AN ACTIVITY OF THE BUREAU OF NAVAL WEAPONS

C. BLENMAN, JR., CAPT., USN, Commander
WM. B. McLEAN, PH.D., Technical Director

FOREWORD

In the infrared, the Michelson interferometer spectrometer has these advantages over classical methods: large aperture, simultaneous recording of all spectral elements, and the fact that detector noise rather than photon noise limits the s/n ratio. On the other hand, a lengthy Fourier transform calculation is required to produce the spectrum.

Mme. Connes has written a fundamental paper on Fourier transform methods applied to the Michelson spectrometer. This paper, which appeared in 1961 in Revue d'Optique, Volume 40, was informally translated from the French for use within our laboratory. However, the content is of such high interest that we believe a wider circulation would be valuable to English-speaking scientists working in the infrared.

The translation was supported by HITAB, part of Project DEFENDER, under Bureau of Naval Weapons WEPTASK RTSA 30013/216-7/F019-01-002.

Released by
T. E. PHIPPS, Head
Research Department
22 January 1963

Under authority of
WM. B. McLEAN
Technical Director

NOTS Technical Publication 3157
NAVWEPS Report 8099

Published by.....Research Department
Collation.....Cover, 88 leaves, abstract cards
First printing.....160 numbered copies
Security classification.....UNCLASSIFIED

CONTENTS

SPECTROSCOPIC STUDIES USING FOURIER TRANSFORMATIONS

by

Mme. Janine Connes
Laboratorie Aimé Cotton, Béllevue

INTRODUCTION

There are two principal ways to look for improvements in spectroscopic techniques [1]. One method is constructing instruments to receive the broadest spectrum possible for a given resolution. Towards this end several methods have been proposed: double or multiple passage of a beam of light through a single dispersive element [2], use of the Fabry-Perot integral spectrometer [3], or of the sisam [4]*. But these methods make poor use of the energy of the source in time because the spectral elements are analyzed successively. A fundamental improvement can be obtained by receiving energy from all the spectral elements simultaneously; this is what is done using spectrographic techniques and the Fourier transform method.

The principle of spectrographic methods which use a two-beam interferometer and a Fourier transform has been known a long time. Michelson conceived the first in 1891. He showed that the intensity I of the light that can be measured at the exit of a two-beam interferometer with a variable phase difference is the Fourier cosine transform of the spectrum of the incident light [5,6]. Since the Fourier transform (F.T.) is an invertible operation, it therefore suffices in theory, to reconstruct the spectrum studied, to make the cosine transform

*Translator's Note: As defined in [4] s.i.s.a.m. is an interference spectrometer for selecting the modulation amplitude.

of the interferogram function representing the variations of I as a function of the phase difference δ between the two interfering beams. But taking the F.T. of a very complex function is an extremely long procedure if there is no high-speed modern computer at one's disposal, and Michelson did not attack the study of an arbitrary and extended spectrum. He perfected a method adapted to a very particular problem: the study at very high resolution of an extremely narrow spectral domain, made by studying the curve of visibility V, the envelope of the interferogram function. Lord Rayleigh explained how the knowledge of V alone permits constructing the spectral profile of the line studied without ambiguity only in the case of the symmetric line [7]. This method, however, permitted Michelson to exceed the highest powers of resolution attained at that time and to make evident the hyperfine structure.

Nowadays to study the structure of a line at very high resolution, one uses large gratings [8], and plane [9] or spherical [10] interferometers. However, Michelson's method retains a certain interest, and recently Terrien showed how the study of V determined by photoelectric observations made under the best conditions resulted in information about the profile of a line (known à priori to be symmetric) which was more precise than that obtained by other methods [11,12].

The possibility of using photoelectric photoconductive, or thermal detectors to record the "interferogram" function and the means now at one's disposal for making the F.T. have opened a field of application of the F.T. method that Michelson never suspected. Rubens and Wood in 1910 obtained the first spectra in the far infrared by taking the F.T. of an interferogram.

Much more recently P. Fellgett [13 to 15] and P. Jacquinot [1,50,51] independently showed that the reconstruction of a spectrum by the Fourier transformation of an interferogram has

a great advantage over the direct recording of the same spectrum: one can, while using a single channel detector, measure simultaneously all the spectral elements as with spectrographic methods--hence the name given by P. Fellgett to the method, "multiplex spectrometry". A simple argument allows one to predict the order of magnitude of gain that can be expected. If with an exploring spectrometer it is desired to measure M spectral elements during time T, each element is observed during time T/M; with a spectrograph or a multiplex method, each element is observed during the whole time T. In the case where the fluctuations have a spectrum of uniform frequency and where the background noise is not increased by the simultaneous arrival of all spectral elements, the precision varies as the square root of the exploration time. The gain in sensitivity is therefore of the order of $\sqrt{M}$. Hence, in the infrared where photon noise is negligible compared with receiver noise, the spectroscopic method using Fourier transformations is the most powerful, no matter what may be the desired resolutions and it is all the more interesting because the spectrum studied contains more spectral elements. This gain in sensitivity can be expressed in several ways:

--the signal/noise ratio can be multipled by $\sqrt{M}$ if the duration of the measurement is the same as in the classical method;

--for equal signal/noise ratio, the duration of the measurement is divided by M;

--finally, for a given s/n ratio and measurement time, one can obtain an increase in resolution and thus treat some problems inaccessible by any other method.

Furthermore, P. Jacquinot [1] showed independently that in addition to the preceding advantage, the use of a Michelson type interferometer allows him to employ a luminous flux which

was far greater than he could use with slit devices, indeed as much as that given by a Fabry-Perot interferometer. Finally, P. Connes [39] showed how this flux could be increased even more if one inserted afocal systems upon each of the interferometer arms.

At a colloquium on interferometric spectroscopy in Bellevue in 1957, the first results obtained by the method were collected. It should be noted that the first problems treated were astrophysical problems because in this domain there exist some feeble sources, the study of which is interesting even at low resolution. Fellgett obtained the first star spectra in the near infrared at a resolution varying from 60 to 100, by using an interferometer with reflecting trihedrals [16]. Strong and his collaborators Vanasse and Gebbie investigated the far infrared region [17 to 19]. For an interferometer, they used a grating with lines of variable depth which did not have symmetry of revolution, but had the advantage of not requiring separating and compensating plates (difficult to effect in this spectral region). Gebbie, with his instrument, measured for the first time the solar spectrum in the region of 300 to 1,000 μ with a limit of resolution of 0.2 cm^{-1} and localized the transmission window with precision [20].

In the visible range Mertz constructed polarization interferometer consisting essentially of a variable retardation plate between polarisers [21]; the maximum resolutions attainable by this system are low, of the order of 100. He hoped to make an empirical classification of star spectral types based on interferograms without making F.T.; Bakhshien seems to have thought of the same instrument but he does not give a single detail about the theory nor about the construction of his apparatus [22].

In each case the work took place in two stages; the interferogram function was recorded and later the F.T. was calculated

by digital computers, using discrete values of this function. Strong made [23] an analogue computer giving the intensities of 10 spectral elements for each passage of the moving part, but this apparatus, requiring several explorations to cover all the spectral domain studied, does not allow one fully to exploit the advantage of the method. Different authors have mentioned the fact that the resolution was proportional to the maximum phase difference attained [1,15,11]; certain ones have studied the conditions under which the numerical Fourier transformation should be made; but they limited themselves to the study of the case where the spectrum extends from frequency 0 to a maximum frequency σ_M [15,21,24] and have not studied the conditions under which the numerical transform ought to be made to obtain the maximum signal/noise ratio in the spectrum.

In Chapter II of this paper a more complete study is considered; one determines the form of the theoretical equipment-function in the case where the Fourier transformation is made by a numerical calculator and one treats the number of points to pick from the interferogram as a function of the spread and position of the spectral domain to be studied.

In Chapter III we study the form of a real apparatus-function; it is different from the theoretic apparatus-function for several reasons:

--necessity of receiving on the detector a beam of finite width;

--imperfections of the optical components and in the adjustment of the instrument;

--irregularities in the motion of the moving part;

--error in the adjusting of the zero phase difference of the interferogram.

Chapter IV is devoted to the calculation of the mean square error of the fluctuations in the reproduced spectrum, Chapter V to the study of the different possible ways to

obtain in a given experimental time, the maximum s/n ratio in the case where the F.T. is computed numerically.

Chapter VI sets forth the practical setting up and results obtained in two experiments: the spectrum of night sky emission and the spectrum of germanium recombination at 1.6 μ.

Finally, Chapter VII is given over to an attempt to synthesize the spectroscopic methods called "classic" and the Fourier transform method; there, it will be shown how in every case the spectrum is obtained by making the cosine transform of the autocorrelation function of the vibration of incident light.

II. THEORETICAL APPARATUS-FUNCTION NUMERICAL FOURIER TRANSFORM

We shall recall the principle of the method before determining the relations which exist between the reproduced spectrum and the spectrum studied. Spectroscopists call the "apparatus-function" the distribution of the spectral density that is obtained if the instrument receives strictly monochromatic radiation. In the classical methods, the spectrum obtained in the general case is the convolution of the spectrum under consideration with the apparatus function; we shall show that it is the same thing in the Fourier transform method. This chapter is devoted to the study of the theoretical apparatus-function, i.e., the instrument is assumed perfect and used with a beam of zero extent. Likewise we shall treat the important problem of the number of points to choose from the interferogram in order to make a numerical Fourier transform.

1. PRINCIPLE OF THE METHOD

Let us consider a two-beam interferometer in which one can vary the phase difference between two beams, for example a Michelson interferometer. For the sake of simplicity we suppose that the beam splitter is attached to a compensating glass plate of equal thickness (Fig. 1). One of the mirrors can be displaced parallel to itself with constant velocity V. 2. Suppose the interferometer to be illuminated by a strictly monochromatic light, of luminance B, with wave number σ_0. The beam splitter divides the light into two equal parts (if it is not absorbing

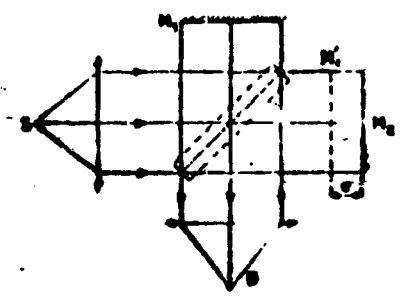

Fig. 1. Diagram of the Principal of a Michelson Interferometer.

and if the reflectivity $\mathcal{R}$ is equal to 0.5) which it recombines to make them interfere after they suffer a relative delay $\delta = 2e$, $2e$ being the difference between the optical paths taken by the two beams. The light on leaving follows the well-known law

$$L = B \cos^2 \pi\sigma_0\delta = (B/2)\ (1 + \cos 2\pi\sigma_0\delta).$$

It is composed of a constant part and a variable part which, up to a constant multiplier, is given by

$$I(\delta) = B \cos 2\pi\sigma_0\delta = B \cos 2\pi Vt\sigma_0 = B \cos 2\pi\nu_0 t,$$

with

$$\nu_0 = V\,\sigma_0 = N_0\ V/c.$$

The detector gives a sinusoidal electric signal with amplitude proportional to the luminance received and frequency equal to the product of the frequency of the light N_0 by the fraction V/c.. For example, in the case of the green Mercu line, if V equals 10^{-3} mm/s, $\nu_0 = 1.83$ cps.

If the interferometer is illuminated by several monochromatic lines, each radiation is treated in the same way, and the resulting signal is the sum of the signals corresponding to each line. In the case of an arbitrary spectrum taken between σ_1 and σ_2, the interferogram has the form

$$I(\delta) = \int_{\sigma_1}^{\sigma_2} B(\nu) \cos 2\pi\sigma\delta\ d\sigma$$

or

$$\mathcal{J}(t) = \int_{\nu_1}^{\nu_2} B(\nu) \cos 2\pi\nu t\ d\nu$$

according to the variable considered. $I(\delta)$ and $\mathcal{J}(t)$ are luminances, $B(\sigma)$ and $B(\nu)$ densities of luminance (luminance/cm^{-1} for the first, luminance/cps for the second). This is the Fourier transform of the spectrum $B(\sigma)$ [or $B(\nu)$]. In the case of strictly monochromatic radiation, the interferogram will be a sine wave of constant amplitude. In practice the lines have a finite width and the sine wave has an amplitude which decreases when the phase difference increases (Fig. 2). When the spectrum is very rich, the different sine waves corresponding to the different frequencies are in phase only for zero phase difference and the interferogram appears to be reduced to some fringes in the neighborhood of this position (Fig. 3). Between these two extreme cases, all intermediate cases are possible, the modulation dropping in direct proportion to the increase in size of the spectral interval (Fig. 4).

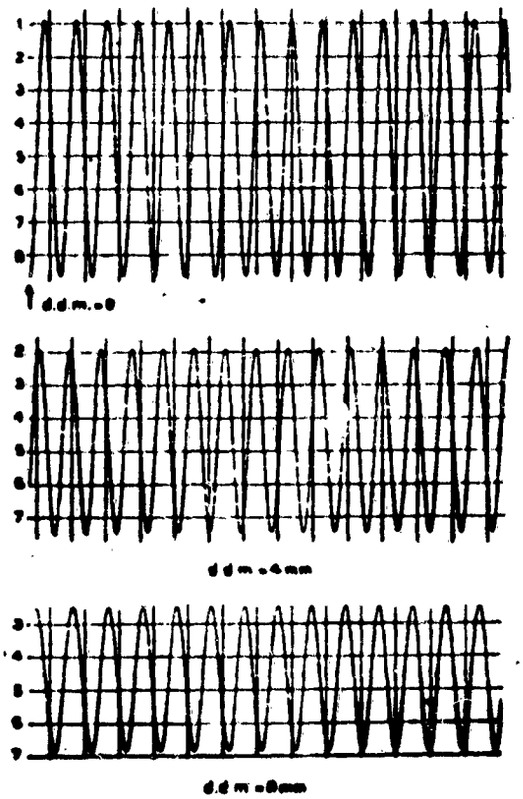

Fig. 2. Interferogram of the Line 5,461 A Produced by a Mercury Lamp Under Low Pressure ["d.d.m." Phase Difference].

In order to reconstruct the spectrum from the interfergram, it is necessary to make the inverse F.T.

$$B(\sigma) = \int_{-\infty}^{+\infty} I(\delta) \cos 2\pi\sigma\delta \, d\delta.$$

One can consider making an harmonic analysis of the signal with the aid of n filters, each having a band pass $\delta\nu$ corresponding to the desired limit of resolution $\delta\sigma$ where $\delta\nu = V\,\delta\sigma$ and centered about the interesting frequencies

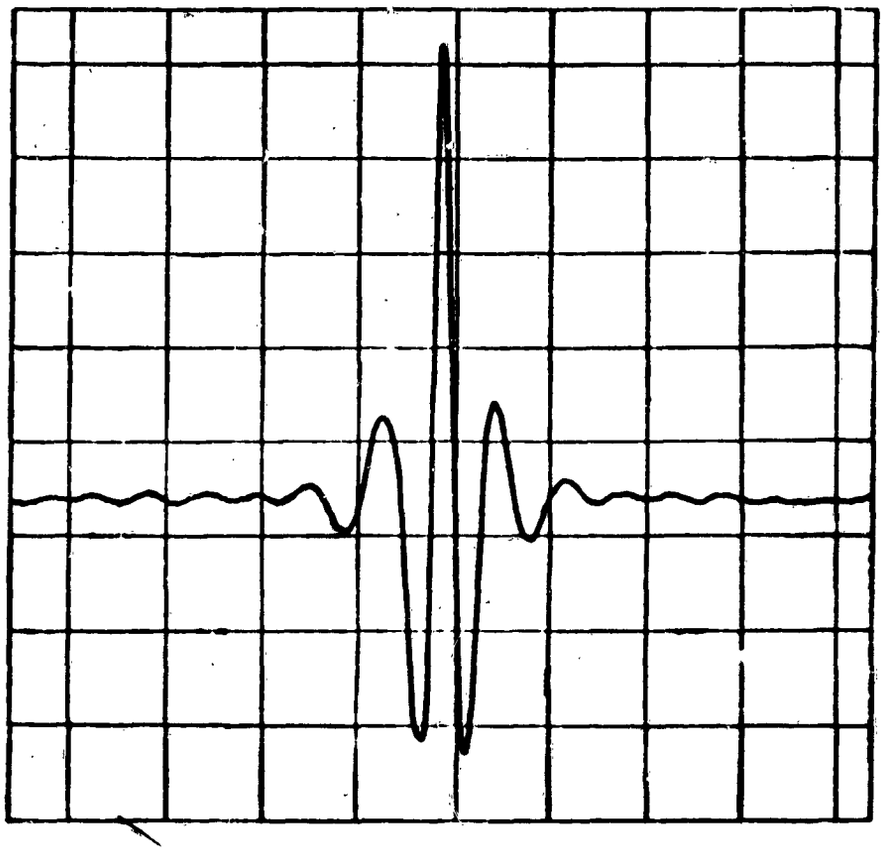

Fig. 3. Interferogram Produced by an Incadescent Lamp, the Detector Being a Lead Sulphide Cell.

$\sigma_1, \ldots, \sigma_n$. This analysis can be made, either during the measurement or afterwards from a magnetic tape upon which the interferogram is recorded. One can also record the interferogram with a recording pen and numerically calculate the F.T. of the function thus obtained.

2. THEORETICAL APPARATUS-FUNCTION

Let us consider a Michelson interferometer illuminated by a point source placed in the focus of the entrance collimator. One of the mirrors is strictly parallel to the image of the other formed by the beam splitter.

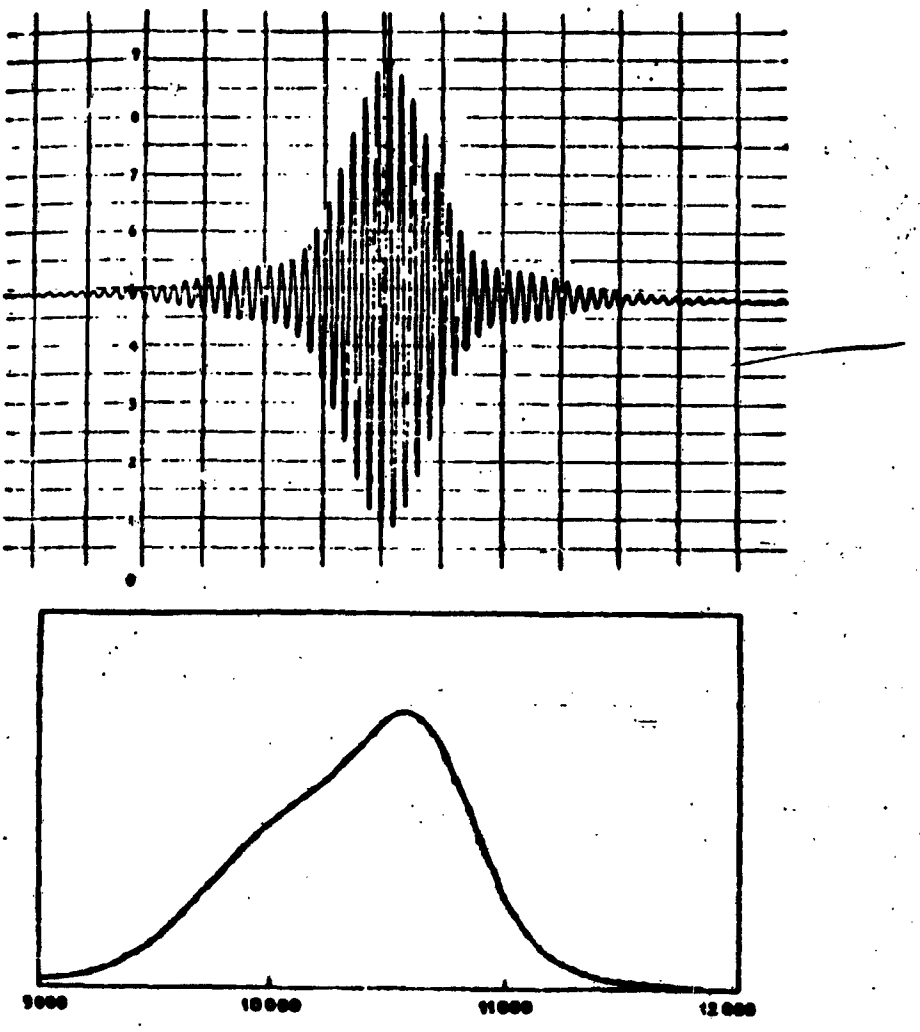

Fig. 4. Above, Interferogram of a Radiation Band About 1.0 μ. Below, the spectrum computed from the interferogram: the abscissa, frequency in cm^{-1}; the ordinate, intensity.

If $B(\sigma)$ is the spectrum of the emitted light, the interferogram has the form

$$(II.1)\quad I(\delta) = \int_0^{\infty} B(\sigma)\cos 2\pi\sigma\delta\, d\sigma = \int_{-\infty}^{+\infty} B_p(\sigma)\cos 2\pi\sigma\delta\, d\sigma,$$

$B_p(\sigma)$ being the even part of the function $B(\sigma)$ defined by

$$B_p(\sigma) = \frac{1}{2}\,[B(\sigma) + B(-\sigma)] \qquad \text{(Fig. 5)}.$$

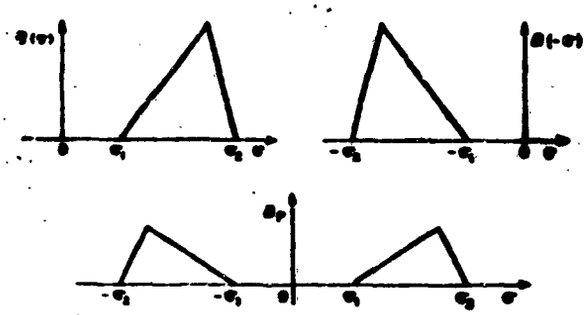

Fig. 5. Even Part of an Optical Spectrum.

If one could know the interferogram completely for δ varying between 0 and ∞ (hence in fact between $-\infty$ and $+\infty$ since it is symmetric), the spectrum could be reproduced exactly by the operation

$$\text{(II.2)} \qquad B_p(\sigma) = \int_{-\infty}^{+\infty} I(\delta) \cos 2\pi\sigma\delta \, d\delta.$$

But in fact, during the measurement, δ varies only between 0 and a maximum value L; the value $B'_p(\sigma_1)$ computed for a particular wave number σ_1 will be only an approximate value of $B_p(\sigma_1)$, which one expresses by saying the resolution is finite. The expression (II.2) can be put in the form

$$\text{(II.3)} \qquad B'_p(\sigma_1) = \int_{-\infty}^{+\infty} I(\delta)\, D(\delta) \cos 2\pi\sigma\delta \, d\delta,$$

$D(\delta)$ being a square pulse function such that

$$D(\delta) = 1 \text{ if } -L < \delta < +L,$$

$$D(\delta) = 0 \text{ for } \delta < -L \text{ and } \delta > +L.$$

(1) Form of the Apparatus-Function

The cosine transform of the product of two even functions is the convolution of the cosine transforms of each of the two functions, whence

(II.4) $$B'_p(\sigma_1) = T_{cos}[I(\delta)] * T_{cos}[D(\delta)].$$

The cosine transform of $I(\delta)$ is precisely the observed spectrum $B_p(\sigma)$. Calling $f(\sigma)$ the cosine transform of $D(\delta)$, (II.4) can be written

(II.5) $$B'_p(\sigma_1) = \frac{1}{2}\int_{-\infty}^{+\infty} B_p(\sigma)\,[f(\sigma_1-\sigma) + f(\sigma_1+\sigma)]\,d\sigma$$

$$= \int_{-\infty}^{+\infty} B_p(\sigma)\, f(\sigma_1-\sigma)\, d\sigma.$$

The spectrum obtained is the convolution of the even part of the initial spectrum with the function $f(\sigma)$ which we shall call the apparatus-function. The apparatus-function thus defined has a dimension, that of length in the case where the spectrum $B(\sigma)$ is calculated, that of time when $B(\nu)$ is calculated.

When the spectrum is reduced to a single line of wave number σ_0, of luminance unity, the reproduced spectrum has the form

(II.5b) $$B'_p(\sigma) = \frac{1}{2}\,[f(\sigma-\sigma_0) + f(\sigma+\sigma_0)].$$

If the F.T. is taken by a method permitting the calculating of luminance densities corresponding to negative wave numbers (which have no physical reality), the apparatus-function contains two maxima centered about σ_0 and $-\sigma_0$ and of height $f_0/2$ (Fig. 6).

When the F.T. of a constant, say one, is taken the only maximum is found to be centered about the zero frequency and of height double f_0, the two preceding maxima being superposed.

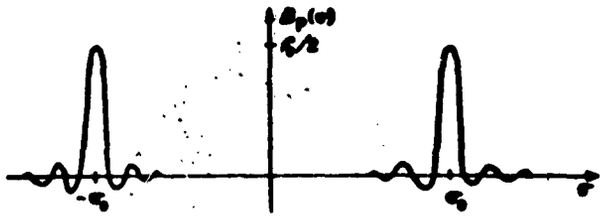

Fig. 6. Apparatus-Function.

One can define a normalized apparatus-function which will be the ratio

$$f'(\sigma-\sigma_0) = B_p(\sigma)/B_p(\sigma_0) \qquad \text{(II.6)}$$

between the density of luminance calculated for the wave number σ near σ_0 to that calculated for the number σ_0 corresponding to the line under consideration. The apparatus-function can be put in the form

$$f(\sigma) = f_0 f'(\sigma), \qquad \text{(II.7)}$$

with

$$f_0 = 2qL \ , \qquad \text{(II.7b)}$$

q being a numerical factor here equal to the mean value of the function $D(\delta)$, hence one, and which, more generally, will be equal to the mean value of the function $A(\delta)$ defined later, whence

$$f(\sigma) = 2L\, f'(\sigma) = 2L\, \frac{\sin 2\pi\sigma L}{2\pi\sigma L} \ . \qquad \text{(II.8)}$$

This function $f'(\sigma)$ has zeros for $\sigma_k = k/2L$ (Fig. 7, curve a); it has very important secondary maxima and one may find it desirable to apodize it. To this end it is sufficient to replace the square pulse function $D(\delta)$ by another function $A(\delta)$ which has a profile better adapted to the problems of spectroscopy. This is especially simple in the case where the F.T. is made numerically. There, it is sufficient to replace the

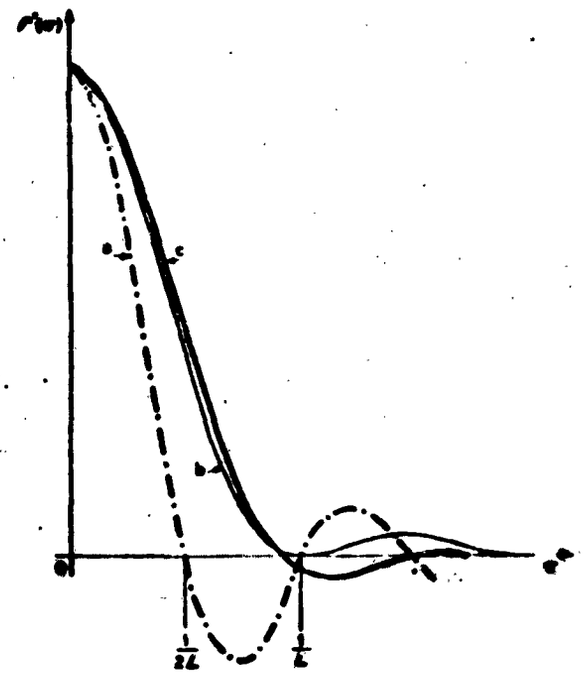

Fig. 7. Theoretical Apparatus-Function.

values of $I(\delta)$ by those of the product $I(\delta)\,A(\delta)$; this is numerical apodizing. The apodizing problem has been the subject of numerous papers, in particular those of Mlle. B. Dossier [26] and J. Arsac [27].

We are going to consider two particular forms of the weighting function $A(\delta)$.

1°. $A_1(\delta)$ is a triangle function such that

$$A_1(\delta) = 1 - |\delta/L| \quad \text{for } -L < \delta < +L$$

and $$A_1(\delta) = 0 \quad \text{for } \delta < -L \text{ and } \delta > +L.$$

Under these conditions

$$q = \frac{1}{2L}\int_{-L}^{+L}\left(1 - \left|\frac{\delta}{L}\right|\right)d\delta = 0.5, \tag{II.9}$$

$$f(\sigma) = L\,f'(\sigma) = L\left(\frac{\sin \pi\sigma L}{\pi\sigma L}\right)^2.$$

This is the same apparatus-function as that of the grating spectrometer (Fig. 7, curve b).

2°. If one chooses [27] (Fig. 8)

$$A_2(\delta) = [1 - (\delta^2/L^2)]^2 \quad \text{for } -L < \delta < +L,$$

$$q = \frac{1}{2L}\int_{-L}^{+L}\left(1 - \frac{\delta^2}{L^2}\right)^2 d\delta = 0.533,$$

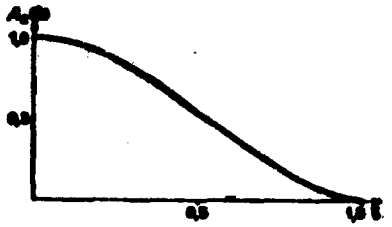

Fig. 8. The $A_2(\delta)$ Function.

(II.10) $$f(\sigma) = 1.066\ L\ f'(\sigma),$$

with

$$f'(\sigma) = (2\pi L\sigma)^{-5/2}\ J_{5/2}(2\pi L\sigma).$$

This function (Fig. 7, curve c) has its first zero for δ very close to $1/L$; its breadth at mid-height is practically the same as that of the function $[(\sin \pi L\sigma)/\pi L\sigma]^2$, but the amplitude of the first minimum is only a twenty-fifth of that of the first maximum, and that of the next maximum is only a hundredth.

(2) Limit of Resolution

The Rayleigh criterion can be applied only in the case where the apparatus-function has zero minima; hence in general one selects a criterion which gives nearly the same results as in the ordinary cases. One is led to take as a measure of the limit of resolution $\delta\sigma$ the breadth at 0.404 of the maximum of the apparatus-function. Since the F.T. of a function gets narrower as the function gets wider, one sees immediately that the limit of resolution varies inversely with L, the exact law being determined for each particular case.

The study of limits of resolution rests on the study of the breadths at mid-height of the functions $f'(\sigma)$.

If there is no apodization, $\delta\sigma = 1/2L$, whence a theoretical resolution $R_0 = 2L\sigma$. With the weighting function $A_1(\delta)$ or $A_2(\delta)$ one has very nearly $\delta\sigma = 1/L$, with a theoretical resolution $R_0 = L\sigma$[1]. Hence, the resolution is proportional to the maximum phase difference attained. This result is completely analogous to that of the classical spectrographic method.

Figure 84b shows two spectra of the night sky taken from the same interferogram. For the first at resolution 350, a F.T. has been made of that portion of the interferogram for which δ varies between 0 and 0.4 mm. For the second at resolution 1,000, the length of interferogram used is nearly triple.

(3) Numerical Fourier Transforms

Any spectrum studied is limited--whether by the emission itself, by the transparency of the materials making up the interferometer, or by the sensibility zone of the detector. It is this important fact that allows us to make F.T. from discrete values of $I(\delta)$ and to use modern high-speed calculators.

A. FOURIER TRANSFORM AND THE THEORY OF SAMPLING. According to the sampling theorem, all information concerning a function of a bounded spectrum is contained in a countable infinity of discrete values of the function, and interpolation formulas can be found which, based on these points permit the reconstruction of the function. These questions are treated in detail by Shannon [28], Woodward [29], and Kohlenberg [30].

And so all the bits of information contained in the interferogram which is known to have a bounded spectrum are given by

[1] In this case one can say further that the theoretical resolution is equal to the number of recorded fringes.

discrete values of $I(\delta)$. As a consequence it is sufficient in calculating the spectrums to deal with a particular number of equidistant values taken from the interferogram. The calculation of the integral

$$(II.11) \qquad B'_p(\sigma_1) = 2\int_0^{+L} I(\delta)\, A(\delta) \cos 2\pi\sigma_1\delta \, d\delta$$

is replaced by that of the sum

$$(II.12) \qquad B''_p(\sigma_1) = h\,[I_0 A_0 + 2I_h A_h \cos 2\pi\sigma_1 h + \ldots + 2I_{nh} A_{nh} \cos 2\pi\sigma nh].$$

I_0, I_h, ..., I_{nh} are the values on the interferogram for the values 0, h, ..., nh of the phase difference; A_0, A_h, ..., A_{nh} are the corresponding values of the apodizing function.

The sum (II.12) is equivalent to the integral

$$(II.13) \qquad B''_p(\sigma_1) = h\int_{-\infty}^{+\infty} I(\delta)\, A(\delta)\, R_h(\delta) \cos 2\pi\sigma_1\delta \, d\delta,$$

$R_h(\delta)$ being a Dirac distribution of periodic support with interval h (Fig. 9); we deduce immediately

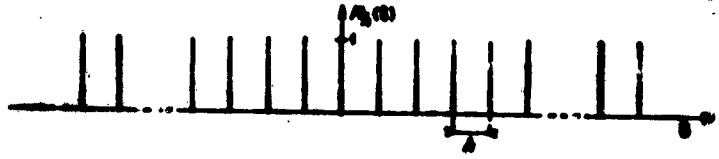

Fig. 9. Grating function $R_h(\delta)$.

$$(II.14) \qquad B''_p(\sigma_1) = \frac{1}{2}\int_{-\infty}^{+\infty} B_p(\sigma)\,[F(\sigma_1-\sigma) + F(-\sigma_1-\sigma)]\, d\sigma.$$

$F(\sigma)$ is the F.T. of the product of the two functions $A(\delta)$ and $h\,R_h(\delta)$; since the F.T. of a periodic Dirac function with interval h is, except for a factor $1/h$, another periodic Dirac distribution with interval $1/h$ (Fig. 10), a new apparatus-

Fig. 10. Grating Function $R_{1/h}(\sigma)$.

function can be found:

$$F(\sigma) = 2\,L\,F'(\sigma),$$

with

$$\text{(II.15)}\quad F'(\sigma) = \sum_{m=-\infty}^{+\infty} \left[\sin 2\pi L \left(\frac{m}{h}-\sigma\right) \Big/ 2\pi L \left(\frac{m}{h}-\sigma\right) \right]$$

in case $A(\delta)$ is a square pulse function and $F(\sigma) = 1.066\,L\,F'(\sigma)$, where

$$\text{(II.16)}\quad F'(\sigma) = \sum_{m=-\infty}^{+\infty} \left[2\pi L \left(\frac{m}{h}-\sigma\right) \right]^{-3/2} J_{3/2}\left[2\pi L \left(\frac{m}{h}-\sigma\right) \right]$$

with the apodizing function $A_2(\delta)$.

The new apparatus-function is made up of a series of identical maxima which occur at every multiple of $1/h$ (Fig. 11). It can be said that the even part of the spectrum is examined simultaneously by two series of apparatus-functions centered one on σ_1, the other on $-\sigma_1$ (Fig. 12). The examination of the spectrum is made here by using a calculation like that of (II.12) for a new value σ_2 of σ. During the spectral examination the two series of apparatus-functions have translations in opposite directions (Fig. 13).

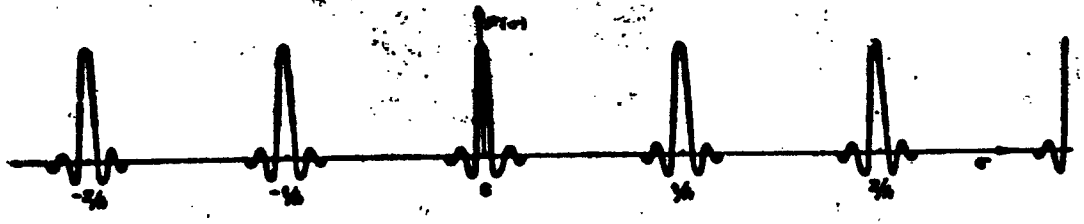

Fig. 11.

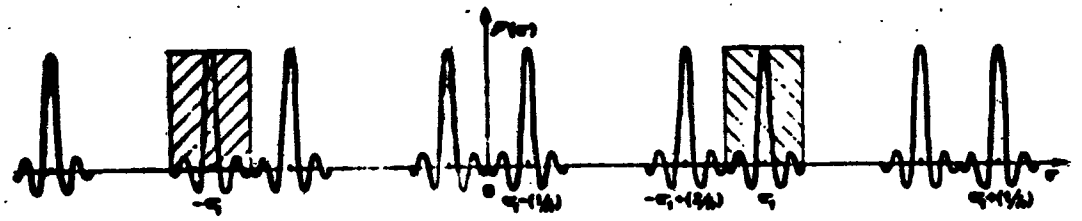

Fig. 12.

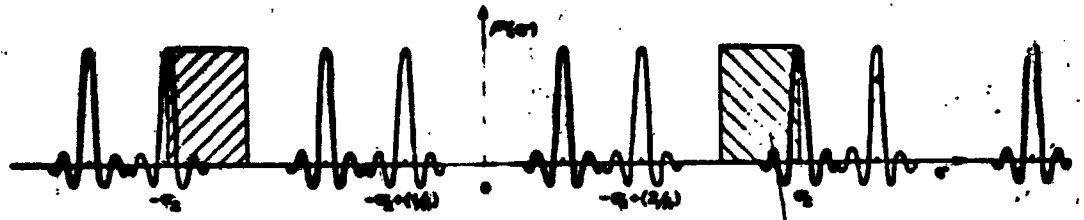

Fig. 13. Apparatus-Function Given by a Numerical F.T., Exploration of the spectrum.

B. CHOICE OF INTERVAL h. This is a very important problem because the computed spectra are going to repeat at multiples of $1/h$ and because, for the result to be usable, they ought not be entangled. This amounts to saying that a single maximum of the apparatus-function ought to explore the spectrum. We shall call σ_M and σ_m the limiting wave numbers of the spectrum and $\Delta\sigma = \sigma_M - \sigma_m$ the spectral interval used (Fig. 14).

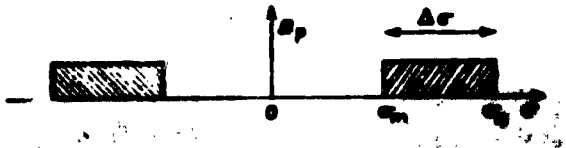

Fig. 14.

a. Relation Between h and $\Delta\sigma$. Three cases can be distinguished according to the position of $\Delta\sigma$ with respect to the zero frequency.

α) $\sigma_m = 0$. σ varies between 0 and σ_M; in order that there be no overlapping of spectra, it is sufficient that $1/h = 2\ \Delta\sigma$ or $h = 1/(2\Delta\sigma) = 1/(2\sigma_M)$ (Fig. 15a). This is the result usually stated by saying that one ought to record two points per period of the signal corresponding to the highest frequency contained in the spectrum.

β) $\sigma_M = \chi\Delta\sigma$ (χ being an integer). It is easily seen in this case also that the orders do not overlap if $1/h = 2\Delta\sigma$ or $h = 1/(2\Delta\sigma)$ (Fig. 15b). The distance between two points taken from the interferogram in centimeters is one half the inverse of the spectral interval used, measured in cm^{-1}.

γ) Any σ_M whatever. $\sigma_M/\Delta\sigma = \chi + f$, χ being an integer and f a fraction. Then $\Delta\sigma$ is replaced by another quantity $\Delta\sigma'$ defined by $\Delta\sigma' = \sigma_M/\chi$. It is larger than $\Delta\sigma$ and has the same upper bound. This reduces to the preceding case with the choice $h = 1/(2\Delta\sigma')$ (Fig. 15c).

Fig. 15. Repetition of Numerically Calculated Spectra.

b. Numerical Examples. The first example illustrates the case where the spectrum extends from 0 to σ_M; we have computed the F.T. of the function $\sin^2 \pi\sigma_M\delta/(\pi\sigma_M\delta)^2$ using 36 discrete values, the distance between any two successive values being $1/(2\sigma_M)$. The calculated spectrum repeats every $2\sigma_M$; the resolution is $R_0 = 18$ because we have used only a short length of $I(\delta)$; also the apexes of the triangle are slightly rounded off (Fig. 16).

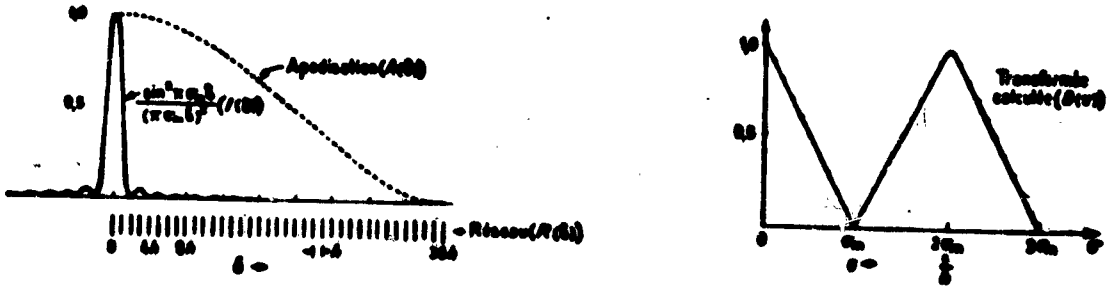

Fig. 16.

In the second example the calculated spectrum is that of an incadescent lamp whose light passes through filters which isolate a band of radiation in the neighborhood of 1 μ.

Knowing the transmission curve of the filters we can deduce from them that

$$\Delta\sigma = 3{,}410 \text{ cm}^{-1},$$

$$\sigma_M = 12{,}850 \text{ cm}^{-1} \text{ and}$$

$$\sigma_M/\Delta\sigma = 3 + 0.8.$$

The domain $\Delta\sigma'$ is then defined such that

$$\Delta\sigma' = \sigma_M/3 = 4{,}283 \text{ cm}^{-1}$$

and so

$$h = 1/(2 \times 4{,}283) = 0.11695\ 10^{-3} \text{ cm}^{-1}.$$

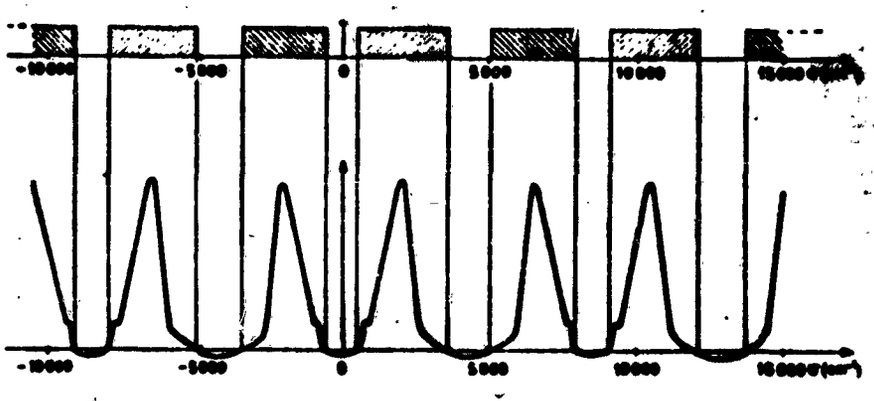

Fig. 17. Spectral Domain Occupied, 3,410 cm^{-1}; $h = 0.11695 \times 10^{-3}$ cm; Number of Points Taken From the Interferogram, 25.

Figure 17 shows, for this value of h, the agreement between the position of the observed spectra and those of the computed spectra.

C. RELATION BETWEEN THE NUMBER OF POINTS CHOSEN AND THE NUMBER OF SPECTRAL ELEMENTS STUDIED

We have just seen that the interval h depends only on the breadth and the position occupied by the spectral interval[2] In addition, the limit of resolution depends essentially on the maximum phase difference L attained and, secondarily on the form of the apodizing function chosen. Hence, the exploration of a given spectral domain with a given resolution poses two distinct problems: determination of L and choice of interval h. The total number of points to choose is given, within a unit, by $n = L/h$, and there exists a relation between n and the number M of spectral elements contained in the spectrum under consideration. The spectral element is that portion of the spectrum included between two points that can be considered as barely separated by the instrument; it has the value $\delta\sigma$ and $M = \Delta\sigma/\delta\sigma$. A general argument, due to Shannon, allows one to predict that starting with n bits of information contained in a function, one can find n independent values of its F.T. [31]. We are going to show that the relation between n and M varies with the spectrum considered, and in certain particular cases, we find $n = M$.

Consider at first the case where $\sigma_m = 0$ or better yet that where $\sigma_M = m\Delta\sigma$, m being an integer. Then $h = 1/(2\Delta\sigma)$ and $n = L/h = 2L\Delta\sigma$.

If the interferogram is not apodized, $\delta\sigma = 1/2L$ and $n = \Delta\sigma/\delta\sigma = M$, that is to say that the number of points to be chosen is equal to the number of spectral elements.

---

[2] This is true in the absence of noise. In practice, to obtain the best signal/noise ratio, one decreases h considerably, the number of points chosen being multiplied by a number of the order of 5.

If apodizing is done as indicated above, then obviously $\delta\sigma = 1/L$ and $n = 2M'$, M' being the new number of spectral elements. Its value is half that of M.

In the most unfavorable case, σ_M is very little under $2\Delta\sigma$ (Fig. 18); then $\Delta\sigma' = \sigma_M$ is nearly equal to $2\Delta\sigma$ and $n = \Delta\sigma'/\delta\sigma$ is very close to 2M' or 4M' according to whether or not apodizing has been used. Hence, in conclusion, with apodizing, the number of points to choose varies between 2 and 4 times the number of spectral elements.

Fig. 18.

Remark.--We have just seen that for a given resolution the number of points to choose is greater the more extended the spectrum. Although the advantage of this method over classical methods is greater the higher M is, one can consider using it for the high resolution study of a weak spectral domain, for example the hyperfine structure of a line in the infrared. If M is of the order of 100, the number of points to take will be rew, in the order of hundreds.

D. COMPUTING METHOD

We constructed a program for computing Fourier transforms on the IBM 704[3]. In order to achieve a reasonable computing time, the problem became one of finding a recurrence formula for calculating $\cos 2\pi\sigma_1 n\delta$ based on $\cos 2\pi\sigma_1 h$. Indeed, computing cosines by using either series or tables resulted in prohibitive calculation times.

We used the Chebyshev formula [32]

$$\cos (p + 1)x = 2 \cos x \cos px - \cos (p - 1)x.$$

[3]The program is now in the IBM general library.

If the cosines are computed to six significant figures, the error between the value computed from a series expansion and that obtained after 12,000 iterations is less than 1/50,000.

Program Checking.--We have calculated the F.T. of a function containing 24.5 sine-wave arcs of unit amplitude, and two points per period have been taken, the interval h being taken equal to unity. The maximum height of the calculated function is f_0 in this case and not $f_0/2$ [see (II.5.b) and (II.10)] because of the overlapping of the orders due to the particular choice of h.

$2qL = 1.066 \times 49 = 52.2634$. The number calculated by the machine is 52.2582, that is to say an error of the order of 1/10,000.

The calculation is made in two parts:

1°.- During the very rapid first part, in each address the value I_{ph} of the interferogram at the point $\delta = ph$ is replaced by the corresponding value $I_{ph} A_{ph}$ of the weighted interferogram.

2°. Then the calculation proper of the F.T. begins. For each new value of σ, the first cosine, $\cos 2\pi\sigma h$, is calculated using series; the cosines which follow are computed by a recurrence formula and the sum

$$B'(\sigma) = h[IA_0+2I_1A_1\cos 2\pi\sigma h+\ldots+2I_nA_n\cos 2\pi\sigma nh].$$

is computed. This calculation is performed in $T = 0.8 \times 10^{-3}$ sec per input point, per output point.

If n points are taken from the interferogram and k spectral densities calculated, the computing time will be $t = 0.8\ nk \times 10^{-3}$ sec.

Assuming that it is necessary to compute the intensity for three points per spectral element in order to facilitate the drawing of the spectrum, the total time t in the most favorable case is $t = 0.8 \times 10^{-3}$ sec $\times$ 2M $\times$ 3M = 0.48 M^2 10^{-3} sec

and in the most unfavorable case, $t = M^2\ 10^{-8}$ sec.

It is interesting to remark that these calculation times correspond to the case where the F.T. is made from an interferogram containing no noise. In practice, to obtain the maximum s/n ratio, it is necessary to pick more points from the interferogram, and the calculation time increase. This question will be studied in detail in Chapter V.

Note.--It suffices to calculate one point per spectral element in order to collect every bit of information contained in the interferogram, or M points in all. But we have granted that it was convenient to calculate Q points per element (Q being at least equal to 3) in order to facilitate drawing the spectrum. But, the spectrum is the convolution of a sequence of Dirac functions with the apparatus-function. The Dirac functions are spaced $\delta\sigma$ apart and have heights the M values which were calculated previously (theorem of Dirichlet).

Since it is possible to perform convolutions with a numerical calculator (see Chapter IV and V) and since the calculation is relatively rapid, one can consider calculating intermediary points in making the convolution of the M Dirac functions with the apparatus-function (limited to the domain where the latter has a non-negligible value). One would thus obtain a reduction of the calculation time by a factor of Q. We propose to write this as a computing program in the near future.

III. REAL APPARATUS-FUNCTION

Under conditions attainable in practice, the spectrum obtained is always different from the one that would result from the convolution of the spectrum under consideration with the theoretical apparatus-function. The preceding results, in fact, have been established for a beam of zero extent. They are modified when the detector receives a line of finite extent. We shall study these modifications in the case where a diaphragm of finite dimensions is placed in the focal plane of the exit lens of a Michelson interferometer.

We shall show that there results, as in the classical method, an increase in the apparatus-function, with a corresponding decrease in resolution. The study of the product luminosity × resolution allows one to determine the best conditions for using the instrument.

In general, the spectrum obtained when the source is reduced to a single line of negligible width is different from the real function defined above. In fact, an instrument is never perfect and the precision of a measurement is always limited. We shall study some of the causes of perturbation of the apparatus-function, such as irregularity in the displacement of the moving element and the maladjustment of the interferometer. Finally when the Fourier transform is made by a method sensitive to phase, the necessarily limited precision of recording the zero phase difference causes a distortion of the apparatus-function.

1. APPARATUS-FUNCTION FOR A FINITE BEAM WIDTH

Several authors have already been concerned with the form of the diaphragm that has to be placed at the exit of a two-beam interferometer [33] and with the dimensions it must be

given in order to have a suitable depth of modulation [34,35] or to measure fractional excesses under the best conditions [11]. We are going to consider this question with the view of using the Michelson interferometer as a spectrometer by means of Fourier transforms.

The effect of the use of slits of finite width upon the luminosity and resolution of a grating spectrometer or a Fabry-Perot spectrometer has been treated by P. Jacquinot and C. Dufour [36] and P. Jacquinot [37]; the same study for the sisam has been made by P. Connes [4]. These are the chief results of the studies: a spectrometer with slits, grating or prism is an apparatus which can operate at very different resolutions, possibly very much below the theoretical resolution R_0. When $R \ll R_0$ the product luminosity × resolution is practically constant, and simply by enlarging the slits, one can increase the luminosity but lose in resolution. A statement of the results is made easier by the introduction of the reduced variables:

R/R_0 ratio of the real resolution to the theoretical resolution;

l reduced diaphragm breadth or ratio of the diaphragm width to the width at a height 0.404 times the maximum of the theoretical apparatus-function;

$\mathcal{L}_r$ ratio of the real luminosity to the maximum luminosity that can be obtained by increasing the opening of the diaphragm. In the case of slit spectrometers, $\mathcal{L}_r$ has a simple interpretation. It is the ratio of the real luminosity to that which can be obtained in the absence of diffraction with slits corresponding to $l = 1$.

Figures 19 and 20 show for the Fabry-Perot and the sisam the variations of $\mathcal{L}_r$, R/R_0, $\mathcal{L}_r R/R_0$ as functions of l. This last product passes through a maximum for a normalized diaphragm width near 1 and, for best results, these instruments should be used near their theoretical resolution.

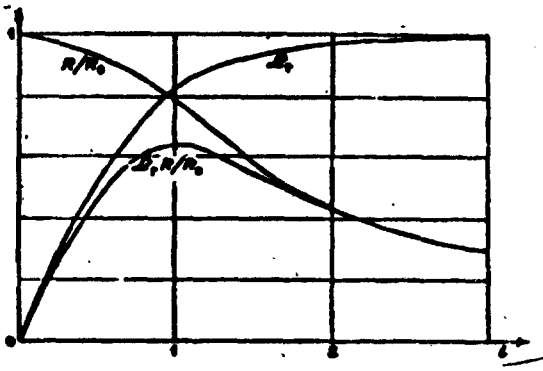

Fig. 19. Fabry-Perot Spectrometer.

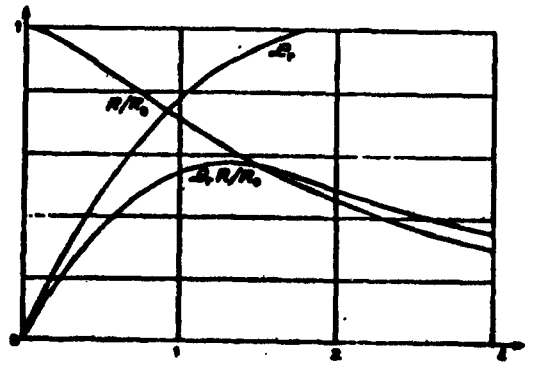

Fig. 20. Sisam.

The use of the Michelson interferometer in spectrometry, like that of the Fabry-Perot étalon, requires a circular diaphragm (entrance or exit), centered about the normal to the mirrors and limiting a bundle of rays with solid angle Ω which is slightly inclined to the normal. Under these conditions, the recorded interferogram $\Phi(\delta)$ is different from the theoretical interferogram $I(\delta)$ and its F.T. is different from the theoretical apparatus-function.

(1) Computation of the Recorded Flux and of the Real Apparatus-Function.

The calculation of the transmissed flux $\Phi(\delta)$ when the spectrum studied is reduced to a single line of negligible width, wave number σ_0, and luminance B is classical [22,24,28]:

$$\Phi(\delta) = BU \frac{\sin(\pi\delta\sigma_0\Omega/2\pi)}{\pi\delta\sigma_0\Omega/2\pi} \cos 2\pi\sigma_0\delta[1 - (\Omega/4\pi)]; \quad \text{(III.1)}$$

$S\Omega = U$ is the beam width. It has already been shown [38] that using a finite width has two consequences; widening the apparatus function, with consequent lowering of resolution, and

displacement of the spectrum towards the lower frequencies. The correction $\Delta\sigma$ to apply to the calculated spectrum is $\Delta\sigma = \sigma\Omega/4\pi$.

Numerical Example.--As we shall see in Chapter VI, the solid angle useable for studying at resolution 1,000, a spectrum about 1.5 μ is $\Omega = \pi\alpha^2 = \pi \times 16 \times 10^{-4}$ steradians. Under these conditions $\Delta\sigma = 6,000 \times 4 \times 10^{-4} = 2.6\ cm^{-1}$.

(2) Determination of the Best Conditions for Using the Instrument

Rigorously, the width of the diaphragm to be used depends upon the weighting function $A(\delta)$ chosen. We consider two types of apodization.

a. Weighting by a Triangle Function $A(\delta) = 1 - (\delta/L)$. The variations of $\mathcal{L}_r$, R/R_0 and $\mathcal{L}_r\ R/R_0$ are exactly the same as for a sisam used with a diamond-shaped diaphragm. In both cases the apparatus-function is like that of a classical grating spectrometer with the sisam, it is necessary to choose a diaphragm such that $l = 1$. Then $R = 0.80\ R_0$ and $\mathcal{L}_r = 0.82$ (Fig. 20).

b. Weighting the Interferogram by $A(\delta) = [1 - (\delta^2/L^2)]^2$. The variation of R/R_0 is then nearly the same as in the preceding case because the two apparatus-functions have the same width at mid-height; the variation of $\mathcal{L}_r$ is slightly different. The product $\mathcal{L}_r\ R/R_0$ still passes through a maximum for l very near to 1. Under these conditions, the effective resolution again is $R_0 = 0.82\ R_0$ and $\mathcal{L}_r = 0.87$ (Fig. 21).

The angular field of the diaphragm is given by the relation

$$\alpha = \sqrt{2/R_0} = 0.9\ \sqrt{2/R}. \qquad \text{(III.2)}$$

Let us suppose that for the maximal phase difference L attained, the rings in the exit plane of the objective have bright centers,

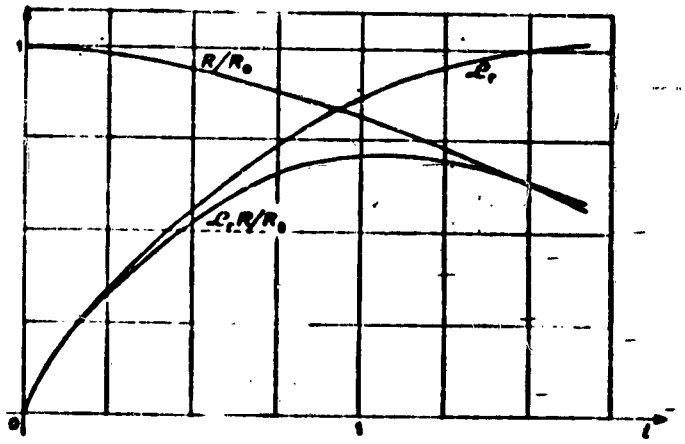

Fig. 21. Variations of R/R_0, $\mathcal{L}_r$ and $\mathcal{L}_r\, R/R_0$ in the Michelson Case.

the diameter of the diaphragm to be used is very close to 9/10 of that of the first bright ring.

(3) Correction to the Calculated Frequencies

The wave number σ_c of the radiation for which the spectral density, B, is calculated, and the interval h of the grating function occur as a product in the calculation of cosine. The wave number σ of the radiation having the same density B in the spectrum studied is related to σ_c by

$$\sigma_c = \sigma[1 - (\Omega/4\pi)]. \qquad \text{(III.3)}$$

In taking as the value of h_1, the interval of the grating function, a number such that $\sigma_c\, h = \sigma\, h_1$, it is possible, when making the F.T. numerically, to correct the frequencies automatically.

One is then led to choose

$$h_1 = h\, \sigma_c/\sigma = h[1 - (\Omega/4\pi)]. \qquad \text{(III.4)}$$

We shall see a little later (§ III.2.(4)) that to eliminate the lead errors of a moving mirror, it is necessary to adjust the phase differences with a reference line recorded at the same time as the interferogram. In this case the interval h of the grating function $R_h(\delta)$ [see (II.13)] is measured by taking as unity the wave length of this reference line.

Now the reference beam has a finite width generally different from that of the beam carrying the signal to be studied. Let us consider the case where the reference beam follows the same path in the interferometer as the light to be analyzed and let us call Ω' the solid angle subtended by the diaphragm in front of the reference source seen from the center of the exit objective. The reference interferogram is a sine wave corresponding to a signal of wave number $\sigma_c = \sigma[1-(\Omega'/4\pi)]$. From this it can be deduced that if h is the value of the period measured in the wave lengths of the reference line, its exact value h' is given by

$$h' = h[1 - (\Omega'/4\pi)].$$

To correct automatically and simultaneously the fact that the beam to be studied and the reference beam have finite widths, it is necessary to take as measure h_2 of the period which occurs in the numerical calculating,

$$h_2 = h[1 - (\Omega/4\pi)]/[1 - (\Omega'/4\pi)] \tag{III.5}$$

where, as Ω and Ω' are always small compared with one

$$h_2 = h\left(1 + \frac{\Omega'-\Omega}{4\pi}\right). \tag{III.6}$$

Remark.--P. Connes [31] showed that the phase difference variation of interfering rays with angle of incidence, which necessitates limiting the width of the beams, is useful when the exploration of the spectrum is made in space (prism and grating spectrograph, and spectrometers, Fabry-Perot used in

connection with photographing the rings), but is detrimental when it is made in time (F.P. or Michelson photoelectric interferometer). If one inserts an afocal system in each of the two beams of a Michelson interferometer, it is possible to combine the relative displacements of the mirrors and of the afocal systems in such a way that the apparatus no longer produces fringes. The interference state is constant in the entire space. Luminosity increase is practically limited only by the aberrations, and the exit aperture if it cannot be completely omitted will be considerably enlarged; all the previous considerations about the variation of the product $\mathcal{L}_r R/R_0$ are obviously no longer valid in the case where afocal systems are used.

2. CHANGES IN THE APPARATUS-FUNCTION CAUSED BY DIVERSE ERRORS

(1) Effects of Imperfections in the Optical Components

As with the sisam, the aberrations of the entrance and exit objectives, if they remain small with respect to the angular diameter of the diaphragm, have practically no effect on the theoretical resolving power. On the other hand, laminar defects in the interferometer (mirrors or trihedrals, separating and compensating plates of a Michelson interferometer, lamellar gratings of Strong's apparatus [13]) bring about a lowering of the modulation which varies with wave length, whence a loss of luminosity in the reconstructed spectrum which increases with decreasing wave length.

With grating or Fabry-Perot [3] spectrometers, the apparatus-function recorded by imperfect optical parts is the convolution of the theoretical apparatus-function with a function representing the surface faults. For example, with surface having a spherical or cylindrical curvature, the fault function is a step function which increases as the ratio of the sagitta to the

wavelength under consideration increases. This is a Gaussian function in the case of poorly micropolished surfaces. These faults are accompanied by a lowering of the resolution and a loss of luminosity.

In the F.T. method, it is the recorded interferogram which is the convolution of the theoretical interferogram with the laminar fault function $D(\delta)$. The calculated spectrum finally is the product of the theoretical spectrum by the F.T. $d(\delta)$ of the fault function $D(\delta)$, i.e., in general, the spectrum will be attenuated with respect to high frequencies. There is no widening of the apparatus-function nor lowering in resolution.

Example.--Consider, for example, the case of a circular mirror having a spherical curvature, the sagitta being $\lambda_0/2$; that of the wave surface will be λ_0, which means that instead of having at a given instant a well-determined phase difference δ, one has all values between δ and $\delta + \lambda_0$. The fault function is a square pulse function of width λ_0 (Fig. 22b). The recorded interferogram $I'(\delta)$ (Fig. 22c) is the convolution of $I(\delta)$ (Fig. 22a) with $D(\delta)$ and the spectrum obtained will be the product (Fig. 22f) of the theoretical spectrum $B(\sigma)$ (Fig. 22d) with the function $(\sin \pi\sigma/\sigma_0)(\pi\sigma/\sigma_0)$ (Fig. 22e), the F.T. of this $D(\delta)$ function which has zeros for $\sigma = k\,\sigma_0$, calling $\sigma_0 = 1/\lambda_0$.

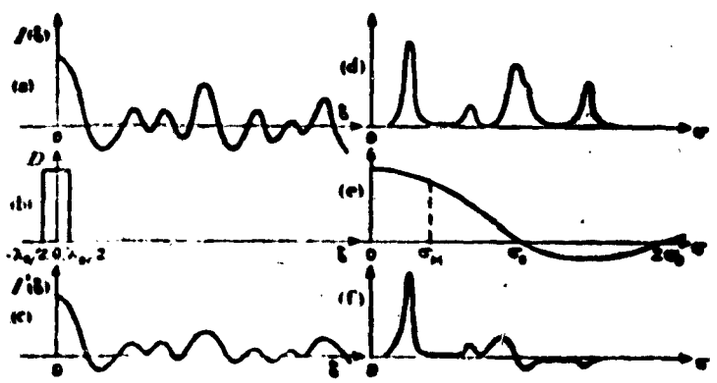

Fig. 22. Effect of a Spherical Curvature of the Surfaces.

In practice, it will obviously be necessary that the magnitude of the flaws be small with respect to the smallest wave length contained in the spectrum; this amounts to saying that the maximal frequency σ_M of the spectrum will be small with respect to σ_0 (Fig. 22e); under these conditions, in the whole spectrum, the attenuation will be weak and vary little.

(2) Effect of a Maladjustment of the Interferometer

We distinguish the two cases in which the maladjustment due simply to an initial poor adjustment of the optical components remains constant or varies with the displacement of the mirror[4].

A. CONSTANT MALADJUSTMENT. The effect of a constant maladjustment is equivalent to a surface fault. If the interferometer mirrors are stopped down by rectangles, and if one of the sides of length L is perpendicular to the line of intersection of the mirror planes which make an angle ϵ (Fig. 23), then the two reflected wave fronts make an angle 2ϵ, and, at a given instant, the phase difference varies between δ and

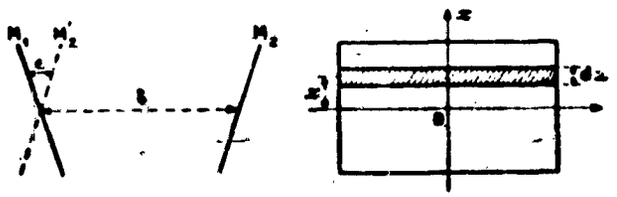

Fig. 23. Maladjustment of the Interferometer.

[4]The effect of a maladjustment upon the photoelectric measure of a displacement has been studied by G. W. Stroke [40].

$\delta + 2\epsilon L$ (This is the simplest case). Here, by putting $\lambda_0 = 2\epsilon L$, one sees that the effects on the interferogram and the spectrum are identical to those of the sagitta λ_0; the calculated spectrum is further attenuated by a factor $(\sin \pi\sigma/\sigma_0)(\pi\sigma/\sigma_0)$.

B. VARIABLE MALADJUSTMENT

If the movement of the mirror is not a translation (as the result of an imperfection in the ways, for example), there is a variable maladjustment in the interferometer. Now one must write that ϵ, hence λ_0 and σ_0, are functions of δ; the signal; corresponding to each frequency σ in the interferogram, is attenuated by a factor depending on δ and σ, $P(\sigma,\delta) = [\sin \pi\sigma/\sigma_0(\delta)][\pi\sigma/\sigma_0(\delta)]$; the new apparatus-function will be the F.T. of $P(\delta)$. In contrast to the preceding case, not only its height but also its shape can be modified, the change always being the greatest for the highest frequencies. A more detailed inquiry into this case appears to be of little use since there exists a method, due to E. R. Peck [41], which removes nearly completely this cause of error: the use of reflecting trihedrals, unaffected by a rotation about their vertex.

(3) Effect of an Error Upon the Determination of the Point on the Interferogram Corresponding to a Phase Difference $\delta = 0$.

We are going to show that this point, called in what follows the "zero point" of the interferogram, ought to be located with great precision (small error with respect to the wave length studied)[5]. Even a very small error strongly

[5] This necessity disappears in the case where the F.T. is made by a method insensible to the phase of the signals contained in the interferogram: the use of an harmonic analyzer

(Cont. on following page)

perturbs the form of the apparatus-function, which becomes asymmetric and has important negative minima. Moreover its shape varies rapidly with σ so that in the case of a broad spectrum the results soon become hard to interpret.

Suppose that we have chosen for the zero point a point which corresponds to a phase difference ϵ. According to whether ϵ is positive or negative, one makes the F.T., not of $I(\delta)$ (Fig. 24a), but of one of the two even functions represented by the Figures 24b and 24c.

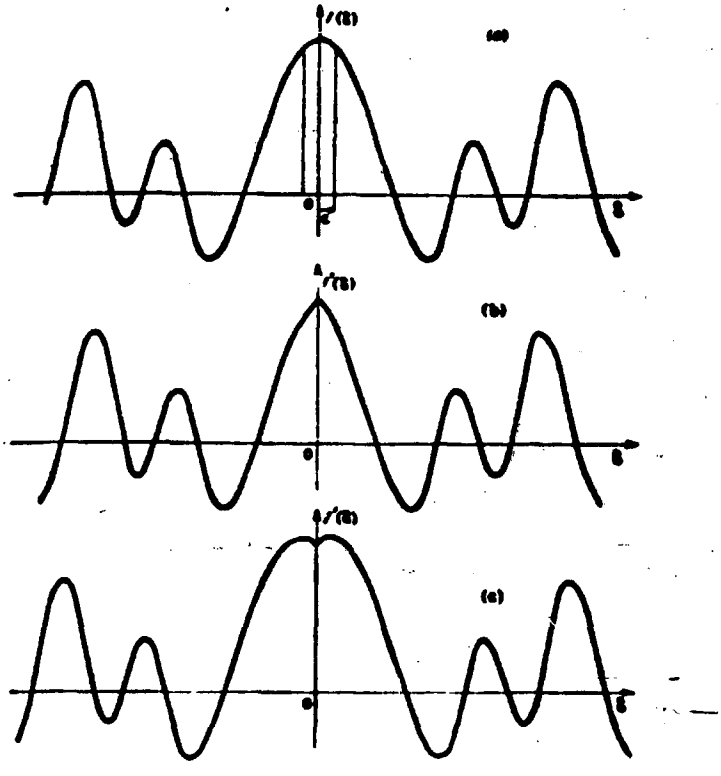

Fig. 24. Effect of an Error in the Choice of Zero-Point on the Interferogram: a. $\epsilon = 0$; b. $\epsilon > 0$; c. $\epsilon < 0$.

(8,cont) like that conceived by P. Jacquinot [1] and made by L. W. Mertz [46] or of a numerical transformation of the type studied in § II.2(3).

A. CALCULATION OF THE APPARATUS-FUNCTION

a. $\epsilon > 0$. In order to calculate the spectral density corresponding to the wave number σ_1, in lieu of using the equality

$$B(\sigma_1) = 2\int_0^\infty I(\delta)\, A(\delta) \cos 2\pi\sigma_1\delta \, d\delta, \tag{III.7}$$

the following operation is performed

$$B'(\sigma_1) = 2\int_0^\infty I(\delta+\epsilon)\, A(\delta) \cos 2\pi\sigma_1\delta \, d\delta. \tag{III.8}$$

To find the form of the new apparatus-function, it is sufficient to consider the case where the spectrum is reduced to a radiation of wave number σ_0 of luminance $B = 1$. Then

$$I(\delta+\epsilon) = \cos 2\pi\sigma_0(\delta+\epsilon), \tag{III.9}$$

so that (III.8) can be put in the form

$$B'(\sigma_1) = 2\Big[\cos 2\pi\sigma_0\epsilon \int_0^\infty A(\delta) \cos 2\pi\sigma_0\delta \cos 2\pi\sigma_1\delta \, d\delta - \tag{III.10}$$
$$- \sin 2\pi\sigma_0\epsilon \int_0^\infty A(\delta) \sin 2\pi\sigma_0\delta \cos 2\pi\sigma_1\delta \, d\delta\Big].$$

We find the integral

$$2\int_0^\infty A(\delta) \cos 2\pi\sigma_0\delta \cos 2\pi\sigma_1\delta \, d\delta$$
$$= \tfrac{1}{2}\,[f(\sigma_0-\sigma_1) + f(\sigma_0+\sigma_1)], \tag{III.11}$$

which gives the two usual maxima of the apparatus-function, the cosine transform of $A(\delta)$ centered on σ_0 and $-\sigma_0$ (Fig. 25a).

On the other hand (Fig. 25b),

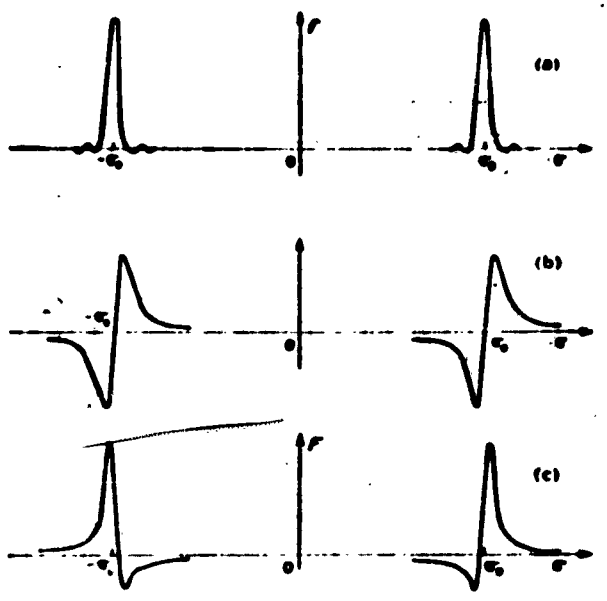

Fig. 25. Apparatus-Functions When There is an Error in the Determination of $\delta = 0$.

$$2\int_0^\infty A(\delta)\sin 2\pi\sigma_0\delta\cos 2\pi\sigma_1\delta\,d\delta \qquad \text{(III.12)}$$

$$\tfrac{1}{2}\left[h(\sigma_0+\sigma_1)+h(\sigma_0-\sigma_1)\right],$$

$h(\sigma)$ being an odd function, the sine transform of $A(\delta)$, that we shall call the apparatus-function in sines:

$$h(\sigma) = 2\int_0^\infty A(\delta)\sin 2\pi\sigma\delta\,d\delta\,. \qquad \text{(III.13)}$$

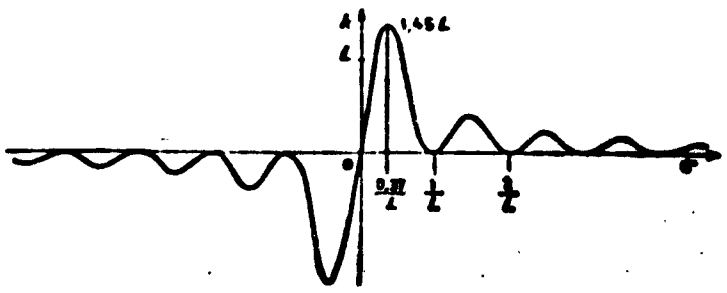

Fig. 26. Sine Transform of a Square-Pulse Function.

It is the convolution of $h(\sigma)$, the sine transform of a square-pulse function (Fig. 26) with $a(\sigma)$, the cosine transform of $A(\delta)$.

The spectral density calculated for wave number σ_1 is then

$$B'(\sigma_1) = \tfrac{1}{2}\,[\cos 2\pi\sigma_0\epsilon\, f(\sigma_1-\sigma_0) + \sin 2\pi\sigma_0\epsilon\, h(\sigma_1-\sigma_0) + \cos 2\pi\sigma_0\epsilon\, f(-\sigma_1-\sigma_0) + \sin 2\pi\sigma_0\epsilon\, h(-\sigma_1-\sigma_0)]. \quad \text{(III.14)}$$

The calculated spectrum is thus formed by the two peaks of the apparatus-function

$$F(\sigma) = \cos 2\pi\sigma_0\epsilon\, f(\sigma) + \sin 2\pi\sigma_0\epsilon\, h(\sigma), \quad \text{(III.15)}$$

centered one on σ_0, the other on $-\sigma_0$ (Fig. 25c).

The expression (III.15) shows that the apparatus-function depends on the frequency analyzed in the spectrum. The term $\sigma\epsilon$ or ϵ/λ measures the error made in the choice of the zero point divided by the wave length studied. When ϵ/λ is equal to 0 or 1, $F(\sigma) = f(\sigma)$. When ϵ/λ is equal to 1/4, i.e., when an error of a quarter of a fringe has been made, $F(\sigma) = h(\sigma)$. Between these two extreme cases, all intermediary ones are possible. Figure 27 gives the function $F(\sigma)$ for values of ϵ/λ taken between 0 and 0.25. The asymmetry of the function increases with the displacement by translation of the principal maximum. In Fig. 28, the variation of the ratio C of the height of the negative minimum to that of the central maximum for ϵ/λ varying from 0 to 0.25 has been studied. It is interesting to note the rapidity with which C increases for low values of ϵ/λ (Fig. 29).

b. $\epsilon < 0$. The case where ϵ is negative is easily deduced from the preceding case. For a given wave number σ and a given negative value ϵ' of the error, the apparatus-function

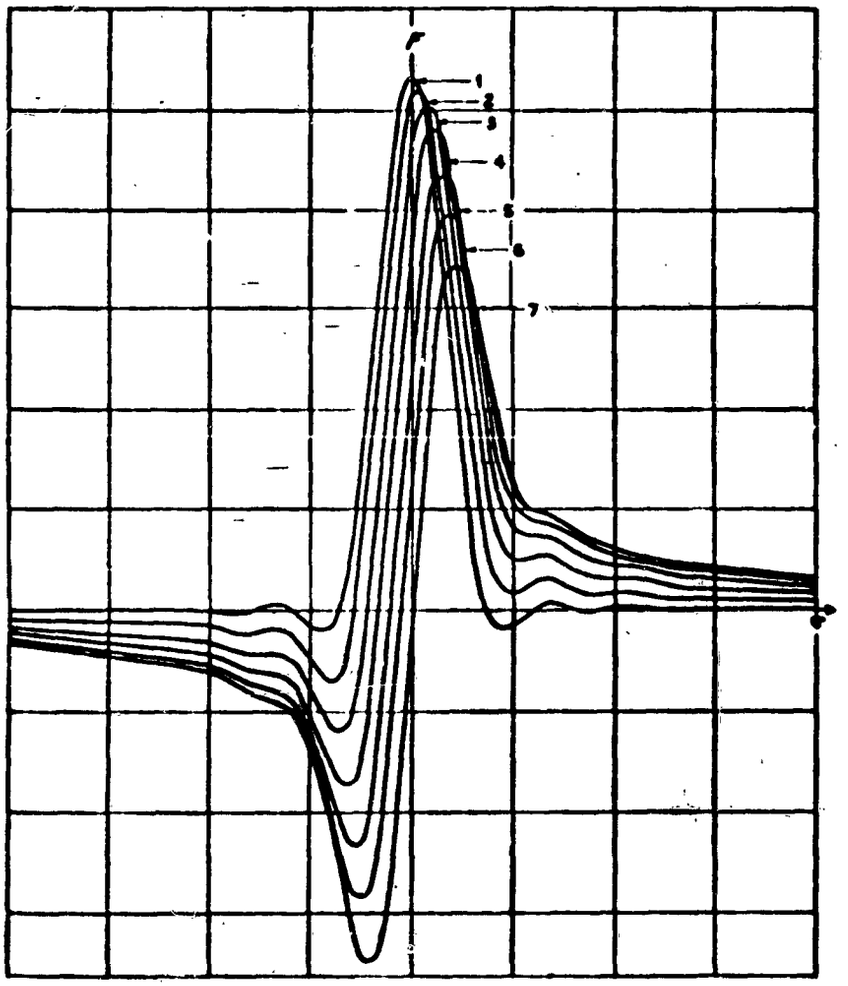

Fig. 27. Different Forms of the Apparatus-Function for Different Values of the Phase Displacement: Curve 1, $\epsilon/\lambda = 0$; Curve 2, $\epsilon/\lambda = 0.042$; Curve 3, $\epsilon/\lambda = 0.084$; Curve 4, $\epsilon/\lambda = 0.126$; Curve 5, $\epsilon/\lambda = 0.168$; Curve 6, $\epsilon/\lambda = 0.210$; Curve 7, $\epsilon/\lambda = 0.250$.

$$F'(\sigma) = \cos 2\pi\sigma\epsilon' \, f(\sigma) - \sin 2\pi\sigma |\epsilon'| \, h(\sigma),$$

is identical to the function $F(\sigma)$ determined for a positive value of ϵ,

$$F(\sigma) = \cos 2\pi\sigma\epsilon \, f(\sigma) + \sin 2\pi\sigma\epsilon \, h(\sigma),$$

under the condition that $|\sigma\epsilon'| = 1 - \sigma\epsilon$.

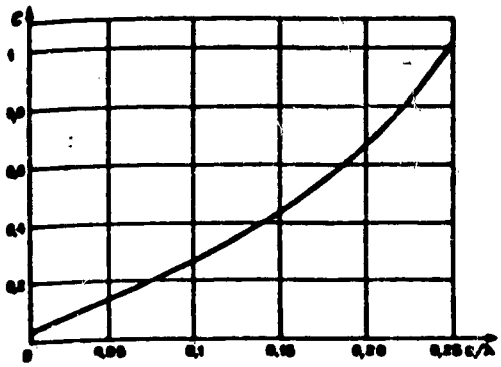

Fig. 28. Variation in the Asymmetry of the Apparatus-Function With Phase Displacement.

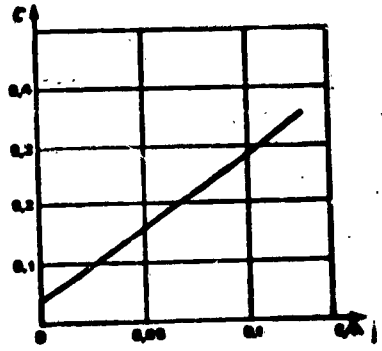

Fig. 29.

When investigations of an extended spectral domain are made, ϵ/λ and, consequently, the apparatus-function vary considerably from one end of the spectrum to the other. Figure 30

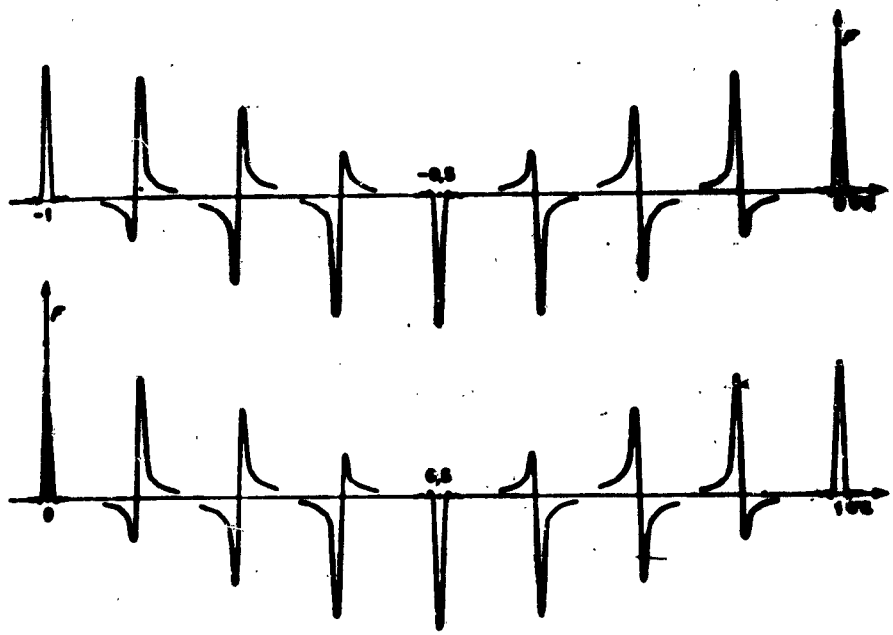

Fig. 30. Deformation of the Apparatus-Function for Phase Displacements Taken Between - 2π and + 2π.

shows the deformation of $F(\sigma)$ for ϵ/λ varying between $-\frac{1}{2}$ and $+\frac{1}{2}$.

B. PRACTICAL PROBLEMS RELATED TO THE DETERMINATION OF THE ZERO PHASE DIFFERENCE. When the spectrum studied is broad, the interferogram in the neighborhood of the zero phase difference has only a few fringes, the intensity of which decreases rapidly and (under the condition that the interferometer used is very symmetric, hence that the interferogram itself is symmetric) the zero can be located with great precision. In general, the precision is limited for two reasons:

1°. in practice, on the ideal interferogram, there are always superposed some fluctuations due to noise;

2°. sometimes the very nature of the interferogram renders the recording difficult. If the spectrum considered consists only of some rather close lines in the neighborhood of the zero phase difference, the modulation is practically constant, and one is uncertain by several fringes.

One solution to these two problems consists in recording simultaneously the interferogram to be studied (interferogram 1) and that given by a source with an intense and broad spectrum (interferogram 2). Practically, one uses an incandescent lamp and a filter isolating a broad radiation band in the same domain as the spectrum to be studied.

When one studies an emission spectrum, there is no inconvenience in replacing a portion of a fringe or an entire fringe, in the center of interferogram 1, by the equivalent part of interferogram 2. At the time of the recording, the passage of the zero phase difference is easily recognized. It is enough then to replace the light coming from the incadescent lamp by the spectrum to be studied. This question will be considered in detail in Chapter VI. The important problem of the determination of the zero phase difference in the case where

the interferogram is recorded with a time constant which makes it asymmetric will be considered in Chapter V.

C. CALCULATION OF THE SPECTRUM BY A METHOD NOT REQUIRING A KNOWLEDGE OF THE ZERO. We are going to show that it is possible correctly to reconstruct the spectrum studied without being bothered about the position of the zero point, when the interferogram is recorded for δ varying from - L to L, to make the cosine transform B_1' of the interferogram; to make the sine transform B_2'; and to take as the measure of the spectrum[6] $B' = \sqrt{B_1'^2 + B_2'^2}$. Suppose that the spectrum contains only a single line of luminance B = 1, of wave number σ_0; the spectrum obtained in this case will be the apparatus-function.

The interferogram reduces to a sine wave having the form

$$I(\delta) = \cos 2\pi\sigma_0(\delta+\epsilon) = \cos 2\pi\sigma\delta_0 \cos 2\pi\sigma\epsilon - \sin 2\pi\sigma_0\delta \sin 2\pi\sigma\epsilon.$$

It is composed of an even part $I_p(\delta) = \cos 2\pi\sigma\epsilon \cos 2\pi\sigma_0\delta$ and of an odd part $I_i(\delta) = \sin 2\pi\sigma\epsilon \sin 2\pi\sigma_0\delta$.

$$B_1'(\sigma) = \cos 2\pi\sigma\epsilon \int_{-\infty}^{+\infty} A(\delta) \cos 2\pi\sigma_0\delta \cos 2\pi\sigma\delta \, d\delta$$

$$= \tfrac{1}{2} \cos 2\pi\sigma\epsilon \, [f(\sigma-\sigma_0) + f(\sigma+\sigma_0)].$$

$$B_2'(\sigma) = - \sin 2\pi\sigma\epsilon \int_{-\infty}^{+\infty} A(\delta) \sin 2\pi\sigma_0\delta \sin 2\pi\sigma\delta \, d\delta$$

$$= - \tfrac{1}{2} \sin 2\pi\sigma\epsilon \, [f(\sigma-\sigma_0) - f(\sigma+\sigma_0)].$$

The calculated spectrum will have the value

[6] This process is used by J. G. Braithwaite and J. Brooks [53].

$$B'(\sigma) = \sqrt{[B'_1(\sigma)]^2+[B'_2(\sigma)]^2}$$

(III.16)

$$= \frac{1}{2}\,[|f(\sigma-\sigma_0)| + |f(\sigma+\sigma_0)|].$$

The new apparatus-function $|f(\sigma)|$ has the same width as the usual function $f(\sigma)$. Hence the limit of resolution remains unchanged. However, this method has several inconveniences:

1°. it requires a double displacement of the movable mirror, which can become difficult for high resolutions;

2°. for equal time durations, the signal/noise ratio is somewhat less advantageous (this question will be studied in greater detail in the following chapter);

3°. the calculation time in the case of numerical analysis is a little more than quadrupled (there are twice as many input points and there are two identical calculations for the cosine and sine transforms; the calculation time of the squares of the F.T. and of the square root of their sum is short compared with that of the F.T. themselves).

(4) Effect of an Error Upon the Measurement of the Phase Difference

The reconstruction of the spectrum based on the interferogram requires the knowledge of the phase difference corresponding to each of its points. This is best accomplished by simultaneously recording (with a two-pen recording device or a two-track magnetic recorder) the interferogram to be studied and a reference signal given by a monochromatic radiation of known wave length. The precision with which δ is known is then limited only by the noise in the reference signal. In practice this last consideration does not matter in problems with low resolution, the only ones we have attempted experimentally up to now; so we have not undertaken

this study. However, having to produce and record this reference signal presents a certain difficulty. Another much simpler but much less precise procedure consists in recording simultaneously the interferogram and reference time pips produced by the rotation of the drive screw[7]. Still more simply, one can drive the screw and the recording paper by synchronous motors. We are going to study the deformations of the apparatus-function introduced in these last two methods, by mechanical errors. Our conclusion will be that they can be used only to treat problems of low resolution, for example in the far infrared.

The movable mirror's advance is never rigorously linear because a screw is never perfect. It always has a periodic error of period θ, the period of the rotation of the screw $\theta = p/V$, p being the pitch of the screw. We shall confine ourselves in the following to the study of the "ghosts" introduced into the calculated spectrum by an error of this type, because it is by far the most annoying.

A. CALCULATION OF THE RELATIVE HEIGHT OF GHOSTS. In a general way, $\delta(t)$ can be considered as the sum of two terms (Fig. 31), one a linear function of time, the other an arbitrary function of time with mean value zero: $\delta = Vt - f(t)$. If $f(t)$ is a periodic function of period θ, we can write it in the form of a Fourier series

$$f(t) = \sum_{n=1}^{\infty} a_n \cos 2\pi n \frac{t}{\theta} + b_n \sin 2\pi n \frac{t}{\theta} = \sum_{n=1}^{\infty} \epsilon_n \cos\left(2\pi n \frac{t}{\theta} - \varphi_n\right).$$

[7] An intermediary precision method (sufficient for mid or far infrared) uses a reference signal provided by the moire fringes obtained with two gratings, one of which is attached to the moving component.

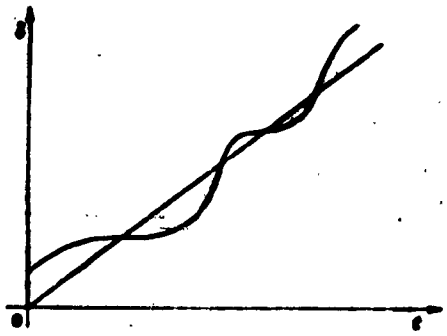

Fig. 31. Variation of δ as a Function of t.

When the error is purely sinusoidal of period θ, only the first term exists and

$$(III.17)\quad \delta = Vt + \epsilon_1 \cos\left(2\pi \frac{t}{\theta} - \varphi\right).$$

Let us take the time origin at $\delta = 0$; the expression (III.17) becomes

$$\delta = Vt + \epsilon_1 \sin (2\pi t/\theta).$$

Under these conditions the interferogram obtained with a monochromatic source of luminance B, of frequency σ_0, can be expressed as

$$(III.18)\quad I(t) = B \cos 2\pi\sigma_0[Vt + \epsilon_1 \sin (2\pi t/\theta)]$$

$$= B \cos (\Omega_0 t + \beta \sin \omega t),$$

where $\Omega_0 = 2\pi\sigma_0 V$ (mean frequency) and $\beta = 2\pi\epsilon_1/\lambda_0$ (modulation index).

One is thus led to the classical problem of studying the spectrum of a frequency-modulated sine wave ([43] p. 407). This problem is familiar to radio engineers. It also occurs in the study of ghosts of a grating which has been drawn with a ruling machine. From this point of view it has been the subject of several papers, the oldest of which is due to Rowland ([25] p. 97, [44], [45]). We are going to take it up in our particular case and we do not limit ourselves to the case where β is small in comparison with the wave length studied, because the interferometer screws are generally of a quality very inferior to that of the screws used in the machines which rule gratings.

Equation (III.18) can be put in the form

(III.19) $I(t) = B \cos \Omega_0 t \cos (\beta \sin \omega t) - B \sin \Omega_0 t \sin (\beta \sin \omega t).$

Using the classical expansions of cos (β sin ωt) and sin (β sin ωt) and noticing that $J_{-n}(z) = (-1)^n J_n(z)$, one gets

(III.20) $$I(t) = B \sum_{n=-\infty}^{+\infty} J_n(\beta) \cos (\Omega_0 + n\omega) t.$$

The spectrum of the signal studied is composed of the principal line of wave number σ_0, and of an infinity of ghosts located on both sides of the principal ray, of intensity $J_n(\beta)$ and of wave number $\sigma_0 \pm n \Delta\sigma$, n being an integer and $\Delta\sigma$ the interval between any two of these ghosts,

(III.21) $$\Delta\sigma = \frac{1}{2p},$$

p being the pitch of the screw.

Since the Bessel functions become negligible when the index is distinctly greater than the argument, the number of ghosts that one sees is, in practice, limited. We can get an idea of their height relative to the principal line by the following comparisons.

Suppose that the screw is used in a machine ruling gratings and that the gratings so obtained are used in a Littrow mounting at grazing incidence (i.e., under the worst conditions, the ghosts' intensity increasing as the square of the sine of the incident angle). One can show that the relative height of the ghosts obtained by the F.T. of the interferogram is equal to the ratio of the <u>amplitude</u> of the luminous vibration diffracted in the ghost to that diffracted in the principal

line whence equal to the square root of their relative intensity. It is thus much greater.

NUMERICAL EXAMPLE. Suppose that with an excellent machine one can get gratings such that the intensity of the first ghost for an incidence of 60° and a given wave length is 10^{-3} times the principal line's wave length. Used to record an interferogram, the same machine would have yielded for the same wave length a ghost whose relative intensity is 3.6×10^{-8}.

These facts give an idea of how much more difficult it is to build a machine sufficiently precise to record an interferogram and to take a F.T. of it without recourse to a reference line than it is to build a grating ruling machine.

B. EXPERIMENTAL STUDY. We didn't check these results directly but we studied our interferometer's screw and we deduced the relative height of the ghost that we would have gotten in taking the F.T. of an interferogram without using the reference line.

As a source we used the red cadmium line and we recorded the 14,100 fringes corresponding to a variation of phase difference of 1 cm. We measured the distances between every hundred fringes on the recording with an estimated error of one-quarter fringe; the displacement of the moving mirror was adjusted to about 0.08 μ. It was then possible to chart the screw errors (Fig. 32). A periodic error was clearly disclosed with period equal to that of the screw whose thread was $p = 1$ mm; the error amplitude was about $\epsilon = 0.5$ μ.

The ghosts which one would obtain would be $\Delta\sigma = 1/2p = 5$ cm^{-1} apart. We computed the relative height in three different cases.

1°. $\lambda_0 = 0.6438$ μ, i.e., the interferometer is to be used in the study of the red cadmium line. The modulation index

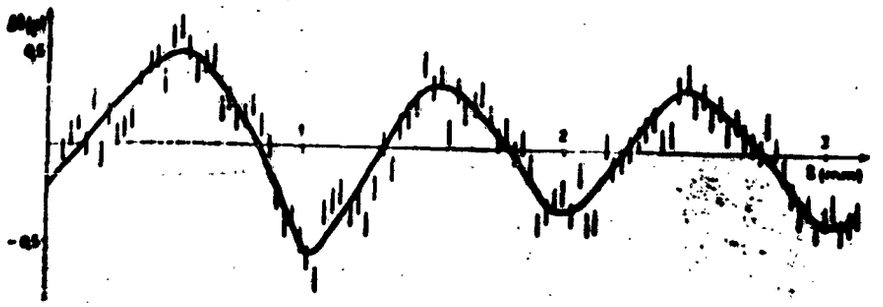

Fig. 32. Screw Errors.

β is 4.88. One must go out to the eleventh ghost to find an intensity which is 2/10,000 times the theoretic intensity of the principal line (Fig. 33a).

2°. $\lambda_0 = 1.5\ \mu$, $\beta = 2$. The line studied is in the near infrared. There are fewer ghosts (Fig. 33b).

3°. $\lambda_0 = 15\ \mu$, $\beta = 0.2$. Only three ghosts have an intensity greater than 2/10,000 (Fig. 33c).

Figure 33 shows that the spectral interval occupied has width 100 cm^{-1}, 60 cm^{-1}, or 30 cm^{-1} according as the line studied is in the visible, the near infrared, or the mid-infrared part of the spectrum. If the limits of resolution are of this order, one cannot, in practice, recognize the ghosts.

These results illustrate very well how necessary it is to use a reference line when it is desirable to exceed a resolution of the order of 100, in the visible and near infrared.

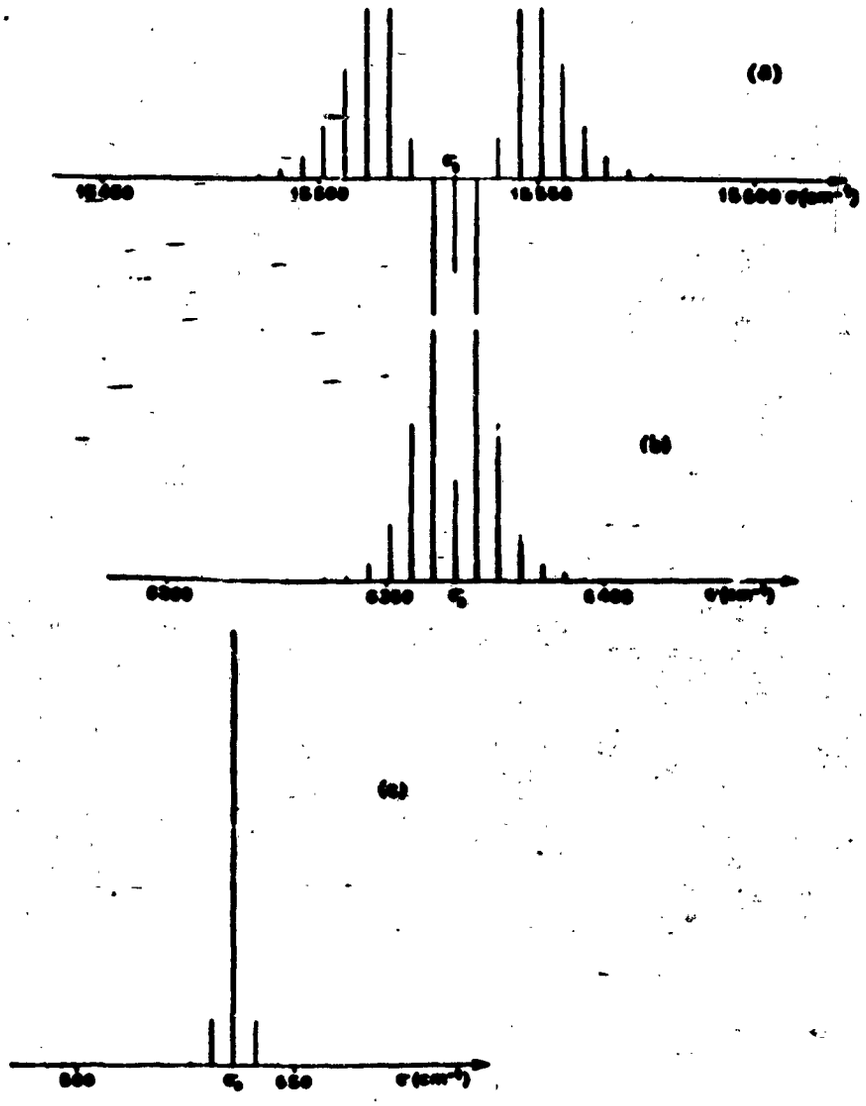

Fig. 33. Frequencies and Relative Intensities of Ghosts:

a. $\beta = 4.88$, $\lambda_0 = 6{,}438.47$ A, $\sigma_0 = 15{,}531$ cm^{-1};

b. $\beta = 2$, $\lambda_0 = 1.570\ 8\ \mu$, $\sigma_0 = 6{,}366$ cm^{-1};

c. $\beta = 0.2$, $\lambda_0 = 15.708\ \mu$, $\sigma_0 = 636.6$ cm^{-1}.

IV. GENERAL NOTES ON NOISE IN THE FOURIER TRANSFORM METHOD

In the introduction we showed by a simple argument the gain in the signal/noise ratio that could be expected for equal resolution and measurement time by the F.T. method instead of a classical method. Recall that this is true only in the infrared region, where the fluctuations perturbing the measurements originate in the detector itself and not in the line studied, i.e., when the photon noise is negligible compared with detector noise.

The noise problem of the F.T. method does not occur in the same way as it does in the classical methods. In fact, here, the result of the experiment is the interferogram. The interferogram noise has the same behavior as the noise in the spectrum obtained by a classical method, but the noise in the spectrum obtained by a Fourier transformation is the F.T. of the noise contained in the interferogram and has a special aspect.

In this chapter we shall study the behavior of the noise in the spectra. We shall show that the s/n ratio in the spectrum varies as the square root of the total measurement time T and how one can predict the s/n ratio in the spectrum using the s/n ratio in the interferogram.

1. CHOICE OF THE BEST CONDITIONS FOR RECORDING THE INTERFEROGRAM. NOISE IN THE INTERFEROGRAM

The procedures for recording an interferogram vary according to whether one intends to make the F.T. of an interferogram with a harmonic analyzer or by a numerical method. In the first case one makes a continuous recording (for example, on magnetic tape [1,46]). In the second case one can use either a pen recorder or a converting system which, at a given instant,

changes a voltage into a number written on punched tape [42]. Whatever method is used, the problems relative to amplification of the signal furnished by the detector remain the same. Fellgett was the first to insist upon the necessity of introducing only perfectly linear elements into the amplification-detection system. We are going to distinguish several possibilities according to the signal frequency to be recorded.

1°. If the detector used is a photomultiplier and if the available energy is low, so that a long recording time is required hence a low velocity V, the electrical frequencies contained in the signal to be amplified which we shall now call Fourier frequencies are low (of the order of one cycle per second). One can then use a direct current amplifier.

2°. Lead sulfide cells have a non-uniform noise spectrum, always maximum in the neighborhood of the zero frequency (scintillation noise). On the other hand their response to a modulated signal, uniform for lower frequencies, decreases rapidly for higher frequencies (of the order of 1,000 cps). Under these conditions the best s/n ratio for a signal occupying a given band width is obtained when the mean signal frequency is of the order of 100 to 1,000 cps.

If the source to be studied is intense enough to permit operating at such speeds that the frequencies to be analyzed are of this order, an alternating current amplifier with a sufficiently large band width can be used. But in the majority of cases the usable energy is low. The Fourier frequencies will be very low, whence the necessity of chopping the luminous flux with a modulator (following the classical method in infrared spectroscopy). The detection of the electric signal necessarily will have to be a synchronous detection [16]. In fact, we shall see in what follows that with the F.T. method one can detect lines which give, in the interferogram, sine

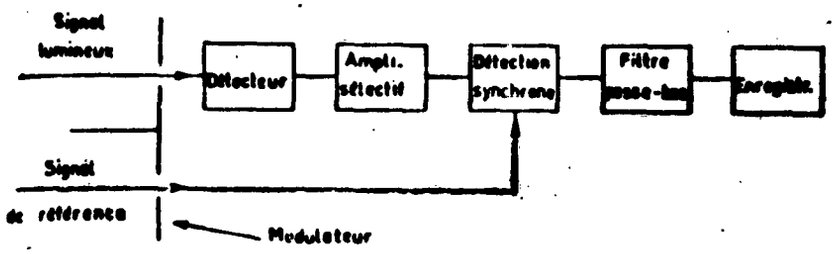

Fig. 34. Schematic Diagram of the Recording of an Interferogram. Captions:

Signal lumineux = Light signal
Détecteur = Detector
Ampli. seléctif = Selective amplifier
Détection synchrone = Synchronous detector
Filtre passe-bas = Low-pass filter
Enregistr. = Recorder
Signal de référence = Reference signal
Modulateur = Modulator

waves whose amplitude is much smaller than the noise. But a classical detection method (so-called linear) is in fact linear only if the s/n ratio is much greater than 1 ([47] p. 359), hence the absolute necessity of synchronous detection.

The detector-amplifier system to use in this case is exactly the same as the one which serves to record the spectrum in classical methods (Fig. 34). The electrical signal before synchronous detection is amplified in a selective amplifier in such a way that the synchronizing frequency corresponds to the frequency of modulation of the light signal. The band pass should be wide enough for all the frequencies to be transmitted without phase distortion or amplitude attenuation. After synchronous detection, the signal passes through a low-pass filter before being recorded. We shall see that this filter plays a fundamental rôle when the F.T. is made numerically using discrete values taken from the interferogram. When it is made by a harmonic analyser (which uses the whole interferogram and not just discrete values)

the s/n ratio in the calculated spectrum does not depend on the time constant of the low-pass filter. The rôle of the latter is simply to reduce the noise which must not saturate the recording device. The spectral densities $A(\nu)$ and $\mathfrak{B}(\nu)$, corresponding to the frequency ν of a signal before and after filtering, are connected by the classic relation

$$\mathfrak{B}(\nu) = A(\nu)\ |G(\nu)|^2, \tag{IV.1}$$

$G(\nu)$ being the complex gain of the filter.

If one assumes that the noise spectrum is constant in the neighborhood of the modulation frequency (white noise) with a noise density $\mathfrak{B}_0$, the power spectrum of the noise contained in the interferogram (or in the spectrum obtained by a classical method) has the form

$$\mathfrak{B}(\nu) = \mathfrak{B}_0\ |G(\nu)|^2. \tag{IV.2}$$

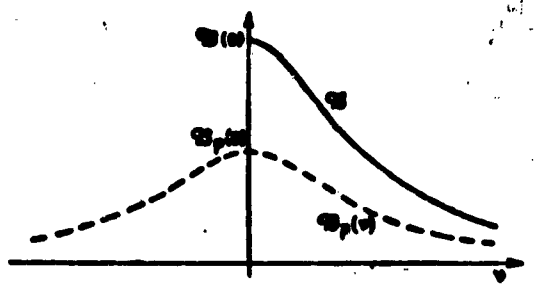

Fig. 35. Noise Spectrum and its Even Part.

In the particular case of a resistance-capacity filter with time constant $RC = \tau$

$$\mathfrak{B}(\nu) = \mathfrak{B}_0/[1 + (2\pi\nu\tau)^2] \tag{IV.3}$$

(Fig. 35).

2. APPEARANCE OF NOISE IN THE CALCULATED SPECTRUM

The cosine transform, as described in Chapter II, is a linear transform. The recorded interferogram $I'(t)$ is the sum of the theoretical interferogram $I(t)$ which we have been considering until now and the noise $x(t)$ which can be regarded as random luminance of mean value zero. The F.T. of $I'(t)$ is the sum of the spectrum $B_p(\nu)$, F.T. of $I(t)$, and noise $X(\nu)$ which is cosine transform of $x(t)$; $X(\nu)$ is a quantity of the same kind as $\mathfrak{B}(\nu)$. It is a density of the random luminance

(luminance per cps), with mean value zero, which is superimposed on the spectrum. There is no signal-noise[8] interaction and to study the sum signal + noise, it is sufficient to study the signal separately in the absence of noise, which has been done in Chapter II, and then study noise. If one represents the sum signal + noise $\mathcal{S}$, i.e., the result of the cosine transform of I'(t) as a function of the signal s which would be the result of the cosine transform of I(t), one gets Fig. 36 in which σ_χ represents the mean square error of the fluctuations in the calculated spectrum. There will be a certain definite probability P, related to the shape of the statistical distribution of noise, that the measured signal $\mathcal{S}$ lies between $s + \sigma_\chi$ (Fig. 36, curve a) and $s - \sigma_\chi$ (Fig. 36, curve b).

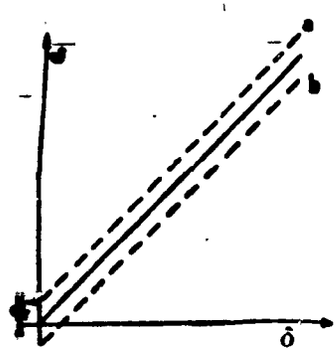

Fig. 36. Variation of the Sum Function Signal + Noise as a Function of the Signal When the F.T. is Made by Referencing the Zero Point.

In the study of a random variable, two problems occur:

1°. the determination of its autocorrelation function, whence the calculation of the radius of correlation from which one deduces the appearance of the curve representing the random variable;

2°. the calculation of its mean power, again called variance.

[8] We shall see in what follows that when the spectrum is obtained as the square root of the sum of the squares of the cosine and sine transforms of the interferogram recorded from - L to + L, as explained in paragraph III.2(3)C, the study of the signal/noise ratio is much more complicated.

A simple argument allows one to predict the appearance of noise in a calculated spectrum without its being necessary to calculate the autocorrelation function. The noise x(t) recorded on the interferogram between instants 0 and T, which we shall call oscillogram noise has no periodicity whatsoever (Fig. 37a). Its radius of correlation is τ. However, if T is

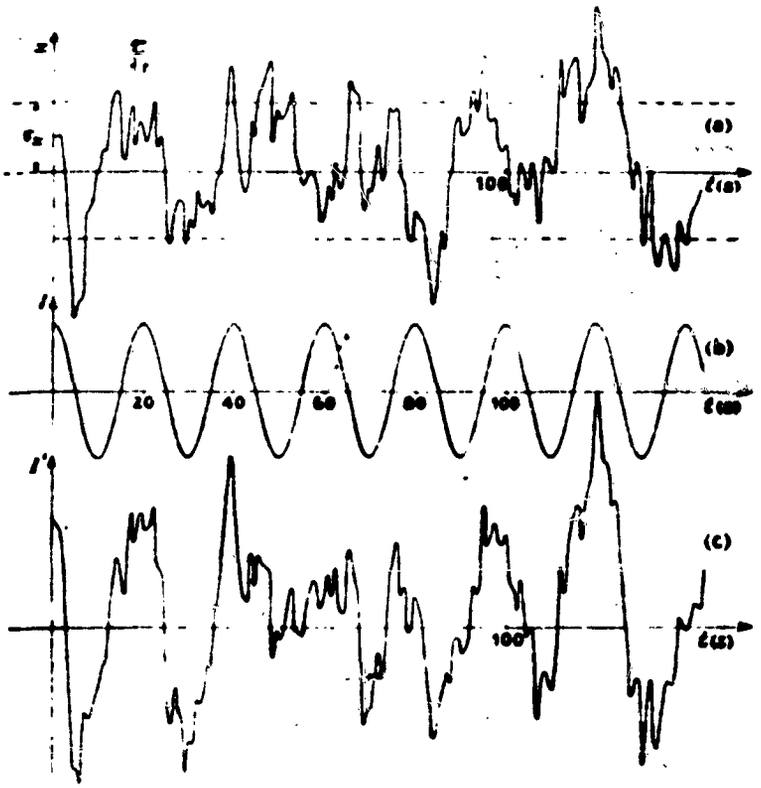

Fig. 37. (a) Noise in the Interferogram; (b) Signal in the Interferogram; (c) Noise + Signal.

chosen sufficiently large with respect to the time constant τ which has been used to record x(t), then practically, one can assume (although in theory, this may not be entirely exact) that x(t) is a periodic design of period T and can make a classic Fourier decomposition of it ([47] p. 307, [48]). In the interval (0,T), x(t) is represented by the Fourier series

$$(IV.4)\quad x(t) = \sum_{n=-\infty}^{+\infty} \frac{C_n}{2T} \cos(2\pi\nu_n t - \varphi_n), \quad \text{with } \nu_n = \frac{n}{T},$$

which we can put in the form

$$(IV.5)\quad x(t) = \sum_{n=-\infty}^{+\infty} \left[\frac{A_n}{2T} \cos 2\pi\nu_n t + \frac{B_n}{2T} \sin 2\pi\nu_n t \right],$$

the coefficients A_n and B_n being given by the expression

$$A_n = \int_0^T x(t) \cos 2\pi\nu_n t \, dt = C_n \cos \varphi_n$$

and

$$B_n = \int_0^T x(t) \sin 2\pi\nu_n t \, dt = C_n \sin \varphi_n.$$

The quantities C_n and φ_n or A_n and B_n are pairs of random coefficients attached to each oscillogram. They are such that

$$(IV.6)\quad \overline{A_n} = 0, \quad \overline{B_n} = 0 \quad \text{and} \quad \overline{A_n^2} = \overline{B_n^2} = \overline{C_n^2}/2.$$

The noise $X(\nu)$ in the spectrum, calculated from the interferogram $I'(t)$, is given by the expression

$$(IV.7)\quad X(\nu) = T_{\cos}[x(t)].$$

It is the cosine transform of a function $x(t)$ which can be considered a sum of sine waves of absolutely arbitrary frequencies ν_n and phases φ_n. To each sine wave there corresponds in the spectrum, the F.T. of the noise oscillogram, a line which is the convolution of the Dirac function, of height $C_n/2T$, with the apparatus-function corresponding to the phase displacement φ_n. Depending on the phase φ_n of the

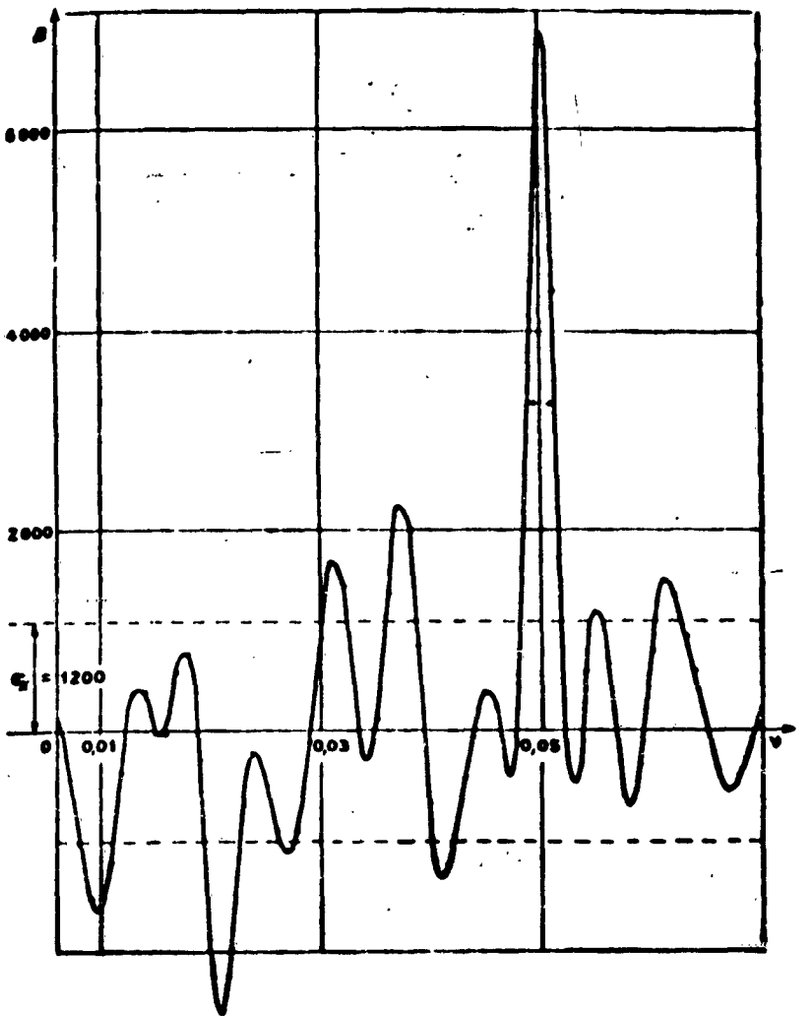

Fig. 38. Spectrum Obtained From the Interferogram I'(t).

corresponding sine wave in x(t), the apparatus-function will have one or the other of the shapes represented in Fig. 30. X(ν) is therefore a random function whose radius of correlation is of the order of 1/T, the width of the apparatus-function (Fig. 38)[8].

[8] this when one has made an apodization. Without apodization the radius of correlation of the noise is effectively divided by 2.

3. STUDY OF VARIANCE AND S/N RATIO IN THE INTERFEROGRAM AND SPECTRUM

We shall call the ratio s/n in the interferogram, $(s/n)_I$ for a line of frequency ν_1, the ratio of the amplitude β of the corresponding sine wave in the interferogram to the mean square error σ_x of the fluctuations of the interferogram.

$$\text{(IV.8)} \qquad \sigma_x = \sqrt{\overline{x^2(t)}}, \qquad (s/n)_I = \beta/\sigma_x.$$

β depends only on the luminance of the source, upon the width of the beam and upon the detector used; it is independent of the recording speed.

To calculate the s/n ratio in the spectrum, we are going to distinguish two cases, according to whether the spectrum is obtained simply by making the cosine transform of a symmetric interferogram recorded for δ varying from 0 to L during the time T or by making the complete Fourier transform of an interferogram recorded from - L to + L during the same time T.

(1) Case Where the Fourier Transform is Made by Adjusting the Zero Point

We have seen in Chapter 2 that the height of the corresponding line in the spectrum was $q\beta T$, q being a numerical factor, the mean value of the apodizing function A(t). It equals 1 when there is no apodization, 0.5 with the weighting function A_1 and 0.53 with the weighting function A_2. We shall call the signal/noise ratio in the computed spectrum the ratio $(s/n)_s$, which is the ratio of the theoretical height of the line, calculated from a sine wave of amplitude β in the interferogram, to the mean square error $\sigma_{\chi(1)}$ of the fluctuations in the computed spectrum.

$$\text{(IV.9)} \quad \sigma_{\lambda(1)} = \sqrt{\overline{\lambda_1^2(\nu)}} \quad \text{and} \quad (s/n)_s = q\beta T/\sigma_{\chi(1)}.$$

The signal thus defined in the spectrum increases proportionately with the duration T of the measurement; we are going to show that $\sigma_{X(1)}$ increases proportionately as the square root of T, hence that the s/n ratio varies also as $\sqrt{T}$.

A. CALCULATION OF VARIANCE IN THE SPECTRUM. The fluctuations due to noise in the neighborhood of the frequency ν_1 in the reconstructed spectrum have the form

$$X(\nu_1) = 2 \int_0^T x(t)\, A(t) \cos 2\pi\nu_1 t \, dt. \qquad \text{(IV.10)}$$

From this one deduces that

$$\sigma^2_{X(1)} = 4 \int_0^T \int_0^T x(t)x(t')\, A(t)A(t') \cos 2\pi\nu_1 t \cos 2\pi\nu_1 t' \, dt \, dt'$$

and, noticing that in this expression only x(t) and x(t') are random variables

$$\sigma_{X(1)} = 4 \int_0^T \int_0^T \overline{x(t)x(t')}\, A(t)A(t') \cos 2\pi\nu_1 t \cos 2\pi\nu_1 t' \, dt \, dt'. \qquad \text{(IV.11)}$$

The function $\overline{x(t)x(t')}$ is the autocorrelation function of the noise in the interferogram. Its study rests entirely on a theorem of Khinchin: the cosine transform of the autocorrelation function of a stationary random variable of order <u>two</u> is its power spectrum. It follows that

$$\rho(\theta) = \overline{x(t)x(t')} = \int_{-\infty}^{+\infty} \Phi_p(\nu) \cos 2\pi\nu\theta \, d\nu, \text{ with } \theta = t - t' \text{ and}$$

$$\Phi_p(\nu) = \int_{-\infty}^{+\infty} \rho(\theta) \cos 2\pi\nu\theta \, d\theta, \qquad \text{(IV.12)}$$

$\mathfrak{B}_p(\nu)$ being the even part of the power spectrum $\mathfrak{B}(\nu)$ of the noise contained in the interferogram (Fig. 35).

From Eqs. (IV.12) one gets immediately the expressions giving the density of noise and the variance of noise in the interferogram:

$$(IV.13) \quad \mathfrak{B}_p(0) = \int_{-\infty}^{+\infty} \rho(\theta)\, d\theta \text{ and } \sigma_x^2 = \rho(0) = \int_{-\infty}^{+\infty} \mathfrak{B}_p(\nu)\, d\nu.$$

Replacing $\rho(0)$ in expression (IV.11), we get

$$\sigma^2_{X(1)} = 4 \int_{-\infty}^{+\infty} \mathfrak{B}_p(\nu)\, d\nu \int_0^T\!\!\int_0^T A(t)A(t') \cos 2\pi\nu_1 t \cos 2\pi\nu_1 t' \, [\cos 2\pi\nu t \cos 2\pi\nu t' + \sin 2\pi\nu t \sin 2\pi\nu t']\, dt\, dt'.$$

After expanding and collecting, the variance can be written

$$(IV.14) \quad \sigma^2_{X(1)} = \frac{1}{4} \int_{-\infty}^{+\infty} \mathfrak{B}_p(\nu) \, [f^2(\nu_1-\nu) + k^2(\nu_1-\nu) + f^2(\nu_1+\nu) + k^2(\nu_1+\nu)]\, d\nu,$$

$f(\nu)$ and $k(\nu)$ being the apparatus functions in cosines and sines defined in the preceding chapter. When the interferogram has been recorded through a filter, the spectrum $\mathfrak{B}(\nu)$ of the noise that it contains is not constant as a function of the frequency. But one can consider $\mathfrak{B}(\nu)$ as constant and equal to $\mathfrak{B}(\nu_1)$ in a frequency interval which is large with respect to the size of the function $f^2(\nu)$ and $k^2(\nu)$. Moreover,

$$(IV.15) \quad \int_{-\infty}^{+\infty} f^2(\nu)\, d\nu = \int_{-\infty}^{+\infty} k^2(\nu)\, d\nu = \int_{-\infty}^{+\infty} A^2(t)\, dt,$$

whence the new expression of the variance

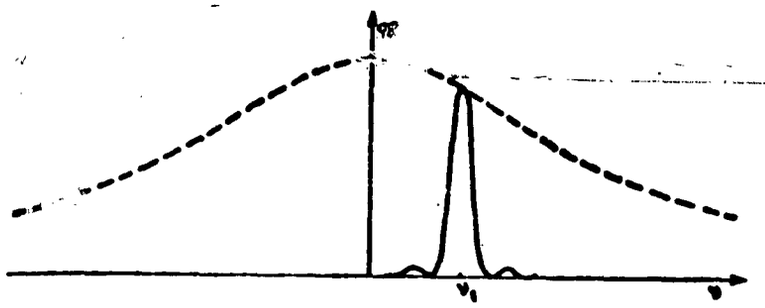

Fig. 39. Square of the Apparatus-Function Exploring the Noise Spectrum.

$$\sigma^2_{\chi(1)} = \mathcal{B}_p(\nu_1) \int_{-\infty}^{+\infty} f^2(\nu_1-\nu)\, d\nu. \tag{IV.16}$$

Replacing $f^2(\nu_1-\nu)$ by $f_0^2 f'^2(\nu_1-\nu)$ [see (II.7)], we get

$$\sigma^2_{\chi(1)} = \mathcal{B}_p(\nu_1)\, f_0^2 \int_{-\infty}^{+\infty} f'^2(\nu_1-\nu)\, d\nu \tag{IV.17}$$

$$= \tfrac{1}{2}\, \mathcal{B}(\nu_1)\, f_0^2 \int_{-\infty}^{+\infty} f'^2(\nu_1-\nu)\, d\nu,$$

a result which may be stated thus (Fig. 39): the mean power of the noise in the spectrum is, within a factor of $\frac{1}{2} f_0^2$, the chopped energy in the power spectrum of the noise contained in the interferogram times the square of the normalized apparatus-function centered about ν_1. The factor 1/2 comes from the fact that the F.T. made under the conditions considered above is a synchronous detection and one finds the usual gain factor 1/2 each time a classic detection is replaced by a synchronous detection [49]. Indeed, we have seen that noise in the interferogram can be put in the form of a sum of even terms and odd terms. When the cosine transform is made one detects only the even terms.

According to (IV.15) the term $\int_{-\infty}^{+\infty} f^2(\nu)\, d\nu$ can be put in the form

$$\int_{-\infty}^{+\infty} f^2(\nu)\, d\nu = 2\, Q\, T\ ,$$

Q being the mean value of the square of the apodizing function:

$$Q = \frac{1}{2T} \int_{-T}^{+T} A^2(t)\, dt\ .$$

This is a numerical factor which is equal to 1 when there is no apodizing, 0.33 when the interferogram is weighted by a triangle function A_1 and 0.406 with the weighting function A_2; (IV.16) then becomes

(IV.18) $$\sigma^2_{\lambda(1)} = 2\, Q\, \mathfrak{B}_p(\nu_1)\, T = Q\, \mathfrak{B}(\nu_1)\, T\ .$$

We shall see in the following chapter that the filter $\mathcal{T}$ is always chosen in such a way that the spectrum of the signal under consideration is in a region where one can as a first approximation identify $\mathfrak{B}(\nu_1)$ with $\mathfrak{B}(0)$ (noise density), in order not to have excessive phase displacement of the signal; under these conditions σ_χ can, whatever the frequency considered, be put in the form

(IV.19) $$\sigma_\chi = \sqrt{Q}\ \sqrt{\mathfrak{B}(0)}\ \sqrt{T}\ .$$

The noise density $\mathfrak{B}(0)$ is a quantity which depends only on the detector used. When one changes the recording speed it is necessary, of course, to modify the time constant of the low-pass filter but, when doing this, one modifies only the width of the band pass of the filter and not $\mathfrak{B}(0)$ (Fig. 40). The spectrum (IV.9) then becomes

(IV.20) $$(s/n)_s = \frac{q\beta T}{\sqrt{Q\mathfrak{B}(0)T}} = \beta\, \frac{q}{\sqrt{Q}}\, \frac{1}{\sqrt{\mathfrak{B}(0)}}\, \sqrt{T}\ .$$

The numerical factor $q/\sqrt{Q}$, which is the result of dividing the mean value of the weighting function by the square root

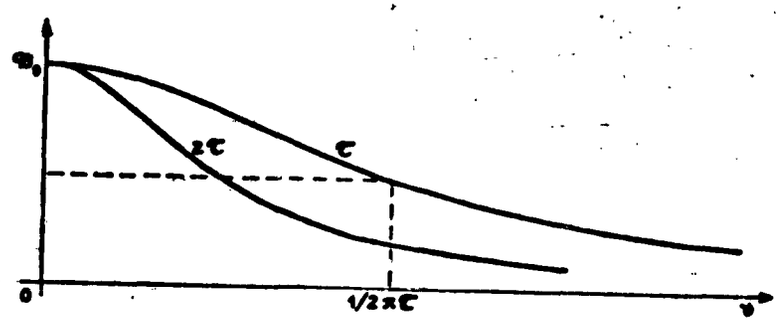

Fig. 40. Noise Spectrum for Two Values of the Time Constant.

of the mean value of the square of this weighting function, is equal to 1 when there is no apodizing, 0.87 with the triangle weighting, and 0.84 with weighting by the function A_2.

B. DISCUSSION OF THE RESULTS. From Eq. (IV.20) giving the expression for the s/n ratio in the spectrum, we can draw three important conclusions:

a. When, by the Fourier transform method, one wishes to treat a given problem with a given resolution, the s/n ratio in the reproduced spectrum varies as the square root of duration of measurement. Thus one meets again an absolutely general result, common to every method. By making the comparison between the coefficients of proportionality in the Fourier transform method with those of classical methods that one can prove the superiority of one of the processes over the others.

Let us suppose that one wishes to record with a classical instrument the monchromatic line of negligible width which will give a sine wave of amplitude β in the interferogram. We assume that the instrument has the same extent as the interferometer used as a spectrometer, that the transmission factors

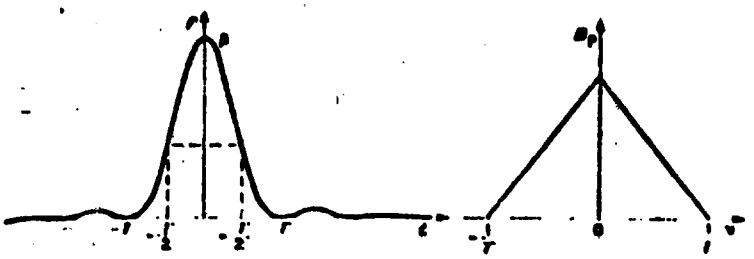

Fig. 41. Signal Recorded by a Grating Spectrometer.

Fig. 42. Spectrum of the Electrical Frequencies Contained in the Recorded Signal.

of the two apparatuses are the same[10], that the two measurements are made with the same detector and that the resolution is the same in both cases. Under these conditions, the signal recorded as a function of time reproduces the apparatus-function. The maximum will have β as its height. Let us suppose that we have taken a time T to record a spectral interval equal to the limit of resolution, that is to say equal to the width of the apparatus-function. In Fig. 41 we show the apparatus-function of a grating spectrometer. The frequency spectrum of the electric signal thus recorded is the cosine transform of it; it extends from $-1/T$ to $+1/T$ (Fig. 42). The ideal filter to use for recording under these conditions is a low-pass rectangular filter having a modulus of gain equal to 1 for ν taken between $-1/T$ and $+1/T$ and the power spectrum $\Phi(\nu)$ of the

[10] In order that the transmittance be equal to one, with the Michelson interferometer one must use the exit beam as described herein and the reflected beam which is sent back in the direction of the source. It suffices then to receive the two beams on a cell and to take the difference of the two electrical signals [16].

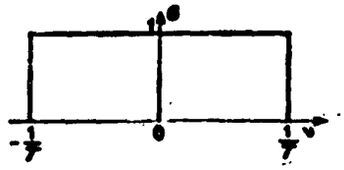

Fig. 43. Ideal Filter for Use With a Grating Spectrometer.

fluctuations in the spectrum is thus determined (Fig. 43). In fact one cannot make a filter whose gain curve is that of Fig. 44 (curve a). One can use a real filter having the same area (Fig. 44, curve b) and the power of the noise in the spectrum stays the same even though its structure may be different. In both cases the variance in the spectrum equals

$$(IV.21) \quad \sigma_X^2 = \int_{-\infty}^{+\infty} \mathfrak{B}_p(\nu)\, d\nu = \int_{-1/T}^{+1/T} \mathfrak{B}_p(0)\, d\nu$$

$$= \frac{2\mathfrak{B}_p(0)}{T} = \frac{\mathfrak{B}(0)}{T} .$$

The s/n ratio in the recording then takes the form $s/n = \beta(1/\sqrt{\mathfrak{B}(0)})\sqrt{T}$. This expression is exactly equal to that giving the s/n ratio in the computed spectrum using the Fourier transform method without apodizing (IV.19). Thus if it is a question of studying a single spectral element, the classical methods and the Fourier transformation method give the same result.

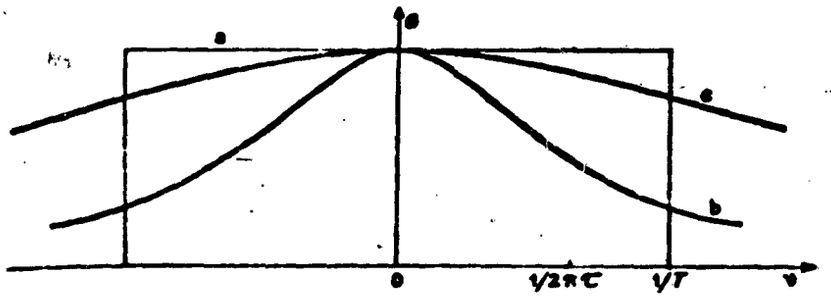

Fig. 44. (a) Theoretical Gain Curve; (b) Gain Curve of a Real Filter Having the Same Area as the Theoretical Filter $\tau = 1/4\ T$; (c) Gain Curve of the Filter Used.

Notice that, with the real filter mentioned above, the high frequencies in a spectrum undergo inadmissible attenuation and phase displacement. In practice, in order that the attenuation and phase displacement of the high frequencies do not exceed a certain amount which has been fixed in advance, one uses a filter with a band pass which is much larger (Fig. 44, curve c). Then the power of the noise in the spectrum is higher, but one can perform a smoothing operation on the spectrum and for all intents and purposes find the same results as before.

When the classical spectrometer used is not a grating spectrometer, the spectrum of the frequencies is no longer necessarily zero for frequencies above 1/T but, the recording time of a spectral element always being T, the maximal frequency of the electrical signal that one may transmit without deformation is always of the order of 1/T and the preceding considerations remain valid.

Let us now suppose that we wish to study a spectrum containing M spectral elements. If one wishes to keep the same s/n ratio by the classical method, the duration of the measurement will become MT. But for a total duration of measurement equal to MT, the s/n ratio in the spectrum obtained by a Fourier transformation, according to (IV.19), $s/n = \beta (1/\sqrt{\mathfrak{B}(0)}\sqrt{MT}$. Hence we see the gain of $\sqrt{M}$ in the s/n ratio that the Fourier transform method permits one to obtain with respect to classical methods in the study of a problem with a given resolution and a given duration of time.

b. The s/n ratio in the spectrum is independent of the time constant of the filter through which one has recorded the interferogram. This is a result to be compared with the fact that in the classical methods the precision of the measurement, but not the s/n ratio, is independent of the time constant which has been used to record the spectrum.

c. For a measurement time equal to T, the s/n ratio in the spectrum varies with the type of apparatus-function chosen. It is maximum when no apodizing has been done. It is lower by a factor 0.87 when the weighting function is a triangle function and by 0.84 when it is the function A_2. Weighting the interferogram improves the shape of the apparatus-function but brings about some losses in resolution and s/n ratio. This weakening in the s/n ratio is moreover, slightly lower than what one gets in optics by using absorbing apodizers in the presence of photon noise and à fortiori in the presence of detector noise. The simple argument which consists in saying that in the case of numerical apodizing used on an interferogram, one does not diminish the s/n ratio because the signal and the noise are divided by the same factor or because the number of photons received is not diminished, is therefore not correct.

C. CALCULATION OF $\mathcal{R}$, RESULT OF DIVIDING THE S/N RATIO IN THE SPECTRUM BY THE S/N RATIO IN THE INTERFEROGRAM. $\mathcal{R}$, the ratio of $(s/n)_s$ to $(s/n)_I$, can be put into different equivalent forms which we shall discuss. In general

$$\mathcal{R} = \frac{q\beta T}{\sigma_\chi} \frac{\sigma_x}{\beta} = q \frac{\sigma_x}{\sigma_\chi} T. \qquad \text{(IV.22)}$$

Theoretically, the interferogram could have been recorded without a time constant, without the s/n ratio in the calculated spectrum varying. Under these conditions, the mean square error σ_x of the fluctuations in the interferogram will be infinite and $\mathcal{R}$ will also be infinite. In practice the interferogram is always recorded through filters, and now we are going to show that the quotient σ_x/σ_χ is nearly proportional to the inverse of the square root of the time constant of the filter used.

If the low-pass filter is an RC filter, the variance in the spectrum in the neighborhood of the frequency $\nu = 0$ has the form

(IV.22b) $$\sigma^2_{X(0)} = 2\,Q\,T\,\mathcal{P}_p(0).$$

The variance of the interferogram is given by

$$\sigma^2_x = \mathcal{P}_p(0) \int_{-\infty}^{+\infty} \frac{1}{1+(2\pi\nu\tau)^2}\,d\nu = \frac{\mathcal{P}_p(0)}{2\tau},$$

whence[11]

(IV.23) $$\sigma^2_{X(0)} = 4\,Q\,T\,\tau\,\sigma^2_x$$

---

[11] There is a very simple way to arrive at this result directly without using relations (IV.14) and (IV.17) which bring in the convolution of the noise spectrum with the square of the apparatus-function. Although the calculation is simpler using this procedure, the first way of looking at the problem is still very useful in order to understand it physically and to treat the case of noise in the numerical F.T., as will be done at the beginning of the following chapter.

The functions $y(t)$ and $X(\nu)$, being reciprocal F.T., are related in the following way

(IV.24) $$\int_0^\infty y^2(t)\,dt = \int_0^\infty X^2(\nu)\,d\nu .$$

In our problem, the noise interferogram has been weighted by the function $A(t)$ in such a way that $y(t) = x(t)\,A(t)$, $x(t)$ being the noise in the interferogram. The fluctuations $X(\nu)$ in the spectrum obtained from the recorded interferogram with the filter of gain $G(\nu)$ are related to those that one would have in the spectrum obtained from an interferogram recorded without the filter $Y(\nu)$ by relation

(cont. on following page)

and so we have

$$\mathcal{R} = \frac{1}{2} \frac{Q}{\sqrt{Q}} \sqrt{\frac{T}{\tau}}.$$

The variance in the spectrum in the neighborhood of frequency ν_1 has the form

$$\sigma^2_{X(1)} = 2\,Q\,T\,\mathcal{P}_p(\nu_1) = \sigma^2_{X(0)}\,\mathcal{P}_p(\nu_1)/\mathcal{P}_p(0),$$

which we can also write as

$$\sigma^2_{X(1)} = \frac{1}{1+(2\pi\nu_1\tau)^2}\,\sigma^2_{X(0)}.$$

(11,cont)

$$\int_0^\infty |X(\nu)|^2\,d\nu = \int_0^\infty |Y(\nu)|^2\,|G(\nu)|^2\,d\nu.$$

Hence (IV.24) may be written

$$\text{(IV.25)}\quad \int_0^\infty x^2(t)\,A^2(t)\,dt = \int_0^\infty |X(\nu)|^2\,|G(\nu)|^2\,d\nu.$$

Let σ^2_x be the variance in the interferogram and σ^2_X the variance in the spectrum in the neighborhood of the zero frequency. Noticing that $A^2(t)$ and $|G(\nu)|^2$ are quantities which vary very slowly compared with $x^2(t)$ and $Y^2(\nu)$ the relation (IV.25) becomes

$$\text{(IV.26)}\quad \sigma^2_x \int_0^\infty A^2(t)dt = \sigma^2_X \int_0^\infty |G(\nu)|^2\,d\nu = \sigma^2_{X(0)} \int_0^\infty |G(\nu)|^2 d\nu,$$

since the filter considered has used unit gain at the zero frequency.

Calling Q the mean value of the square of the apodizing function and replacing $|G(\nu)|^2$ by its value $1/|1+(2\pi\nu\tau)^2|$, one concludes $Q\,T\,\sigma^2_x = \sigma^2_{X(0)}/4\tau$, whence $\sigma^2_{X(0)} = 4\,Q\,T\,\tau\,\sigma^2_x$, an expression equivalent to (IV.23).

The expression

(IV.23b) $$\sigma^2_{X(1)} = \frac{4\,Q\,T\,\tau}{1+(2\pi\nu_1\tau)^2}\,\sigma^2_X$$

allows one to calculate the variance in the spectrum in the neighborhood of any frequency whatsoever as a function of the variance in the interferogram.

The ratio $\mathcal{R}$ varies as the square root of the ratio of the duration of measurement to the time constant of the filter τ. It suffices to increase T in order to make it as large as one wants. Let us take the case where the F.T. is made without apodizing: $q/\sqrt{Q}$ then equals 1 and $\mathcal{R} = 0.5\sqrt{T/\tau}$; if $T = 4 \times 10^4\tau$ (which results in an interferogram recording lasting three hours if the time constant used is τ = 1 sec), $\mathcal{R}$ = 100. We deduce from this that in order to have the s/n = 2 in the calculated spectrum it is enough that the s/n ratio in the interferogram by 1/50. The corresponding sine wave will be totally invisible in the noise. Hence one must be careful not to stop recording the interferograms when one no longer sees fringes and when one has the impression of recording only noise.

D. EXPERIMENTAL VERIFICATIONS. Our experimental verifications have been concerned with three precise points. By means of a synchronous detection amplifier and low-pass filter, described previously, we have recorded the fluctuation of a lead sulfide cell. We calculated the correlation function of the fluctuations $x(t)$ and their spectrum by making the cosine transform of the autocorrelation function. Then we composed a synthetic interferogram by adding a sine wave of known period and amplitude to the noise under consideration and we made the F.T. of this interferogram. Thus we have been able to verify the agreement between the predicted s/n and the s/n measured in the spectrum, as well as the variation $\mathcal{R}$ with the s/n ratio when one passes from the interferogram to the spectrum.

a. Correlation Function and Noise Spectrum in the Interferogram. We wish to verify that no other sources of noise have been introduced other than those considered and that we would be able to calculate G from the expression that we had when the interferogram was recorded through an RC filter. We chose $\tau = 2$ sec (Fig. 37a). The recorded fluctuations have a mean square error $\sigma_x = 37.5$ u, u being the value of an arbitrary unit which serves to measure the deviations on the recording (here millimeters). The correlation function was computed by the IBM-704 calculator[12].

If the recording time of x(t) were infinite, its autocorrelation function $\rho(\theta)$ would have the form $\exp(-t/\tau)$ (Fig. 46, curve a). Since the recording time is limited, $\rho(\theta)$ is slightly different from $\exp(-t/\tau)$ and the error increases as

[12] It is possible to calculate the autocorrelation function of a function f(x) which is known to have a bounded frequency spectrum of width $\Delta\nu$ using equidistant discrete values of this function. It is sufficient to choose the distance h between two points in such a way that the repetition frequency $1/2h$ of the spectrum of the frequencies of the new function thus defined, is equal to or greater than $2\Delta\nu$. If the frequency spectrum of f(x) is not bounded, the approximation with which one calculates its autocorrelation function by this method is better the smaller h is. The complete discussion of this question is similar to the one that will be made in the following chapter to determine the distance h between two points picked from the interferogram in order to have the maximum s/n ratio when one makes a numerical F.T. Figure 45 shows a function f(x) and its autocorrelation function Cf(x) computed numerically using discrete values of f(x). There is perfect agreement between the calculated and predicted Cf(x).

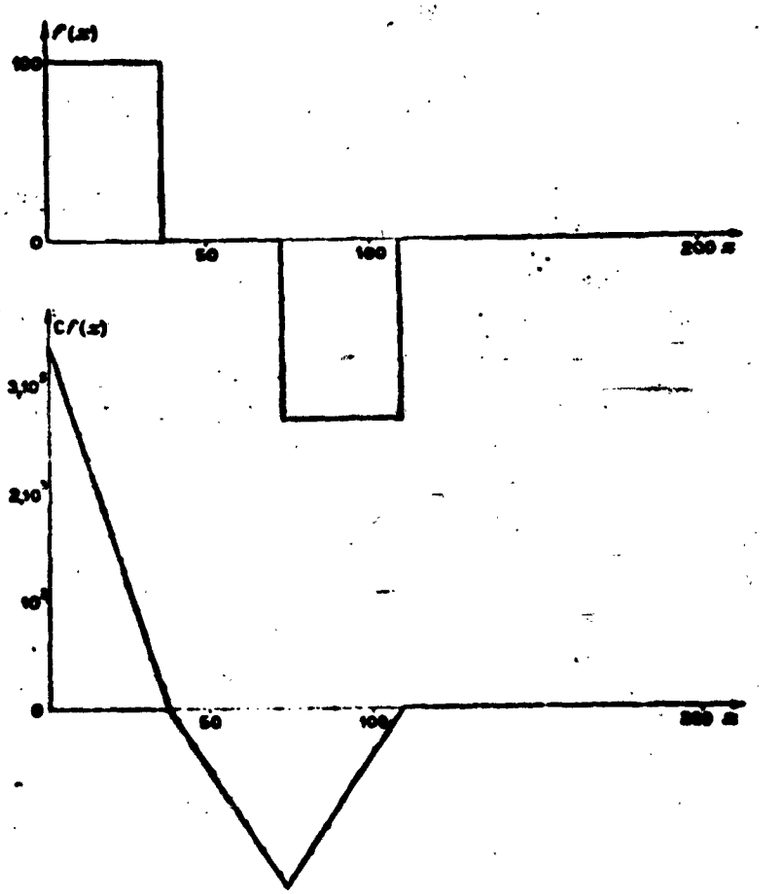

Fig. 45. Illustrating the Calculation of the Autocorrelation Function Cf(x) of a Function f(x).

T/τ decreases. Curves b and c of Fig. 46 show $\rho(\theta)$ for T/τ = 90 and T/τ = 180. The fluctuations are considerably reduced in the second case, as predicted. The cosine transform of $\rho(\theta)$ gives the power spectrum of the noise x(t) (Fig. 47, curve b). It departs little from the theoretical curve (Fig. 47, curve a).

b. S/N Ratio in the Calculated Spectrum. We made up a theoretical interferogram I'(t) (Fig. 37c) formed from the superposition of the portion of the noise x(t) such that T/τ = 180--this was considered earlier--and of a sine wave

$$I(t) = 37 \cos 2\pi\, 0.05t \qquad \text{(Fig. 37b)}.$$

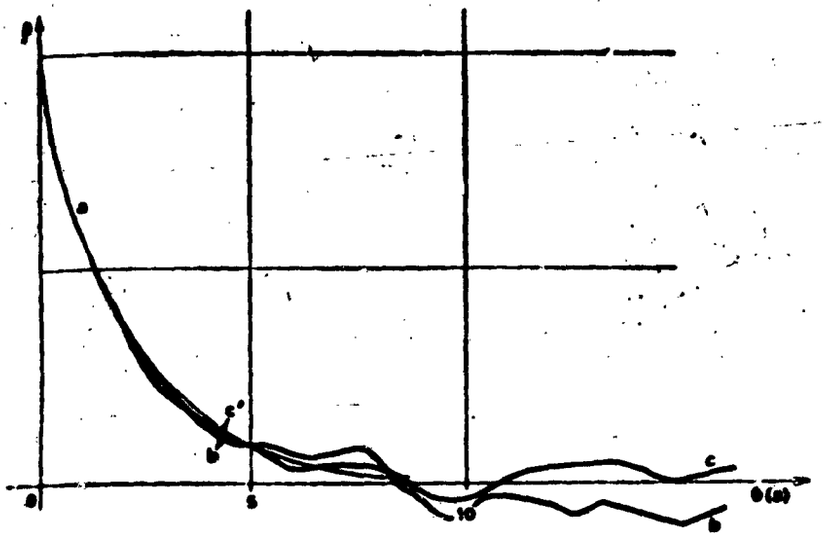

Fig. 46. Autocorrelation Function of the Noise in the Interferogram.

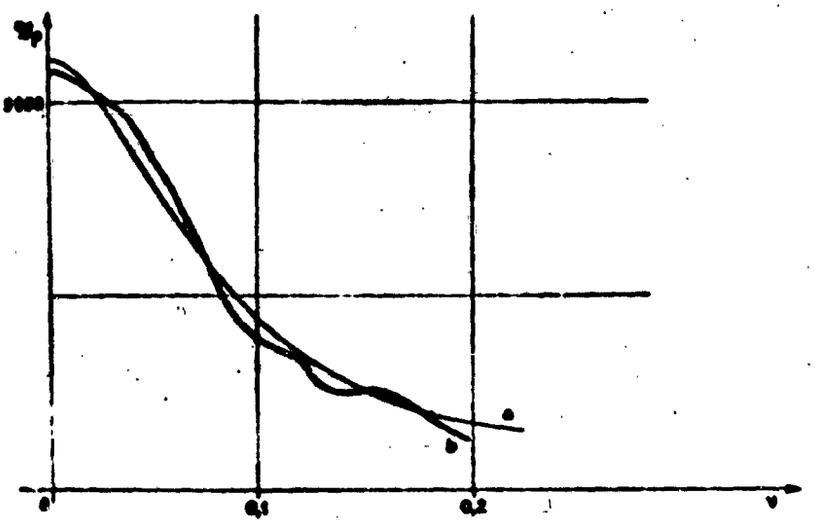

Fig. 47. Noise Power Spectrum in the Interferogram.

Under these conditions the s/n ratio in the interferogram equals 1 and it is practically impossible to distinguish which of the two graphs 37a or 37c is pure noise.

The spectrum $B_p(\nu)$ of I'(t) has been numerically calculated by choosing $h = 1.2$ (Fig. 38). We shall see in the following chapter that the s/n ratio in the calculated spectrum is then 98/100 of the maximum s/n ratio that would have been obtained by using every value of I'(t). The formula (IV.20) permits the prediction of $(s/n)_s$. According to Fig. 47,

$$\mathfrak{w}_p(0.05) = 4{,}950 \text{ u}^2\text{sec}, \text{ where } (s/n)_s = 37 \times 0.84 \times$$

$$\times \frac{1}{\sqrt{2 \times 4{,}950}} \sqrt{360} = 5.91.$$

The s/n ratio measured ~~in the~~ spectrum equals 6.4. It has been obtained by taking the ratio of the measured height of the line at $\nu = 0.1$ to the mean square error of the fluctuations in the spectrum. This mean square error is the mean value of the square of the fluctuations in the neighborhood of $\nu = 0.1$. The noise sample has been chosen sufficiently long so that $\overline{X(\nu)} = 0$. Under these conditions the calculated σ_X equals 1,200 u sec. Notice that the formula (IV.19) allows one to predict

$$\sigma_X = \sqrt{0.406 \times 2 \times 4{,}950 \times 360} = 1{,}200 \text{ u sec}$$

The theoretical signal has the value

$$s = q\,\beta\,T = 0.53 \times 37 \times 360 = 7{,}059.6 \text{ u sec}$$

It is probable that the measured s/n ratio lies between the two limits $(s + \sigma_X)\,\sigma_X = 6.8$ and $(s - \sigma_X)/\sigma_X = 4.9$. We found it equal to 6.4.

c. Variation in S/N Ratio in Passing From the Interferogram to the Spectrum. The s/n ratio in the interferogram being equal to 1, the measured value of $\mathcal{A}$ is equal to 6.4. Its theoretical value can be calculated using formula (IV.22) which gives

$$\mathcal{A} = 0.53 \times \frac{37.5}{1,200} \times 360 = 5.905.$$

(2) Case Where the Fourier Transform is Made Without Locating the Zero

We showed (§III.2(3)C) that it was possible to reconstruct the spectrum without knowing the zero point of the interferogram. It is enough to record the interferogram for δ varying between - L and + L and to take the square root of the sum of the squares of the sine transform and the cosine transform, in other words to make the complete F.T. We propose to study the signal/noise ratio in the computed spectrum by this method and to compare the results with those obtained in the case where only the cosine transform is used. When one takes squares, one introduces nonlinear elements and one can predict that it will not be sufficient to consider separately the F.T. of the interferogram without noise and the F.T. of the noise; there will be signal-noise interaction.

We shall suppose that in the two cases the measurement has lasted the same total time T. In the absence of noise the two methods are strictly equivalent. But the study of the signal-noise ensemble is much more complex when one takes a complete F.T.

In the first place, the noise in the calculated spectrum has a Gaussian distribution. Its mean value is zero. We have called "signal" the height s of a line obtained in the absence of noise taken from a particular interferogram. We designate by ρ the variance σ_x^2 in the spectrum in the presence of noise (a quantity that one can measure in a spectrum by making the

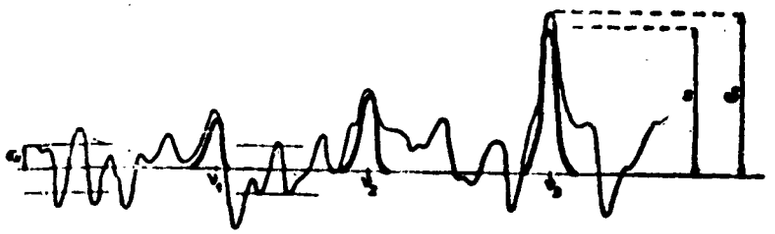

Fig. 48. Appearance of a Spectrum Calculated by Taking the Cosine Transform of an Interferogram in Which the Zero Point Has Been Located.

mean square of the fluctuations in a region where there is no line.) (Fig. 48). There is a definite probability P that the number $\mathcal{S}$ measuring the height of the line lies between the $s + \sqrt{\rho}$ and $s - \sqrt{\rho}$, for any s. In other words, the operation is perfectly linear and the mean square error of the fluctuations in the spectrum is independent of the signal. Figure 51 shows the variation $\mathcal{S}/\sqrt{\rho}$ as a function of $s/\sqrt{\rho}$. Curve a represents the mean value of the signal $\mathcal{S}/\sqrt{\rho} = s/\sqrt{\rho}$. The curves a', $\mathcal{S}/\sqrt{\rho} = (s/\sqrt{\rho}) + 1$, and a", $\mathcal{S}/\sqrt{\rho} = (s/\sqrt{\rho}) - 1$, mark the two limits between which there is the probability P of finding the value of the measured signal divided by $\sqrt{\rho}$. We have called the signal/noise ratio s/n the quotient $s/\sqrt{\rho}$.

If the complete Fourier transform is taken, the results are different; in order to compare the two methods more easily, we are going to express the quantities that we shall call signal and noise in this case as a function of s and ρ. Being given the signal-noise interaction, one cannot, when making the complete Fourier transform, deal with the noise alone and then with the signal-noise ensemble. It is necessary to treat the signal and the noise together and from them to deduce what happens in those regions of the spectrum where the signal is zero. Here are the principal results that we put in evidence:

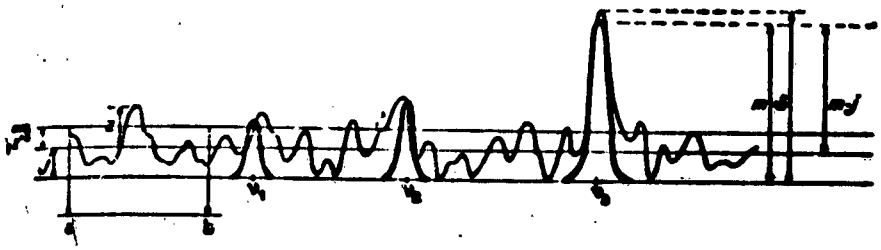

Fig. 49. Spectrum Calculated by Taking the Complete F.T. of the Same Interferogram as in Fig. 48, but in Which the Zero Point Has Not Been Located.

1°. In regions of the spectrum where there is no line (Fig. 49, section ab), the noise is a random function $J(\nu)$ that one can consider as the superposition of a constant nonzero component $\overline{J(\nu)} = j$ and of a fluctuating part $z'(\nu)$ of mean value zero $\overline{z'(\nu)} = 0$ and of mean square value $\overline{z'^2(\nu)}$;

2°. The number $\mathcal{S}$ measuring the height of a line in the reproduced spectrum no longer will be simply a number taken between s + a and s - a, a being a mean square error to be determined. Each value $\mathcal{S}$ can always be put in the form

$$\mathcal{S} = m + z \,, \tag{IV.27}$$

m being the mean value of $\mathcal{S}$ and z being a random function of mean value zero. But the important fact is that m no longer is equal to s and, moreover, is a function of ρ. On the other hand, $\overline{z^2}$ is likewise a function of s; the mean value m becomes an approximately linear function of s when $s/\sqrt{\rho} \gg 1$.

Let us state the meaning of m. If one calculates an infinity of spectra using an infinity of interferograms recorded under the same conditions (constituting an infinity of experiments belonging to a single category), the numbers $\mathcal{S}$ measuring the signal corresponding to a certain frequency ν_1 in each spectrum group themselves about the value m, mathematical expectation of $\mathcal{S}$, i.e., $E\{\mathcal{S}\} = m$.

We shall call "signal" in the case of the complete F.T., the difference $m - j$, i.e., the height of the line above the mean value of the noise (Fig. 49) because it is effectively this quantity which will be accessible to the experimenter. The signal/noise ratio in the calculated spectrum is measured by the quotient $(m - j)/\sqrt{\overline{z'^2}}$.

A. STUDY OF THE SIGNAL-NOISE ENSEMBLE. We shall study the signal-noise ensemble at each stage of the reproduction of the spectrum by assuming that the sine wave in the interferogram corresponding to the frequency under consideration has a displacement ψ_0 with respect to the origin, as was assumed in the preceding chapter. The final result clearly ought not to depend on ψ_0. We shall then study successively the results of the cosine transform of the interferogram, of its sine transform, and of the square root of sum of the squares of these two transforms.

a. Cosine Transform. The height of the line resulting from the cosine transform of the interferogram, if there is no noise, will be (§II.2(3)C)

$$s_c = s \cos \psi_0. \tag{IV.28}$$

The corresponding value of a claculated spectrum s_c can be put in the form

$$\mathcal{S}_c = s \cos \psi_0 + X(\nu_1). \tag{IV.29}$$

We have seen before that the noise recorded on the interferogram can be considered as a superposition of sine waves of random amplitude and phase and, we can write that the noise component at the frequency ν_1 has the form ([47] p. 351)

$$y(t) = \frac{C_1}{2T} \cos(2\pi\nu_1 t - \varphi)$$

$$= \frac{C_1}{2T} \cos\varphi \cos 2\pi\nu_1 t + \frac{C_1}{2T} \sin\varphi \sin 2\pi\nu_1 t,$$

in such a way that the result of the cosine transform of y(t) is written

$$X(\nu_1) = \mathcal{R} \cos \varphi.$$

This is a random variable whose characteristics, mean value and mean square error, are the same as those of the quantity $X(\nu)$, the cosine transform of x(t) for the different values of ν[13].

Then one has

(IV.30) $\overline{\mathcal{R} \cos \varphi} = 0$ and $\sigma^2_{X(1)} = \overline{\mathcal{R}^2 \cos^2 \varphi} = \overline{\mathcal{R}^2}/2 = \rho$.

Let us suppose that we can record an infinity of interferograms under the same conditions and that we plot on a graph the values $\mathcal{S}_c$ measured from each spectrum obtained from each interferogram. The curve joining these points will have the general shape shown in Fig. 50a. The values of $\mathcal{S}_c$ group themselves about the mean value s cos ψ_0, the mean square error of fluctuations being equal to $\sqrt{\rho}$.

b. Sine Transform. Obviously the results are analogous, and in the same way one can define

(IV.31) $$\mathcal{S}_s = s \sin \psi_0 + \mathcal{R} \sin \varphi,$$

with

$$\overline{\mathcal{R} \sin \varphi} = 0 \quad \text{and} \quad \overline{\mathcal{R}^2 \sin^2 \varphi} = \rho \qquad \text{(Fig. 50b)}.$$

[13] The means of $X(\nu_1)$ will be taken from an infinity of trials, i.e., an infinity of values $X(\nu_1)$ obtained by making the cosine transform of an infinity of interferograms recorded under the same conditions. One has the relation $\overline{X(\nu_1)} = \overline{X(\nu)} = 0$.

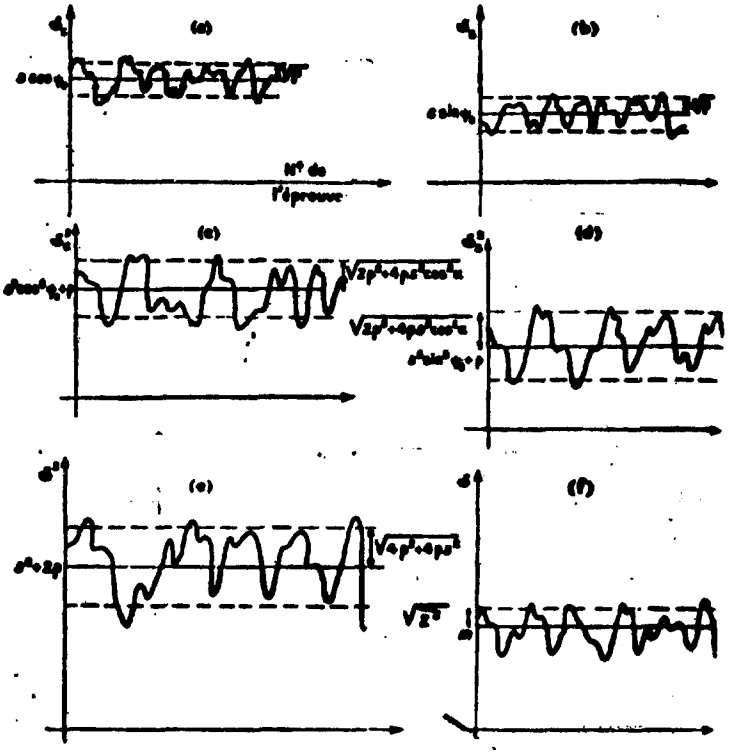

Fig. 50. Study of the Signal-Noise Ensemble When the F.T. is Taken Without Locating the Zero Point of the Interferogram.

The two random functions are $\mathcal{A}$ cos φ and $\mathcal{A}$ sin φ have the same mean value, same mean square error, same autocorrelation function, but their coefficient of correlation is zero[14].

[14] Their correlation function is also zero for a zero delay; but the variables $\mathcal{A}$ sin φ and $\mathcal{A}$ cos φ are not independent variables and their correlation function is different from zero for a delay which is not zero, which, however, doesn't happen in the present case.

c. Sum of the Squares of the Sine and Cosine Transform. The square of $\mathcal{S}_c$ has a constant component and a fluctuating component of mean value zero. The two quantities which are interesting to consider are the constant component which equals $\overline{\mathcal{S}_c^2}$ and the variance of the fluctuating part, i.e., $\overline{(\mathcal{S}_c^2 - \overline{\mathcal{S}_c^2})^2}$ (Fig. 50c):

$$\mathcal{S}_c^2 = s^2 \cos^2 \psi_0 + \mathcal{R}^2 \cos^2 \varphi + 2 s \mathcal{R} \cos \psi_0 \cos \varphi,$$

whence

$$\overline{\mathcal{S}_c^2} = s^2 \cos^2 \psi_0 + \rho. \tag{IV.32}$$

Thus the mean value of $\mathcal{S}_c^2$ depends not only on s and on ψ, but also on ρ, hence on the density $\mathfrak{D}_0$ of noise in the interferogram.

The fluctuating part has the value

$$\mathcal{S}_c^2 - \overline{\mathcal{S}_c^2} = \mathcal{R}^2 \cos^2 \varphi - \rho + 2 s \mathcal{R} \cos \psi_0 \cos \varphi.$$

Its variance is then

$$\overline{(\mathcal{S}_c^2 - \overline{\mathcal{S}_c^2})^2} = \overline{\mathcal{R}^4 \cos^4 \varphi} + \rho^2 + 4 s^2 \cos^2 \psi_0 \, \overline{\mathcal{R}^2 \cos^2 \varphi} - 2\rho \, \overline{\mathcal{R}^2 \cos^2 \varphi}. \tag{IV.33}$$

One can evaluate the term $\overline{\mathcal{R}^4 \cos^4 \varphi}$ using the following classical theorem.

If x(t) is a Laplacian stationary random function of mean value zero with autocorrelation function $C(\tau)$, i.e., such that $\overline{x^2} = C(0)$, the autocorrelation function of its square $x^2(t)$ can be written [51]

$$\overline{x^2(t)\, x^2(t-\tau)} = 2 C^2(\tau) + C^2(0).$$

From this one deduces that

$$\overline{x^4(t)} = 3 C^2(0).$$

In our case since $\overline{\mathcal{R}^2 \cos^2 \varphi} = \rho$, $\overline{\mathcal{R}^4 \cos^4 \varphi} = 3\rho^2$, (IV.33) takes the form

$$\overline{(\mathcal{J}_c^2 - \overline{\mathcal{J}_c^2})^2} = 2\rho^2 + 4\rho s^2 \cos^2 \psi_0. \qquad \text{(IV.34)}$$

The fluctuations will be the greater for greater ρ and also for higher signal. The relations (IV.32) and (IV.34) show the signal-noise interactions very well.

In the same way one calculates the constant component of $\mathcal{J}_s^2$ and the variance of its fluctuating component:

$$\overline{\mathcal{J}_s^2} = s^2 \sin^2 \psi_0 + \rho \text{ and} \qquad \text{(IV.35)}$$

$$\overline{(\mathcal{J}_s^2 - \overline{\mathcal{J}_s^2})^2} = 2\rho^2 + 4\rho s^2 \sin^2 \psi_0 \qquad \text{(Fig. 50d).}$$

In forming the sum $s^2 = \mathcal{J}_c^2 + \mathcal{J}_s^2$, the constant components are added together while the fluctuating components add their variances. Hence one has

$$\overline{\mathcal{J}^2} = s^2 + 2\rho \text{ and} \qquad \text{(IV.36)}$$

$$\overline{(\mathcal{J}^2 - \overline{\mathcal{J}^2})^2} = 4\rho^2 + 4\rho s^2 \qquad \text{(Fig. 50e).}$$

d. Calculation of $\mathcal{J}$. In the last stage of the calculation, the square root of $\mathcal{J}^2$ remains to be taken; we propose to determine the mean value of $\mathcal{J}$, say m and $\sqrt{z^2}$ the mean square error of the fluctuating component of $\mathcal{J}$ as functions of s and of ρ.

In order to determine these quantities, we are going to make use of the two relations (IV.36) in which we are going to replace $\mathcal{J}^2$ and $\overline{\mathcal{J}^2}$ by their values as functions of m and z

$$\overline{\mathcal{J}^2} = \overline{m^2 + 2mz + z^2} = m^2 + \overline{z^2} \qquad \text{(Fig. 50f)} \qquad \text{(IV.37)}$$

and according to (IV.36),

(IV.38) $$m^2 + \overline{z^2} = s^2 + 2\rho,$$

(IV.39) $$\overline{(\mathcal{S}^2 - \overline{\mathcal{S}^2})^2} = \overline{[\mathcal{S}^2 - (s^2 + 2\rho)]^2}$$

$$= \overline{\mathcal{S}^4 - 2\mathcal{S}^2(s^2+2\rho) + (s^2+2\rho)^2} = \overline{\mathcal{S}^4} - (s^2+2\rho)^2.$$

After replacing $\mathcal{S}$ by its value as a function of m and z we get

$$\overline{\mathcal{S}^4} = m^4 + 6\, m^2\, \overline{z^2} + \overline{z^4}.$$

We can substitute for m^4 and m^2 their values as functions of s and ρ taken from (IV.38) and notice that $\overline{z^4} = 3\,(\overline{z^2})^2$. The second equation (IV.36) can then be written

(IV.40) $$(\overline{z^2})^2 - \overline{z^2}(4\rho + 2s^2) + 2\rho^2 + 2\rho\, s^2 = 0,$$

from which one deduces

(IV.41) $$\overline{z^2} = 2\rho + s^2 - \sqrt{s^4 - 2\rho\, s^2 + 2\rho^2}$$

and

(IV.42) $$m = (s^4 + 2\rho\, s^2 + 2\rho^2)^{1/4}.$$

The results are gathered together in Fig. 51 (curves b, b', b") in which we represented $\mathcal{S}/\sqrt{\rho}$ as a function of $s/\sqrt{\rho}$, i.e., of the signal/noise ratio in the spectrum which would have been obtained simply by making the cosine transform of the same-interferogram in which one would have located the zero point. Curve b indicates the variation of $m/\sqrt{\rho}$ as the function of $s/\sqrt{\rho}$ and the curves b' and b" the limits between which there is a definite probability of finding the measured value $\mathcal{S}/\sqrt{\rho}$.

We see immediately that, in the presence of noise, m is not a linear function of s. To be precise, we are going to begin by examining the two extreme cases, one where the signal is zero (s = 0) and one where $s/\sqrt{\rho}$ is large.

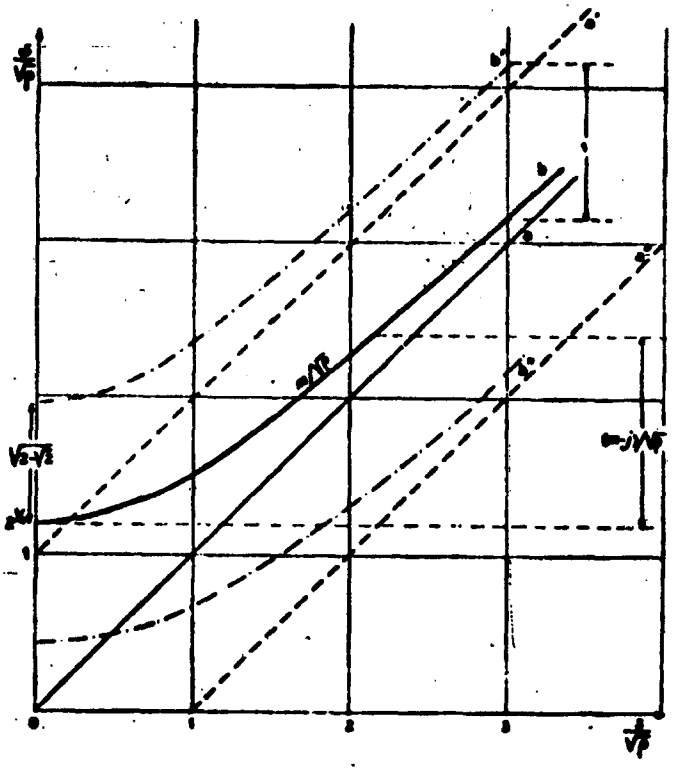

Fig. 51. Variation of $\sigma/\sqrt{\rho}$ as a Function of $s/\sqrt{\rho}$ in the Case of a Cosine Transform above and in the Case of a Complete F.T.

1°. $\underline{s = 0}$. The relations (IV.41) and (IV.42) are written

$$\overline{z^2} = 2\rho - \rho\sqrt{2} = \rho(2 - \sqrt{2}) \quad \text{and} \quad m = 2^{1/4}\sqrt{\rho}.$$

This means that in a place in the spectrum where there is no line (Fig. 49, portion ab), one sees noise made up of a constant component which equals $2^{1/4}\sqrt{\rho}$ and of a fluctuating component which has mean square error $(2 - \sqrt{2})^{1/2}\sqrt{\rho} \simeq 0.8\sqrt{\rho}$, i.e., 4/5 of the mean square error of the fluctuations in the spectrum calculated by taking the cosine transform of the interferogram recorded from 0 to L.

2°. $s/\sqrt{\rho}$ is Large. If ρ/s^2 can be considered as first-order infinitestimal, the relations (IV.41) and (IV.42) become, by neglecting terms of the second order,

$$\overline{z^2} = 2\rho + s^2 - s^2[1 + (2\rho/s^2)]^{1/2} = \rho_1 \quad m = s + (\rho/2s).$$

Hence for lines which would appear with a large s/n ratio in the spectrum calculated by the cosine transform of an interferogram in which zero phase difference is located, the complete F.T. gives an approximately linear result and the mean square error of the fluctuations which affect $\mathcal{B}$ is then the same as in the first method.

3°. Values of $s/\sqrt{\rho}$ in the Neighborhood of 1. It remains to examine the intermediary cases, for values $s/\sqrt{\rho}$ in the neighborhood of 1. The signal m - j is weak and does not vary proportionately to s at all.

To s/n ratios of 2, 3, 6 in the spectrum that one would obtain by taking the cosine transform (lines of frequencies ν_1, ν_2, ν_3 in Fig. 48) correspond the signal/noise ratios of 1, 2, 5 in the spectrum that one would obtain by taking the complete F.T. (frequencies ν_1, ν_2, ν_3 in Fig. 49).

B. EXPERIMENTAL VERIFICATIONS. These have been carried on only in the case where s = 0. They have been made using the recording of noise x(t) of which one part is represented by Fig. 37a and which has been used for the experimental verifications of the preceding chapter (§III.1(3)); $\mathcal{B}_c$ and $\mathcal{B}_s$, cosine and sine transforms of x(t), are represented by Figs. 52a and 52b. The calculated band width equals 0.1 cps, i.e., 20 times the correlation radius of noise. The values of the crests lie between ± 8 u sec (u being an arbitrary unit) and the mean square errors measured have respectively the values $\sqrt{\rho_1}$ = 4.25 u sec and $\sqrt{\rho_2}$ = 4.20 u sec. The functions $\mathcal{B}_c^2$ and

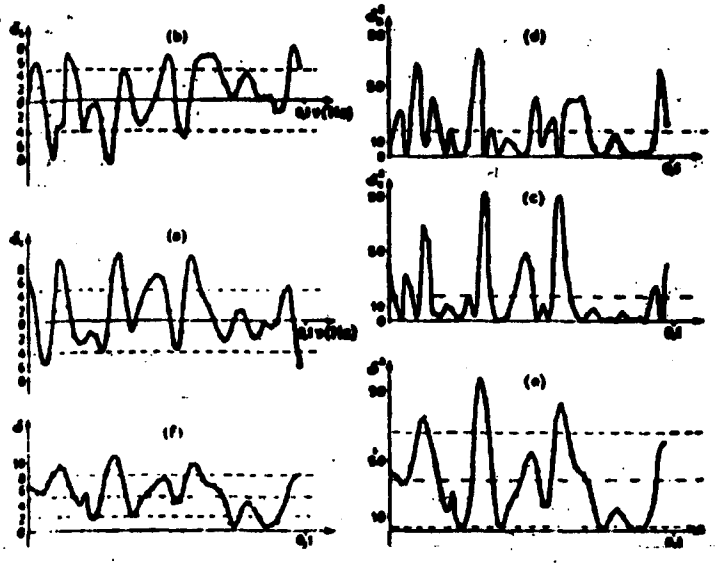

Fig. 52. Study of the Complete F.T. of an Interferogram Containing Only Noise.

$\mathcal{J}_s^2$ (Fig. 52c and 52d) have respectively the mean value $\overline{\mathcal{J}_c^2}$ = 18.06 u² sec², and $\overline{\mathcal{J}_s^2}$ = 17.79 u² sec², very similar values. If $\mathcal{J}_c$ and $\mathcal{J}_s$ had been calculated on a frequency band of infinite width, the variances $\overline{\mathcal{J}_c^2}$ and $\overline{\mathcal{J}_s^2}$ would be exactly equal. The mean value of the sum $\overline{\mathcal{J}^2} = \overline{\mathcal{J}_c^2} + \overline{\mathcal{J}_s^2}$ = 35.85 u² sec².

From the conclusions of the preceding paragraph the predicted value of the variance of the fluctuations of $\mathcal{J}^2 - \overline{\mathcal{J}^2}$ would be $\mathcal{J}^2 - \overline{\mathcal{J}^2}$ written $\overline{(\mathcal{J}^2 - \overline{\mathcal{J}^2})^2} = 2\rho_1^2 + 2\rho_2^2$ = 1,296 u² sec².

The same quantity measured in Fig. 52c equals 1,240 u² sec². The predicted value of the mean of $\mathcal{J}$ is $\overline{\mathcal{J}} = m = (\rho\sqrt{2})^{1/2}$ = 4.9 u sec and that of the mean square error of the fluctuations of $\mathcal{J} - m$ is

$$\sqrt{\overline{(\mathcal{J} - m)^2}} = \sqrt{\rho(2 - \sqrt{2})} = 3.2 \text{ u sec.}$$

The same quantities measured in Fig. 52d have the values m = 5.2 u sec and $\sqrt{\overline{(\mathcal{J} - m)^2}}$ = 2.9 u sec.

C. CONCLUSIONS. We are now in a position to compare the two methods more completely than in the preceding chapter. The second method is never strictly linear (in the same way that a classic detection is never, in the presence of noise, rigorously linear). It is catastrophic for the low values of signal/noise ratio but, for high values of the signal/noise ratio, the two methods are practically equivalent.

One can show that, if the Fourier transformation is made with a harmonic analyzer (a method which does not necessitate referencing zero) the study of the linearity and of $(s/n)_s$ ratio leads to the same results as when the complete F.T. is made. On the other hand let us recall the two inconveniences of this last method: The displacement of the moving part is doubled and the calculation time is more than quadrupled.

V. NOISE IN NUMERICAL FOURIER TRANSFORMATIONS. DIFFERENT METHODS FOR OBTAINING THE MAXIMUM S/N RATIO

When the F.T. is calculated numerically from a finite number of values of the interferogram, the s/n ratio in the calculated spectrum is always lower than the maximum s/n ratio that can be obtained by using a continuous succession of values of I(t). We shall establish the expression giving the mean square error of the fluctuations in the numerically calculated spectrum; we shall treat the important question of the choice of the time constant to use during the recording and we shall discuss different procedures that can be used to obtain a maximum s/n ratio from a given interferogram.

1. NOISE IN A NUMERICAL F.T.

Let us recall the fundamental result of the preceding chapter: The mean power of the noise in the calculated spectrum is the chopped energy in the spectrum of the noise contained in the interferogram times the square of the apparatus-function: now, when one makes a numerical F.T., we have seen in Chapter I that the apparatus-function is composed of several peaks the distance between them being $1/L$ (Fig. 13), L being the interval of the grating function used to pick points from the interferogram; the expression (IV.16)

$$\sigma_\chi^2 = \int_{-\infty}^{+\infty} \mathcal{P}_p(\nu)\, f^2(\nu_0 - \nu)\, d\nu$$

then becomes, in the case of the numerical Fourier transformation,

$$\text{(V.1)} \qquad \sigma_\chi^2 = \sum_{m=-\infty}^{m=+\infty} \int_{-\infty}^{+\infty} \mathcal{P}_p(\nu)\, f^2\left[\left(\nu_0 + \frac{m}{L}\right) - \nu\right] d\nu.$$

One thus sees that several peaks of the apparatus-function explore the noise spectrum, even in the case where the spectrum

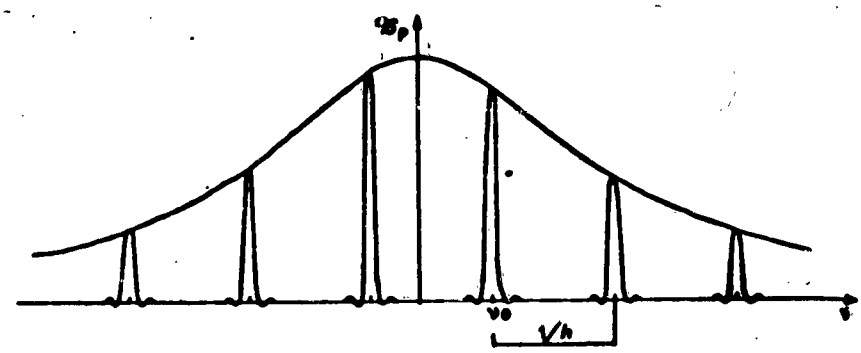

Fig. 53. Different Peaks of the Apparatus-Function Exploring the Noise Spectrum.

to be studied is limited in such a way that it may not be explored except by one peak. If the noise spectrum $\mathfrak{P}(\nu)$ contained in the interferogram were constant, the mean power of the noise in the calculated spectrum would increase indefinitely with the number of peaks in the apparatus-function, hence the absolute necessity of using, during the recording, a filter which limits the noise spectrum in the interferogram. We shall consider, in what follows, the case of the RC filter (it is difficult to make more efficient low-pass filters for the very low frequencies used in our experiment); the noise spectrum contained in the interferogram then has the form

$$\mathfrak{P}_p(\nu) = \mathfrak{P}_p(0)/[1 + (2\pi\nu\tau)^2], \quad \text{with} \quad \tau = RC$$

and in the neighborhood of a frequency ν_0 in the calculated spectrum, the mean power of the noise is the sum of the chopped energies in the spectrum $\mathfrak{P}_p(\nu)$ multiplied by the series of peaks corresponding to the square of the apparatus-function centered about $\nu_0 \pm (m/h)$ (Fig. 53). One concedes that one will have used nearly all the information contained in the recorded interferogram if one chooses the interval h (measured in units of time) close to the time constant. We are going to state this idea precisely in studying the variance as a function of interval h.

(1) Mean Power of Noise in a Numerical F.T.

By replacing $\mathfrak{P}_p(\nu)$ by its value in Eq. (V.1), we get

$$(V.2)\quad \sigma_\chi^2 = \mathfrak{P}_p(0) \sum_{m=-\infty}^{m=+\infty} \frac{1}{1+\left[2\pi\tau\left(\nu_0+\frac{m}{h}\right)\right]^2} \int_{-\infty}^{+\infty} f^2(\nu)\, d\nu.$$

Again we find in the expression for σ_χ^2 the product

$$\sigma_{\chi(0)}^2 = \mathfrak{P}_p(0) \int_{-\infty}^{+\infty} f^2(\nu)\, d\nu$$

which gives the variance in the calculated spectrum as an integral, in the neighborhood of the 0 frequency which we have already seen in the preceding chapter to be (IV.22b)

$$(V.3)\quad \sigma_{\chi(0)}^2 = 2\,Q\,T\,\mathfrak{P}_p(0).$$

In the case of a numerical F.T. one can put σ_χ^2 in the form

$$(V.4)\quad \sigma_\chi^2 = \sigma_{\chi(0)}^2\, \Phi_{\nu_0}(h,\tau),$$

by putting

$$(V.5)\quad \Phi_{\nu_0}(h,\tau) = \sum_{m=-\infty}^{m=+\infty} \frac{1}{1+\left[2\pi\tau\left(\nu_0+\frac{m}{h}\right)\right]^2}.$$

It is necessary to evaluate this series. We can do this in a particularly easy fashion because it happens that the F.T. of the function $1/[1 + (2\pi\nu\tau)^2]$ is easy to calculate. The calculation is based upon the following property: let $P(\nu)$ and $Q(t)$ be two functions which are the F.T. of each other. Then there exists between them the relation

$$\int_{-\infty}^{+\infty} P(\nu)\, d\nu = Q(0).$$

Fig. 54.--(a) Grating Function $\mathcal{R}_{1/k}$; (b) Grating Function $\mathcal{R}'_k$.

Notice that the series (V.5) is none other than the integral

$$(V.6)\quad \Phi = \int_{-\infty}^{+\infty} \frac{1}{1+(2\pi\tau\nu)^2} R_{1/k}(\nu)\, d\nu,$$

$R_{1/k}$ being the convolution of a Dirac distribution of periodic support of interval $1/k$ with the Dirac function centered about the frequency $\nu = \nu_0$ (Fig. 54a).

We put

$$P(\nu) = \frac{1}{1 + (2\pi\nu\tau)^2} R_{1/k}(\nu) = \mathcal{D}'_p(\nu)\, R_{1/k}(\nu).$$

In order to calculate $\Phi = \int_{-\infty}^{+\infty} P(\nu)d\nu$ it then suffices to find the F.T. $Q(t)$ of $P(\nu)$ and to take the particular value $Q(0)$.

The F.T. of $P(\nu)$ is the convolution of the F.T's of $\mathcal{D}'_p(\nu)$ and of $R_{1/k}(\nu)$. The F.T. of $\mathcal{D}'_p(\nu)$ is known; it is

$$T_{\cos}\left[\frac{1}{1+(2\pi\nu\tau)^2}\right] = \frac{1}{2\tau} e^{-t/\tau}.$$

The F.T. of $R_{1/k}(\nu)$ has the expression

$$T_{\cos}[R_{1/k}(\nu)] = k\, R'_k \cos 2\pi\nu_0 t,$$

R'_k being a Dirac distribution of periodic support of interval k (Fig. 54b). From this one deduces immediately the value of Φ,

$$\Phi = \frac{k}{2\tau} e^{-t/\tau} R'_k \cos 2\pi\nu_0 t,$$

that one can put in the form

$$\Phi = \frac{h}{2\tau}\left[\mathrm{Re}\left(2\sum_{m=0}^{m=\infty} e^{-mh/\tau}\, e^{2\pi i\nu_0 mh} - 1\right)\right]$$

or

$$\Phi = \frac{h}{2\tau}\left[\mathrm{Re}\left(\frac{2}{1-\exp\{-h[(1/\tau)-2\pi i\nu_0)]\}} - 1\right)\right]. \tag{V.7}$$

After expanding and collecting, (V.7) becomes

$$\Phi = \frac{h}{2\tau}\,\frac{\sinh(h/\tau)}{\cosh(h/\tau)-\cos 2\pi\nu_0 h}\ , \tag{V.8}$$

from which the expression for the mean power of the noise in the case of a numerical F.T. is

$$\sigma_X^2 = \mathcal{P}_p(0)\ 2\ Q\ T\ . \tag{V.9}$$

The expression (V.8) of $\Phi_{\nu_0}(h,\tau)$ permits one to calculate the variations of the power of the noise as a function of the interval h, when the recording has been made with a certain time constant τ. In the particular case where $\nu_0 = 0$, $\Phi_0(h,\tau)$ then becomes a function only of the quotient h/τ (Fig. 55, curve a):

$$\Phi_0(h/\tau) = \frac{h}{2\tau}\,\frac{\sinh(h/\tau)}{\cosh(h/\tau)-1}\ ; \tag{V.8b}$$

h/τ (h measured in time units) is the inverse of the number of points taken from the interferogram during a time equal to τ.

The curve $\Phi_0(h/\tau)$ has a horizontal tangent at the origin. For $\nu_0 = 0$ and $h/\tau = 0$, $\Phi_0(h/\tau) = 1$ and again we encounter the familiar expression for the variance corresponding to this case

$$\sigma^2_{X(0)} = 2\ \mathcal{P}_p(0)\ Q\ T\ .$$

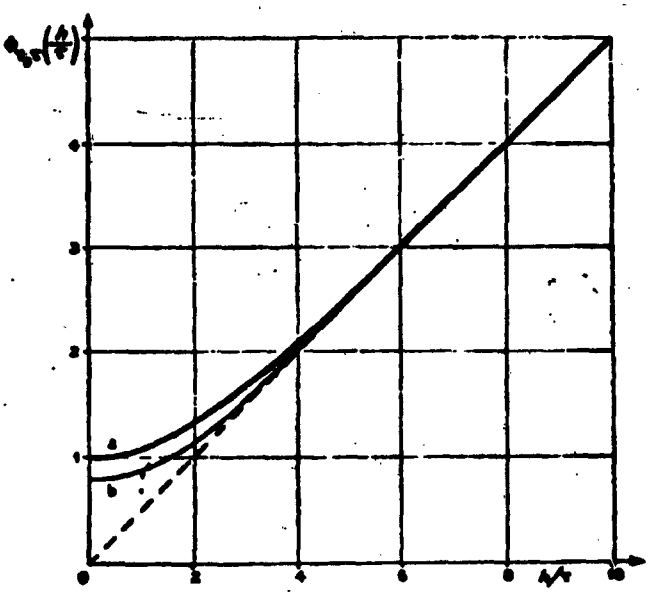

Fig. 55. Study of the Variance in the Spectrum as a Function of the Ratio of the Interval to the Time Constant: Curves b, $\nu_0 = 0$; Dashed Line, $\nu_0 = (1/2)\,(1/2\pi\tau)$.

When the analyzing frequency is an arbitrary frequency ν_0 different from 0, one can define a function $\Phi(h/\tau)$ valid for a certain value of the product $\nu_0\tau$. It can be written

$$\Phi_{\nu_0\tau}\left(\frac{h}{\tau}\right) = \frac{h}{2\tau}\,\frac{\sinh(h/\tau)}{\cosh(h/\tau)-\cos(2\pi\nu_0\tau h/\tau)}\,. \tag{V.8c}$$

This gives the variations of the power of the noise in the spectrum in the neighborhood of the frequency ν_0, as a function of the quotient h/τ when the interferogram has been recorded through a filter with time constant τ. Curve b of Fig. 55 has been constructed for $\nu_0\tau = 1/4\pi$, i.e., the frequency ν_0 considered equals $1/4\pi\tau$; it is such that $\mathfrak{m}_p(\nu_0) = 0.8\ \mathfrak{m}_p(0)$ (Fig. 56). The functions Φ_0 and $\Phi_{\nu_0\tau}$ are

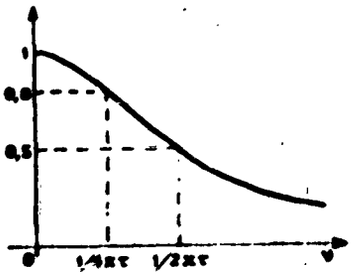

Fig. 56.

extremely close. They have the same asymptote $\Phi' = h/2\tau$. For values of h/τ of the order of a few units they are practically the same.

An examination of these curves furnishes several important results. No matter what the frequency of analysis ν_0 is:

1°. The smaller h/τ is, hence the more points one uses from the interferogram, the less noise there is in the spectrum;

2°. For values of h/τ above a few units, the power of the noise is proportional to the interval h;

3°. One gains practically nothing in choosing $h/\tau < 1$ (rather than $h/\tau = 1$), i.e., in choosing more than one point per time constant.

These results can be stated exactly when one studies the variation of the s/n ratio, in the calculated spectrum based on a particular interferogram, as a function of h/τ.

(2) Variation of the S/N Ratio as a Function of the Interval h

Noise is minimum when one uses a continuous sequence of values of I(t); it is then characterized by

$$(V.10) \qquad (\sigma_\chi^2)_m = 2\,Q\,T\,\mathfrak{w}_p(0)\,\Phi_{\nu_0\tau}(0).$$

Let us call $(s/n)_M$ the maximal value that the s/n ratio then takes in the calculated spectrum:

$$(s/n)_M = s/(\sigma_\chi)_m = s/\sqrt{2\,Q\,T\,\mathfrak{w}_p(0)\,\Phi_{\nu_0\tau}(0)}.$$

The s/n ratio, obtained for a value h of the grating interval, has a form

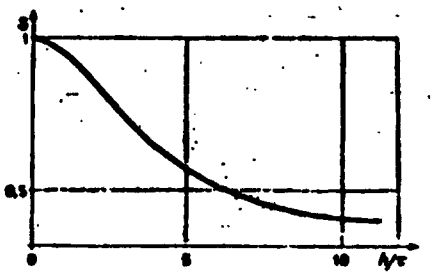

Fig. 57. Variation of S as a Function of h/τ.

$$s/n = s/\sigma_\chi =$$

$$= s/\sqrt{2QT\Phi_p(0)\Phi_{\nu_0\tau}(h/\tau)}.$$

The quotient $S = (s/n)/(s/n)_M$ measures the loss in the s/n ratio due to the fact that one uses only discrete values of I(t):

$$S = \sqrt{\Phi_{\nu_0\tau}(0)/\Phi_{\nu_0\tau}(h/\tau)}.$$

It is represented by a curve which, in principal, is valid for a single value of the product $\nu_0\tau$. But being given the weak variations of Φ with $\nu_0\tau$, the curves S will be practically identical. Figure 57 corresponds to $\nu_0 = 0$. One sees that by taking the F.T. by using, instead of a continuous sequence of values of I(t), discrete values taken at time intervals equal to the time constant, a slight weakening of the s/n ratio in the spectrum is brought about; it is multiplied by 0.95.

(3) Experimental Verifications

These have been made based on a synthetic interferogram I'(t) having a constant component I(t) = 40 u (arbitrary unit), whose F.T. will be a line centered on the frequency 0, and some fluctuations of mean square error σ_χ = 37.5 u registered with a time constant τ = 2 sec and represented by Fig. 37a. The total recording time is T = 360 sec.

The F.T. of this interferogram made by using a continuous sequence of values I(t) is composed of a line centered on the zero frequency and some fluctuations whose mean square error is, according to (IV.23),

$$\sigma_\chi = \sqrt{4 \times 0.406 \times 360 \times 2 \times 37.5 \times 37.5} = 1,281 \text{ u sec.}$$

The F.T. of I'(t) has been calculated numerically with three different values of h.

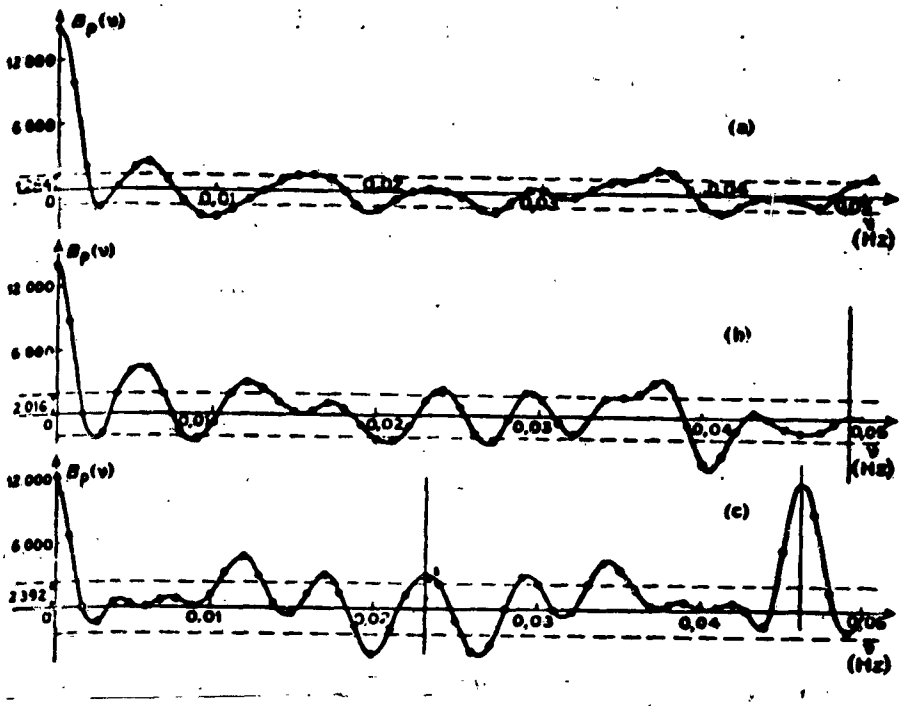

Fig. 58. Spectra Obtained From the Same Interferogram for Different Values of h.

1°. h = 1.2 sec. Number of points taken from the interferogram, N = 300; h/τ = 0.6. According to Fig. 57, S then equals 0.98 whence the predicted value of the mean square error of the fluctuations in the calculated spectrum: σ_χ (predicted) = 1,281/0.98 = 1,307 u sec. The mean square error of the fluctuations measured in the calculated spectrum (Fig. 58a) by taking the square root of the mean of the squares of the ordinates chosen from this spectrum every 10^{-3} cps (thus three points per correlation radius) is

$$\sigma_\chi \text{ (measured)} = 1{,}284 \text{ u sec.}$$

2°. h = 10.8 sec, N = 33 and h/τ = 5.4, whence S = 0.55.

σ_χ (predicted) = 1,281/0.55 = 2,329 u sec. The calculated spectrum repeats every 1/10.8 = 0.0924 cps (Fig. 58b). If one were to trace the spectrum above the frequency ν = 0.046 cps one would observe a symmetry in the spectrum with respect to

this value. To measure the mean square error of the fluctuations we have thus used only a portion of the noise between ν = 0.004 cps (starting with this frequency, the line centered on 0 has a negligible height) and ν = 0.046 cps:

$$\sigma_\chi \text{ (measured)} = 2{,}016 \text{ u sec.}$$

3°. b = 21.6 sec, N = 17 and b/τ = 10.8, whence S = 0.4.

σ_χ (predicted) = 1,281/0.40 = 3,200 u sec. The calculated spectrum repeats every 1/21.6 = 0.0462 cps (Fig. 58c). The curve representing it is therefore symmetric with respect to the frequency ν = 0.02305 cps. The mean square error of the fluctuations was then calculated using only that portion of the noise taken between ν = 0.004 cps and ν = 0.023 cps.

$$\sigma_\chi \text{ (measured)} = 2{,}392 \text{ u sec.}$$

The errors can be explained by the fact that, being given the frequency of the repetition of the spectra, the mean square errors have been calculated from noise samples extending over frequency bands much too narrow to hope to get a correct value of σ_χ. If the noise sample were sufficiently long, the mean value of the fluctuations would be zero; but, it equals - 24 u sec in the first case, + 133 u sec in the second and + 427 u sec in the third, which explains why the error is larger in the third case.

(4) Problems Posed by the Choice of τ and by Locating the Zero Point

The interferogram recorded through a low-pass filter is the convolution of the theoretical interferogram with the impulse response of the filter which is necessarily asymmetric. This is equivalent to saying that the filter introduces a phase shift, a nonlinear function of the frequency hence of phase distortion. Let us choose as time origin that instant where the geometric phase difference is zero. If the phase shift were linear one would have

$$I(t) = \int_0^\infty B(\nu) \cos [2\pi\nu t + \varphi(\nu)]\, d\nu ,$$

with $\varphi(\nu) = \tau\nu$, τ being the time constant of the filter, whence

$$I(t) = \int_0^\infty B(\nu) \cos 2\pi\nu(t+\tau)\, d\nu = I'(t+\tau),$$

i.e., the interferogram would be recorded with a certain delay τ, but without any deformation. In order to have a correct spectrum, it is sufficient to choose as origin for the analysis the time $t = \tau$.

Since with ordinary filters, the phase shift is never linear, it is no longer proper to speak of the zero point of the interferogram. The origin can be chosen correctly only for a single frequency. In the reproduced spectrum, the image of the line corresponding to this frequency will be symmetric. The images of the lines corresponding to all the other frequencies will be asymmetric, the asymmetry for a given frequency being greater the greater the time constant of the filter used. We are going to examine how it is necessary to choose the time constant in order that, from one extremity to the other of the spectrum, the asymmetry doesn't exceed a certain value chosen in advance and how one determines the zero point of the interferogram. Our study will be limited to the case of the RC filter, the most frequently used with very low frequencies. The phase displacement $\varphi(\nu)$ introduced by the frequency ν is then

(V.11) $$\varphi(\nu) = \arctan 2\pi\nu\tau,$$

which corresponds for this same frequency to a delay

(V.12) $$\tau = \frac{1}{2\pi\nu} \arctan 2\pi\nu\tau.$$

Let us continue to choose for the 0 instant the one where the geometrical phase difference is zero. One can locate it, for

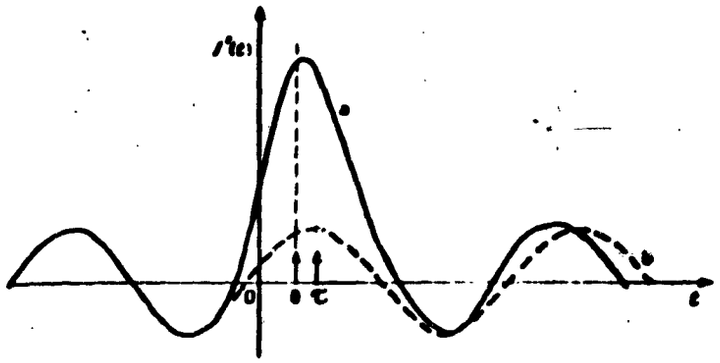

Fig. 59. Curve a, Interferogram Recorded Through an RC Filter; Curve b, the Particular Sine Wave Contained in This Interferogram.

example, by recording at the same time the interferogram to be studied and the one originating from a continuous intense source, the latter recorded without an RC filter.

If one chooses as the zero point of the interferogram the one which corresponds to t = 0, the delay of every frequency in the spectrum will be given by the formula (V.12); only the apparatus-function corresponding to the 0 frequency will be symmetric. But it is possible to make a better choice of the origin for analysis in order that the relative phase shift from one extremity of the spectrum to the other may be smaller.

Let θ be the instant corresponding to the point that we have chosen as the zero point on the recorded interferogram (Fig. 59, curve a). With this new origin for analyzing the interferogram, the delay for a frequency ν present in the interferogram (Fig. 59, curve b), becomes $\alpha = \tau - \theta$, which corresponds, by calling η the period of the phase-shifted signal,

(V.13) $$2\pi\alpha/\eta = \arctan 2\pi\nu\tau - 2\pi\theta\nu,$$

α/η and the coefficient c/λ, considered in Chapter III, which measures the error made in choosing the zero point by taking

as unity the wave length of the signal, are equal. In what follows we replace α/η by ϵ/λ,

(V.13b) $$\frac{\epsilon}{\lambda} = \frac{1}{2\pi} \text{ arc tan } 2\pi\nu\tau - \theta\nu$$

which can also be put in the form

(V.13c) $$\frac{\epsilon}{\lambda} = \frac{1}{2\pi} \text{ arc tan } 2\pi\nu\tau - \frac{\theta}{2\pi\tau} 2\pi\nu\tau.$$

ϵ/λ will be zero for $\nu = 0$ and for a frequency ν_0 which will be given as a function of θ by the relation

(V.14) $$\nu_0 = \frac{1}{2\pi\theta} \text{ arc tan } 2\pi\nu_0\tau.$$

Hence in the spectrum the apparatus-functions corresponding to the frequencies 0 and ν_0 will be symmetric. Those which correspond to the other frequencies will be asymmetric. Since the expressions (V.13b) and (V.13c) allow us to calculate the coefficients ϵ/λ corresponding to them, we can determine their appearance as in Fig. 30. We tried to represent the variations of ϵ/λ in the same spectrum as a function of $2\pi\nu\tau$ for different choices of the zero point, i.e., for different values of $2\pi\nu_0\tau$.

In Fig. 60 we considered the case corresponding to $2\pi\nu_0\tau = 0$, $2\pi\nu_0\tau = 1$ and $2\pi\nu_0\tau = 2$. Curve d represents the function $(1/2\pi)$ arc tan $2\pi\nu\tau$. The lines a, b, c, corresponding to the three cases considered have respectively the slopes $\theta/2\pi\tau = 0.159$, $\theta/2\pi\tau = 0.125$ and $\theta/2\pi\tau = 0.099$. According to (V.13c) one deduces immediately the corresponding values of ϵ/λ (curves a', b', c').

An examination of the figures shows that:

1°. For $\theta = 0$, the phase shift is always negative (Fig. 60, curve a');

2°. For the other values of θ, the phase shift increases starting with 0, passing through a maximum $(\epsilon/\lambda)_M$ for a

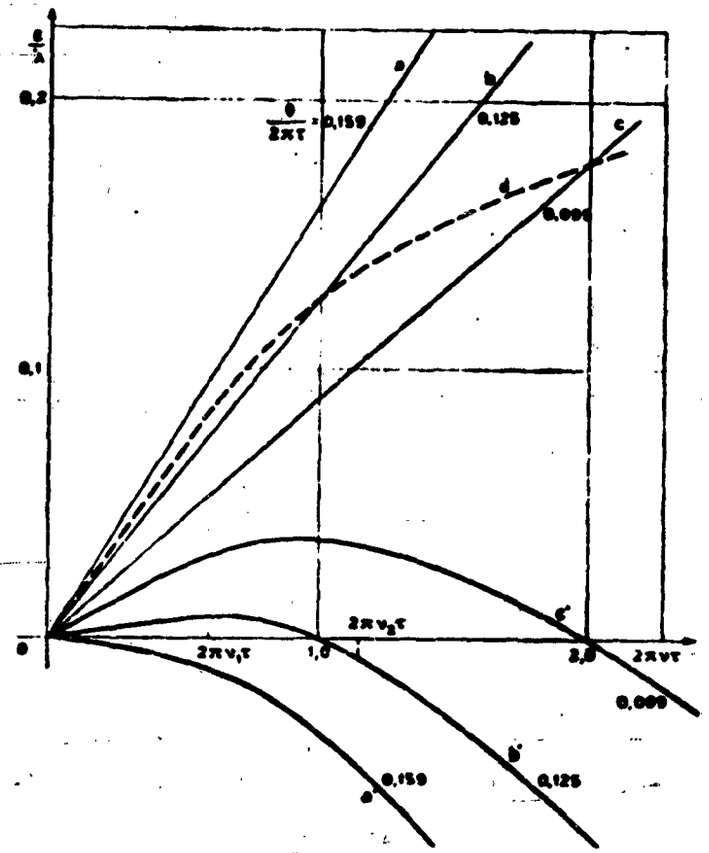

Fig. 60. Changes in ϵ/λ as a Function of $2\pi\nu\tau$ With the Choice of $2\pi\nu_0\tau$.

frequency ν_1, decreases to 0 for a frequency ν_0 and becomes negative. For a frequency ν_2, it equals $-(\epsilon/\lambda)_M$. Hence if the frequencies contained in the spectrum to be analyzed are all taken between 0 and ν_2, ϵ/λ for these frequencies never exceeds $|(\epsilon/\lambda)_M|$ and all the corresponding apparatus-functions will have a coefficient of asymmetry below $C[(\epsilon/\lambda)_M]$ which one can measure from Fig. 28 or 29.

If one chooses $\nu_0 = 1/2\pi\tau$ (Fig. 60, curve b') one has $\nu_2 = 1.25/2\pi\tau$ and C = 0.06.

For $\nu_0 = 1/\pi\tau$ (Fig. 60, curve c'), C = 0.09.

From Fig. 60 we have been able to deduce Fig. 61 in which we have represented as a function of the maximum

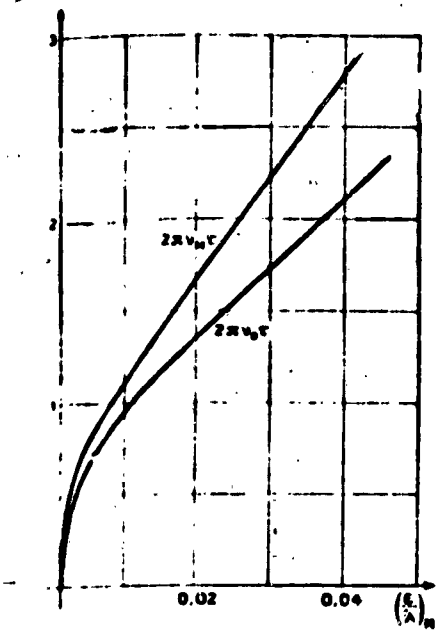

Fig. 61. Variations of $2\pi\nu_M\tau$ and $2\pi\nu_0\tau$ as Functions of the Maximum Coefficient c/λ Allowed in the Spectrum

coefficient c/λ that one allows in the reproduced spectrum the values of $2\pi\nu_0\tau$ and $2\pi\nu_M\tau$, ν_M being the limit frequency contained in the spectrum to be studied.

Curves 28 and 29 relating C and c/λ, you may recall, were established in the case where the weighting function is $A_2(t)$. It is easy to establish them for each type of apparatus-function. Figure 62 gives directly $2\pi\nu_0\tau$ and $2\pi\nu_M\tau$ as functions of C in the case where one uses $A_2(t)$.

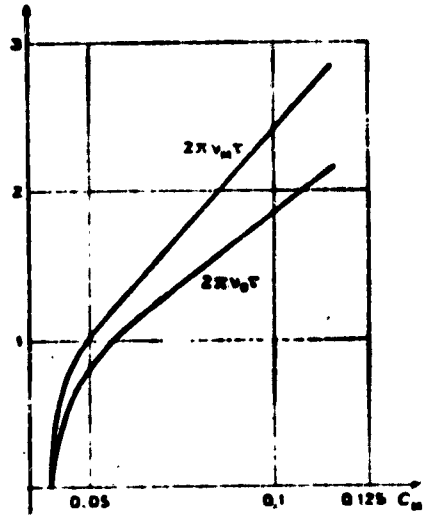

Fig. 62. A Plot of $2\pi\nu_M\tau$ and $2\pi\nu_0\tau$ as Functions of the Maximum Coefficient of Asymmetry C_M Allowed in the Spectrum.

In Conclusion, when one does not want the relative phase shift from one extremity to the other of the spectrum to exceed a certain value, two problems are posed simultaneously: The choice of the time constant and that of the zero point of the interferogram. The two known quantities are: the maximum frequency ν_M contained in the spectrum to be studied and the maximum coefficient ϵ/λ that one can allow. Figure 61 permits one to determine the corresponding value of $2\pi\nu_M\tau$, then of τ since ν_M is known; the same figure then permits one to determine ν_0 from the corresponding value of $2\pi\nu_0\tau$. When one knows ν_0, (V.14) permits calculation of the corresponding value of θ.

This is the rigorous method for determining the time constant to use and the zero point. There exists an approximate method to resolve the latter problem; it consists in recording at the same time as the interferogram another produced by a band of radiation isolated in a continuous spectrum by a filter, whose maximum of transmission coincides with the spectral region to be studied, and recorded with the same time constant. The maximum of the central fringe of the corresponding interferogram then indicates approximately the point that one ought to choose as the origin for analyzing the interferogram.

(5) Study of a Particular Case.

Suppose that we study a spectrum extending from 0 to ν_M (Fig. 66). If one allows C = 0.05 (this leads to an asymmetry of the order of 1/100, since C = 0.04 for a perfectly symmetrical function) one deduces (Fig. 61): $\tau = 1/2\pi\nu_M$ and $\nu_0 = 0.84/2\pi\tau = 0.84\ \nu_M$.

Under these conditions the noise spectrum is such that $\mathcal{P}(\nu_M) = \frac{1}{2}\mathcal{P}(0)$ (Fig. 63) and the frequency ν_M in the reproduced spectrum is reduced by a factor $1/\sqrt{2}$. If one makes a

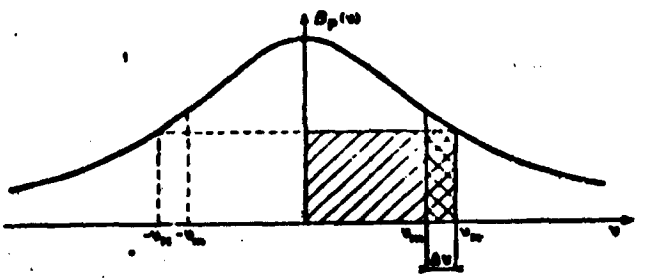

Fig. 63.

numerical F.T., by choosing the minimum interval h for which there is no overlapping of the optical spectra, hence $h = 1/2\ \nu_M$, the quotient h/τ equals π; according to Fig. 57, S then equals 0.7.

Hence when one studies a spectrum extending from the 0 frequency to a maximum frequency ν_M, one can, in picking the minimum number n of points in the interferogram, obtain an s/n ratio which equals 7/10 of the maximum s/n ratio that one could obtain with the given interferogram, with a distortion of the apparatus-function of the order of 1/100, providing the constant and the zero point of the interferogram are properly chosen. In order to make a comparison of the intensities of the lines in the calculated spectrum, it would evidently be necessary to make a correction taking into account the variation of the filter gain in the domain of the frequencies under consideration.

Suppose now that the spectrum of the Fourier frequencies is limited between ν_m and ν_M with, for example, $\nu_m = 4\ \nu_M/5$ (Fig. 63). The time constant to be used remains the same as before if we fix the same tolerances and, in order to obtain the same s/n ratio from an interferogram recorded during the same time T, the interval h ought always to be equal to $1/2\ \nu_M$. But according to Chapter II, in order that there be no overlapping of the optical spectra it would have been sufficient

to choose an interval $h = 1/(2\Delta\nu) = 5/2\ \nu_M$. The number N of the points to choose in order to obtain the signal/noise ratio $s/n = 0.7\ (s/n)_M$ is equal to five times the minimum number n of points that it would be necessary to choose in order that the different optical spectra calculated do not infringe upon each other. The duration of the calculation hence is multiplied by 5. We shall study in what follows different processes permitting the reduction of this calculating time, all the while keeping this same s/n ratio in the calculated spectrum.

2. STUDY OF DIFFERENT METHODS FOR OBTAINING A MAXIMUM S/N RATIO WITH A MINIMUM CALCULATION TIME FROM AN INTERFEROGRAM RECORDED DURING A TIME T

We have seen in Chapter IV that the s/n ratio in the spectrum varies as the square root of the duration of measurement. Suppose that we have at our disposal a certain time to make the measurement and that we have chosen then to take the numerical F.T. of the interferogram obtained. We have seen in the preceding paragraph that the numerical F.T. of an interferogram recorded through a low-pass filter always gives an s/n ratio below that which one could obtain by using the entire interferogram. One way of illustrating this fact consists in saying that several peaks of the square of the apparatus-function explore the noise spectrum when one has chosen the minimum number n of the points even though a single peak of the apparatus-function explores the optical spectrum.

In order to obtain the maximum s/n ratio from an interferogram recorded during time T, at the same time using the greatest interval h possible to make the numerical F.T., it is necessary that the noise spectrum be zero and outside the domain of the Fourier frequencies. Below we are going to consider this and to describe in detail four different methods for obtaining this result.

a. Use of a Band-Pass Filter. The low-pass filter which is used for recording the interferogram is replaced by a band-pass filter. This method, contrary to the three following ones, has never been used in any practical way.

b. Change of Frequency by Heterodyne Before Recording. This method which has been proposed by Mertz [54] under the name of "Heterodyne Spectrometry" is equivalent to the preceding, but in fact is more elegant and easier to put into practice.

c. Static Recording. In the absence of noise, all the pieces of information concerning the spectrum are contained in a number of points n in the interferogram. One easily concedes that, in the presence of noise, one obtains the maximum s/n ratio in the spectrum if one uses the total time T for the measurement of these points. Hence the method consists in stopping the moving mirror of the interferometer for each of the n interesting values of the phase difference in integrating the signal during a time T/n for each one of these points and in displacing the moving mirror very quickly without recording between these different values of δ. The mechanical realization of this type of displacement being somewhat difficult, we have used a variant of this method, registering at variable speed: rapid displacement of the mirror, then slowing up in the neighborhood of the useful points.

d. Mathematical Filtering. In this last method, the recording is done with a simple low-pass filter and the number of points N to choose remains determined by the considerations developed in the preceding paragraph (k is of the order of τ). But before proceeding with the calculation of the spectrum, one makes an intermediate calculation: that of the convolution of the recorded interferogram $I'(\delta)$ with the impulse response of an ideal filter whose band pass would have as its

width that of the spectral interval occupied by the Fourier frequencies. The result is a new interferogram $I''(\delta)$ identical to that which would have been obtained by directly filtering the signal by a perfect band-pass filter. It can then be completely represented by a number of points n reduced with respect to N in the same ratio as the band passes. One then makes the F.T. of $I''(\delta)$ and the calculation time is reduced very nearly in the same ratio n/N (the calculation time of the convolution is very short) which constitutes the clear advantage of the method.

(1) Electric Filtering

The filters should have a band pass centered about the mean frequency of the useful spectrum. The phase-shift considerations introduced by this filter are like those introduced by a low-pass filter. In this case one will find, for a suitable choice of the origin for the analysis of the interferogram recorded between 0 and L and a simple cosine transform, a single frequency for which the image of the line will be perfectly symmetric. We have not studied this process in detail since at the very low frequencies that we use, it is difficult to make band-pass filters and the same result can be obtained more elegantly by the process of changing the frequency.

Let us remark that the process of electrical filtering is interesting only if the width of the interval $\Delta\nu$ of the spectrum of the Fourier frequencies and the frequency ν_{max} satisfy the relation $\nu_{max} > 2\Delta\nu$. In fact, we have shown (Fig. 18) that as long as ν_{max} stays below $2\Delta\nu$, the interval h chosen so that there is no overlapping of the calculated spectra has the same width $h = 1/2N$ if the Fourier frequencies extend from 0 to ν_{max}.

(2) Method of Changing the Frequency

This method has been proposed by Mertz. We do not discuss it here, limiting ourselves with recalling very briefly its principle and giving an example of its use in Chapter VI.

In lieu of recording I(t) as before, one records simultaneously I'(t) and I"(t) obtained as the product of I(t) with two sinusoidal signals of frequency respectively in phase and 90° out of phase with I(t). The sum of the cosine transform of I'(t) and of the sine transform of I"(t) gives the spectrum we are looking for. A delicate problem which presents itself is the adjustment of the phases of the signals.

If the phases are correctly adjusted, the method of changing the frequency gives, for an appropriate choice of ν_0 in the interior of the domain ν_1, ν_2, a s/n ratio equal to that obtained with a band-pass filter and with a calculation time divided by 2. But it is necessary to make the simultaneous recording of the two interferograms which presents a certain complication.

One can be satisfied with recording a single interferogram if one chooses ν_0 outside the domain ν_1, ν_2 or if the signal of frequency ν_0 is out of phase by $\pi/4$ with respect to the Fourier frequencies contained in the interferogram before changing the frequency; but in the two cases the calculation time is at least multiplied by 2 and the s/n ratio in the calculated spectrum is reduced by the factor $\sqrt{2}/2$.

If the signals are out of phase by an angle $\varphi = 2\pi\nu_0\epsilon$, in the case where ν_0 is outside ν_1, ν_2, the s/n ratio in the calculated spectrum by taking a simple cosine transform of the interferogram recorded for δ varying between - L and + L is weakened by a factor cos φ, the calculation time being double that which one would have if the signals were in phase. If ν_0 is inside ν_1, ν_2, in order to obtain a correct spectrum, the calculation time is multiplied by 8 with respect to the

case where the signals are in phase and one can make the same remarks about the lack of linearity in the procedure as were made in paragraph IV.3(2)A. In the case where φ is exactly equal to $\pi/4$, the calculation time will simply be multiplied by 4, but the s/n ratio will be reduced by the factor $\sqrt{2}/2$.

(3) Static Recording

Let us recall that the interferogram I'(t) recorded without a filter when the phase difference δ varies linearly as a function of time is the superposition of the interferogram I(t) that one would have in the absence of noise and the fluctuations x(t) for which one may assume a constant spectrum [noise density $\mathfrak{D}(0)$].

Let n be the minimum number of points to choose from the interferogram. The total measurement time T can be used either to record I'(t) as has been considered earlier, or to determine uniquely the indispensable n values needed to make a numerical F.T., each being measured during the time T/n.

In the second case the operation is performed in the following way: the interferometer is adjusted to the zero phase difference. If there were no noise the signal I'(0) would be constant and would keep the value I(0). But in the presence of noise, the signal I'(0), when the phase difference keeps the constant value $\delta = 0$, fluctuates with time. The mean value which we shall call I"(0) taken for a time $T' = T/n$ is

$$I''(0) = \frac{1}{T'} \int_0^{T'} I'(0)\, dt \ .$$

Let h' be the phase difference corresponding to the second point to be measured. Suppose that the passage from $\delta = 0$ to $\delta = h'$ can be made instantaneously. At the instant T', then δ equals h' and during a time T' we take the mean of the signal; the number found is I"(h'). In the same way one determines I"(2 h'), ..., I"(n h'), etc. so that one can write I"(0),

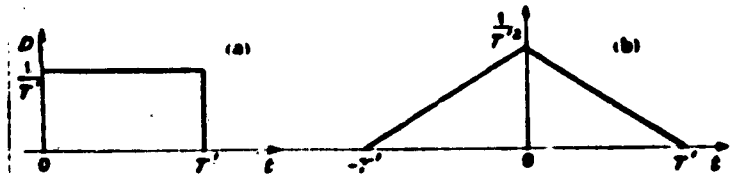

Fig. 64. (a) Square-Pulse Function D(t); (b) Autocorrelation Function of D(t).

I"(T'), ..., I"[(n-1)T']. Hence one obtains at the end of the measurement, n equidistant discrete values of a new interferogram I"(t) which is the superposition of I(t) and the fluctuations x'(t) for which we are going to determine the spectrum with respect to that of x(t). Vinokur [55] studied a particular case of this problem: he showed that under the double condition that the signal y(t) be periodic and that the period T is known precisely, the process called "summation" which consists in adding up the successive elongations y(t+kT) leads to an improvement in the signal/noise ratio. We can give a quick proof, valid in the general case, showing that the spectrum $\mathfrak{B}'(\nu)$ is of the form $\mathfrak{B}'(\nu) = \mathfrak{B}(0)|G(\nu)|^2$, $G(\nu)$ being the filter gain produced by the integration.

The noise x'(t) has the form

$$(V.15)\quad x'(t) = \frac{1}{T'}\int_0^{T'} x(t)\,dt = \int_0^{\infty} x(t)\,D(t)\,dt\ ,$$

D(t) being a square pulse function which equals 1/T' for t taken between 0 and T' and is zero outside of this interval (Fig. 64a).

The mean square error of x'(t) can be put in the form

$$(V.16)\quad \rho'(0) = \overline{x'^2(t)} = \int_0^{\infty}\int_0^{\infty} \overline{x(t)x(t')}\,D(t)D(t')\,dt\,dt'\ .$$

The term $\overline{x(t)x(t')}$ is the autocorrelation function $C_x(\mu)$ of x(t). The term $\int_0^{\infty} D(t)D(t')\,dt'$, that one can also write

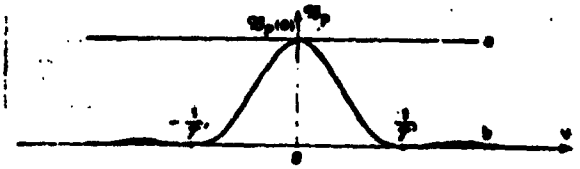

Fig. 65. Noise Spectrum After Integrating the Signal.

$\int_0^{T'} D(t)\, D(t-\mu)\, dt$ by putting $t' = t-\mu$ is, within a factor of $1/T'$, the autocorrelation function of the square pulse function D(t):

$$\int_0^{T'} D(t)\, D(t-\mu)\, dt = T'C_D(\mu).$$

(V.16) can then be written

$$\rho'(0) = T' \int_0^{\infty} C_x(\mu)\, C_D(\mu)\, d\mu. \qquad \text{(V.17)}$$

From Parseval's theorem,

$$\rho'(0) = T' \int_0^{\infty} T_{cos}[C_x(\mu)]\, T_{cos}[C_D(\mu)]\, d\nu. \qquad \text{(V.18)}$$

The cosine transform of the autocorrelation function of x(t) is, by definition, the power spectrum of x(t), i.e., $\mathcal{P}(0)$ [Fig. 65, curve a]. The autocorrelation function $C_D(\mu)$ is a triangle function of base 2 T', of height $1/T'^2$ (Fig. 64b). Its cosine transform is the function $(1/T')\,[\sin^2 \pi\nu T'/(\pi\nu\, T')^2]$, whence

$$\rho'(0) = \int_0^{\infty} \mathcal{P}(0) \left(\frac{\sin \pi\nu\, T'}{\pi\nu\, T'}\right)^2 d\nu\ ,$$

which can also be written

$$\int_{-\infty}^{+\infty} \mathcal{P}_p(\nu) = \int_{-\infty}^{+\infty} \mathcal{P}_p(0) \left(\frac{\sin \pi\nu\, T'}{\pi\nu\, T'}\right)^2 d\nu. \qquad \text{(V.19)}$$

Fig. 66. Noise Spectrum Explored by the Square of the Apparatus-Function.

The integration therefore has had the effect of filtering the noise by a filter of gain $G(\nu)$ such that

$$(V.20) \quad |G(\nu)|^2 = \frac{\sin^2 \pi\nu\, T'}{(\pi\nu\, T')^2} \qquad [18] \quad \text{(Fig. 65, curve b).}$$

The noise in the spectrum will be the F.T. $X(\nu)$ of $x'(t)$ taken by choosing $h = T'$. The mean square error $(\sigma_\chi)^2$ will then be the chopped energy in the noise spectrum times the square of the apparatus-functions centered about $\nu \pm m\,(1/T')$. The result of calculating $(\sigma_\chi)^2_0$ is obvious: one of the maxima is centered about the 0 frequency, the others about $\pm m\,(1/T')$, the values of the frequency for which $\varpi'_p(\nu)$ is zero. From this one concludes immediately

$$\sigma^2_{\chi(0)} = 2\,Q\,T\,\varpi_p(0) \qquad \text{(Fig. 66)},$$

an expression which is identical to (IV.22b).

---

[18] The different "lobes" which are 1/T apart in the filter introduced by Vinokur in the case of the summation that he uses, come from the fact that he does not make a true integration, but a sum of the discrete values of the signal. These different lobes are close to the different peaks of the apparatus-function that one obtains in the case where the F.T. is made numerically using discrete values of the interferogram.

Fig. 67. Grating Function $R_{1/T'}$ Centered on the Frequency ν_0.

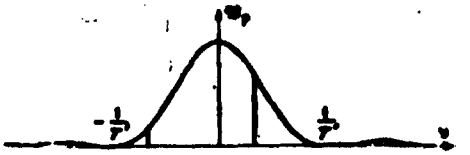

Fig. 68. Product of $m_p(\nu)$ by $R_{1/T'}$.

The signal/noise ratio of the calculated spectrum is therefore the same as when the interferogram I'(t) is recorded in a continuous fashion during time T and when the F.T. is made using all the value. of I'(t).

It remains to show that if the F.T. is made for a frequency ν_1 different from 0, the mean square error of the fluctuations preserves the same value.

$$\sigma^2_{X(\nu_1)} = \sigma^2_{X(0)} \int_{-\infty}^{+\infty} \frac{\sin^2 \pi\nu\, T'}{(\pi\nu\, T')^2} R_{1/T'}\, d\nu,$$

$R_{1/T'}$ being a Dirac distribution of periodic support of interval $1/T'$ centered about the frequency ν_0 (Fig. 67). If we put

$$P(\nu) = \frac{\sin^2 \pi\nu\, T'}{(\pi\nu\, T')^2} R_{1/T'}(\nu) \qquad \text{(Fig. 68)},$$

and $Q(t) = T_{\cos}[P(\nu)]$ we have

$$\sigma^2_{X(\nu_1)} = \sigma^2_{X(0)}\, Q(0) \,. \tag{V.21}$$

The F.T. of P(ν) (Fig. 69) is the convolution of a triangular function of height $1/T'$ and of base $2T'$ with the function $R'_{T'} = T' R''_{T'}$, $\cos 2\pi\nu_0 t$, $R''_{T'}$, being a Dirac distribution of periodic support of interval T'. One sees immediately, according to Fig. 69, that Q(0) = 1 whence

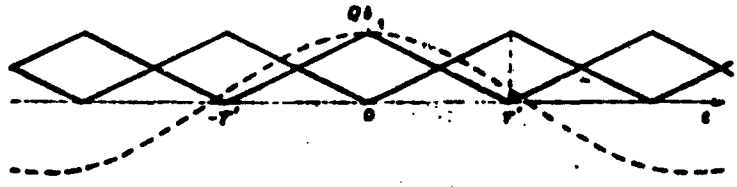

Fig. 69. Determination of Q(0).

$$\sigma^2_{X(\nu_1)} = \sigma^2_{X(0)}.$$

This method of recording is difficult enough to use even given the requisite precision to vary the phase difference. Nevertheless one can consider it for the far infrared where the tolerances are always larger. In the near infrared we have used a variant of this method, variable speed recording.

The spectral domain occupied $\Delta\sigma = 369\ cm^{-1}$ is such that the interval h chosen in order that there be no overlapping of the Fourier frequencies is

$$1/(2\ \Delta\sigma) = 13.519 \times 10^{-4}\ cm^{-1} = 21\ \lambda_0\ ,$$

λ_0 being the wave length of the reference line, here the red cadmium line.

The phase differences are referenced with the aid of preselection counters and adding counters whose indicators increase 1 unit each time that the phase difference increases by λ_0. The carriage is displaced alternately at a slow speed V_1 during which δ varies by $3\ \lambda_0$ and at a speed V_2 16 times larger during a variation $\Delta\ \delta = 18\ \lambda_0$, the changes in speed being triggered by the preset counters. The operation is done in the following way (Fig. 67). The zero point is selected by a white fringe while the interferometer is moving at a speed V_1; when $\delta = 22.5\ \lambda_0$ a preset counter set on 18 triggers the speed V_2; when the counter has returned to 0, it triggers speed V_1 and at the same time a preset counter set on 3, etc. The ordinates

are picked from the interferogram for $\delta = 0, 21\,\lambda_0, 42\,\lambda_0, \ldots, n.\ 21\,\lambda_0$, as indicated in Fig. 87. The method has worked correctly, but we have abandoned it because the signal/noise ratio in the calculated spectrum is insufficient. The reason is that, under the described conditions, the ratio of the useful measurement time (useful time that one can write $\tau\ L/2\ \lambda_0$, τ being the time constant used) to the total time T is too low. There are two reasons:

1°. Being given the quality of the mechanism used, the constant rate of speed is not established instantaneously; three fringes must file by at V_1 and 1/6 of the course is run at a lower speed;

2°. The preset counters used cannot count more than 25 impulses a second, and the ratio of the two speeds can be only 16. The elapsed time between the measured points hence is too large a fraction of the total measurement time.

(4) Numerical Filtering.

Since this question is the subject of a more detailed publication [56], here we shall give only a succinct résumé.

If one takes the convolution of the interferogram $I'(\delta)$, recorded as above through a simple low-pass filter, with the impulse response $\mathfrak{J}(\delta)$ of an ideal filter $G(\sigma)$ whose band pass coincides with the optical spectrum to be studied, one obtains an interferogram $I''(\delta)$ whose F.T. coincides with that of $I'(\delta)$ in the domain of the filter and is zero outside. In order to have the maximum s/n ratio in the calculated spectrum it is then sufficient to pick off from $I''(\delta)$ the minimum number of points compatible with the width of the optical spectrum and its position with respect to the origin (see paragraph II.2(3)B).

Suppose, for example, that the relative positions of the noise spectrum and of the optical spectrum are represented by

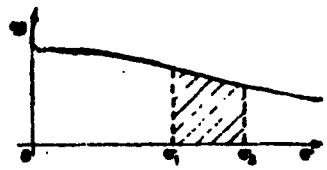

Fig. 70. Noise Spectrum and Optical Spectrum.

Fig. 70. The impulse response $\mathfrak{F}(\delta)$ (Fig. 71a) corresponding to $G(\sigma)$ (Fig. 71b) has the form

$$\mathfrak{F}(\delta) = T_{\cos}[G(\sigma)] = \Delta\sigma \frac{\sin\pi\Delta\sigma\delta}{\pi\Delta\sigma\delta} \cos 2\pi\sigma_m\delta,$$

with $\sigma_m = (\sigma_1+\sigma_2)/2$. If the functions $\mathfrak{F}(\delta)$ and $I'(\delta)$ had a band-limited spectrum it would be possible to calculate their convolutions exactly using discrete values of these functions. Since their spectra are unbounded, from discrete values of these functions one can calculate only a value $\mathfrak{J}(\delta)$ near $I''(\delta)$, the approximation improving as the interval h' chosen for taking the convolution is the smaller. One shows that the s/n ratio obtained by taking the F.T. of $\mathfrak{J}(\delta)$ with the maximum interval h (see paragraph II.2(3,8) is exactly the same as with the spectrum obtained by taking the F.T. of $I'(\delta)$ with the interval h'. Since the convolution is calculated numerically much faster than is a F.T., the calculation time gain for the same final s/n ratio is of the order of h'/h, i.e., of the order of $\sigma_m/\Delta\sigma$. We shall see an application of this method in Chapter VI.

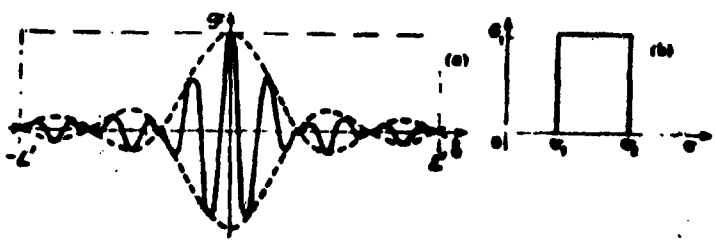

Fig. 71. (a) Impulse Response $\mathfrak{F}(\delta)$ of the Filter; (b) Theoretical Gain of the Numerical Filter.

3. CONCLUSION

We have just seen several methods enabling one to obtain for a minimum calculation time the maximum s/n ratio compatible with the measurement time T: use of a band-pass filter, method of changing frequency, numerical filtering. The conclusion of this study is the following: Each time that the relative width $\Delta\nu/\nu_M$ of the spectral domain to be studied is small, it is advantageous to record the interferogram by the method of changing the frequency, the frequency ν_0 being chosen close to the middle of the occupied interval $\Delta\nu$; nevertheless this method presents a certain instrumental complexity and it is sometimes possible to do without it and record the interferogram through a simple low-pass filter. Under these conditions it is advantageous to make a numerical filtering. This last method can be useful, even if the relative width of the spectral domain to be studied is large, provided that one is interested only in one portion of this domain.

VI. EXPERIMENTS AND RESULTS

With the aid of the Fourier transform method we treated two problems in the near infrared: the study of the emission of the night sky near 1.6 μ, the region where the atmosphere is transparent, and the study of the re-emission light of germanium about 1.7 μ. These two sources had already been studied with grating spectrometers [57,58]. But their low energy level permitted obtaining in a reasonable measurement time only low resolutions of respective orders of 150 and 1,500, and with a signal/noise ratio which was not sufficient to make evident the feeble components whose existence was in question [59] or to determine the law of displacement of a line as a function of the magnetic field. The end pursued is thus an increase in resolution and an amelioration of the signal/noise ratio. For the two studies we used the same Michelson interferometer that we are going to describe summarily.

1. DESCRIPTION OF THE INTERFEROMETER-DETECTOR ENSEMBLE

The interferometer used is completely classical (Fig. 72).

OPTICS. Everything optical is glass; hence the instrument can be used only in the near infrared up to about 2.7 μ, that region where glass becomes absorbent. The two mirrors are 7 in. in diameter and are aluminized; the beam splitter and compensating plate measure 7 cm × 8 cm; they have the same thickness, about 1 μ. They are held by the same support, the face of the beam splitter which is half-aluminized being against the compensating plate. There is no ruling, either on the beam splitter or on the compensating plate. We have adopted this arrangement in order to obtain easily a good

Fig. 72.

parallelism between the two plates, which is necessary in order that the apparatus be perfectly symmetric and that the recorded interferograms have a zero point. But the solution is not perfect (because of the difference of the dispersions and of the phase shift of the reflection on the semi-aluminized glass side and the air side). In order that it be perfect, it would be necessary that the two plates be glued together with a substance having the same index as glass which would hold the plate together although it is very thin.

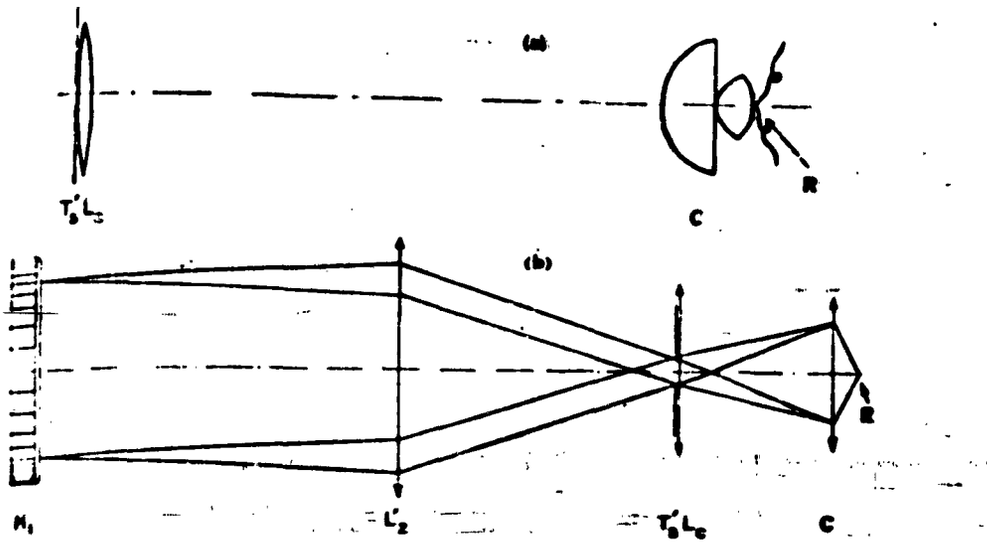

Fig. 73. (a) Diagram of the Detector Mounting; (b) Optical Diagram: M_1, Mirror; L_2', Exit Lens; L_c, Field Lens; C, Condenser; R, Detector.

DETECTOR. The detector is a Kodak cell of lead sulfide. The noise power of these cells increases nearly proportionally to their surface; hence it is advantageous to choose a cell having the smallest surface possible. If one calls **S** the area of the cross section of a beam, Ω the aperture of the exit beam, s the area of the cell and ω the solid angle of the beam that is received, in order to use all the light, it is necessary that $S\Omega = s\omega$. Several arrangements have been proposed to allow the largest possible ω. Williamson recommended the use of a "cone channel condenser" [60], P. Connes that of a microscopic condenser on the rear face of which is fastened the cell [4]. We adopted this last solution (Fig. 73a). The numerical aperture of the condenser used is $n \sin \theta_{max} = 1.4$. The solid angle finally accepted by the cell would correspond in air to the value of $\omega = 1.45 \times 2\pi sd$. A field lens makes the image of the mirrors on the front face of the condenser and the condenser makes the image of the exit hole on the lens (Fig. 73b). The cell is cooled to the temperature of dry ice.

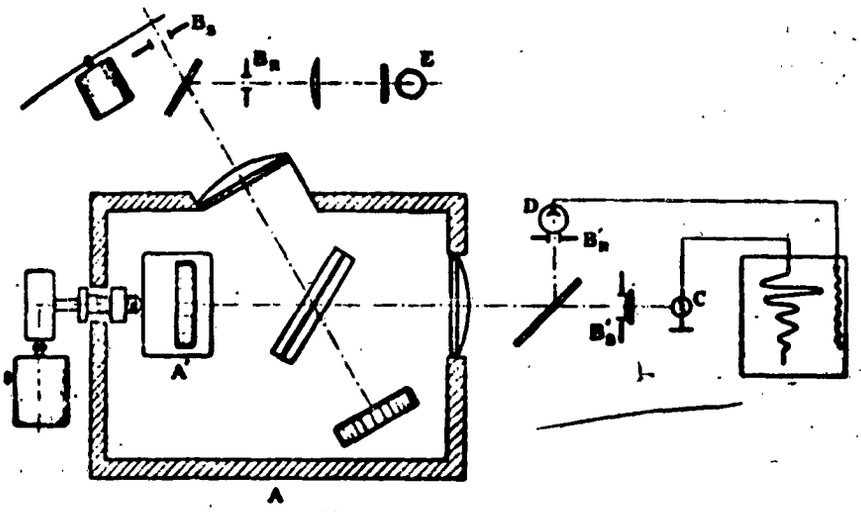

Fig. 74. Schematic Diagram: A, Michelson Interferometer; A', Movable Mirror With Gear Drive; B, Entrance and Exit Holes; C, Lead Sulfide Detector; D, Photon Multiplier; E, Cadmium Lamp.

In the interferometer the reference beam follows exactly the same path as the light beams to be studied (Fig. 74); it is received by a photomultiplier because we have always used as a reference line, a line taken in the visible part of the spectrum.

MECHANICAL PART. The moving mirror is locked on a carriage which travels on parallel slides. The quality of the slides is such that the parallelism is preserved to about 1/10 of a fringe of a red cadmium line, for an 8mm translation of the moving mirror (hence a variation of the phase difference of 16mm) with a 5 cm usable diameter of the mirrors.

The adjustments for parallelism act on the supports for the mirror. The gross adjustments are made following a classical procedure of working directly on the back of the moving mirror with the aid of three leveling screws placed 120° apart and which one draws out once the screw adjustment is made.

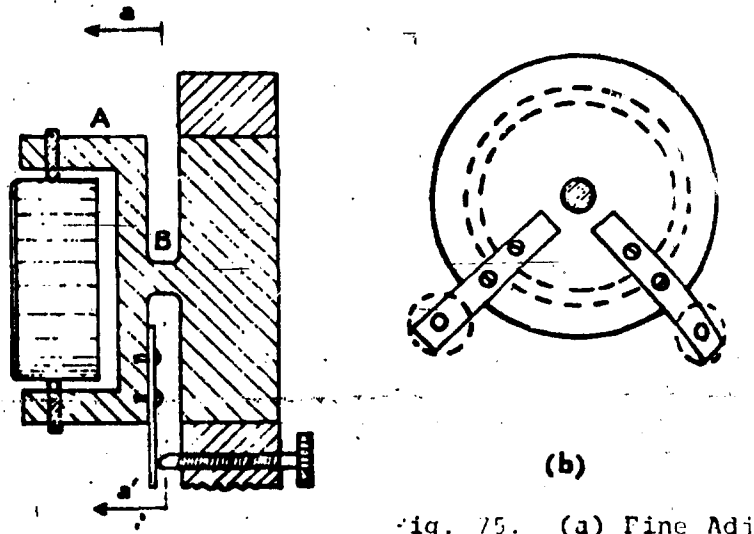

Fig. 75. (a) Fine Adjustment Mechanism of the Fixed Mirror, (b) Cross-Section aa'.

The fine adjustments are located on the fixed mirror. The mirror is mounted on a flexible part which can be oriented by bending and which has the form shown in Fig. 75a. The cylindrical part B has an 8mm diameter and is 10mm long. Part A has two steel arms with perpendicular springs and at 45° to the vertical on the extremity of which one can operate a screw with a fine pitch of 0.5mm (Fig. 75b). The torsion of B which results therefrom gives two completely independent adjustments. One complete turn of the screw corresponds to a misadjustment of a half fringe. It is necessary that the ensemble be very rigid since the optical beams are relatively long (about 15 cm). Also the two consoles bearing the fixed mirror and the separating-compensating ensemble are locked in a heavy cement support. The support for the two slides is locked in the same block of cement.

DRIVE MECHANISM. The carriage is driven by the aid of a micrometric screw with 0.5mm pitch of any quality. It is useless to use a screw of superior quality since we have seen that even with a very good screw the phase differences have to be marked with the aid of a reference line. The screw is displaced by the action of a synchronous motor turning at 750 rpm through the use of a gear box and of a tangent screw giving a reduction ratio of 100. The gear box permits one to use reduction varying by powers of 2 between 1 and 4,096, in such a way that the displacement speed of the moving mirror varies between 6.25×10^{-2} and 1.5×10^{-5} mm/sec. The apparatus is extremely sensitive to vibrations which affect the length of the interfering beams; there are two principal sources of vibrations: those coming from the earth and those which are due to the motor and all of the components of reduction and transmission. In order to suppress the first kind as much as possible the block of cement is mounted upon rubber shock absorbers, and in order to attenuate the second kind, the drive axis and all the transmission components are linked together by flexible joints. Of course, it is necessary to avoid temperature variations. Hence the interferometer is placed in the interior of a box lined with insulating material and covered with aluminum foil. This thermo-isolation proved to be sufficient even when one is working in a room without temperature control. In order to diminish the absorbtions in the glass the windows of the enclosure are formed by entrance and exit collimating lenses.

2. STUDY OF THE EMISSION SPECTRUM OF THE NIGHT SKY

The interpretation of the results of this study has already been the subject of two publications [61,62]. Here we are going to give a brief description of the conditions under which the experiments have been made.

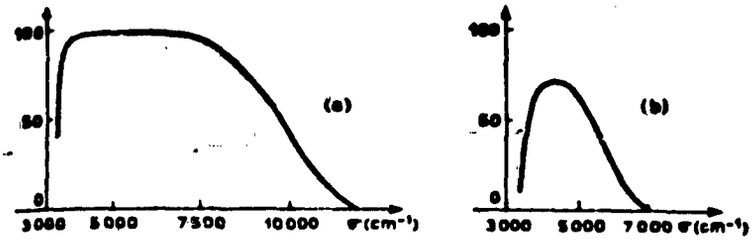

Fig. 76. Filter Transmission Curves; the Ordinates are Transmission Factors in Percent.

The setup is the one shown in Figs. 72b and 74. A simple reflection mirror shown in Fig. 72b permits one to look to the northwest at 20° above the horizon. Hence there is no optical intermediary between the sky and the entrance lens of the interferometer. The diameter of the hole has been chosen in such a way that the apparatus works under the best luminosity-resolution conditions. Under these conditions the angle of the maximum opening of the beam when we wish to obtain an effective resolution of 2,000 measures 3×10^{-2} radians and the solid angle of the beam used is $\Omega = 2.7 \times 10^{-3}$ steradians. The modulator placed before the entrance hole B_s chops the flux at a frequency of 125 cps. The electric signal coming from the lead sulfide cell is amplified in a classical synchronous detection apparatus, filtered by an RC filter and recording potentiometer.

We have studied the region near 1.6 μ with a lead sulfide cell in the region near 1 μ with a Lallemand photomultiplier.

(1) Study of the Region in the Neighborhood of 1.6 μ

A filter, placed directly before the cell and whose transmission curve is represented by Fig. 76a, eliminated wave lengths below 1 μ. As reference line we used the red cadmium line isolated in the spectrum of an Osram lamp by colored filters. The infrared, which comes from the Osram lamp and

which can reach the lead sulfide cell was cut by an ensemble of filters whose transmission curve is given in Fig. 76b and by a 2.5% copper sulfate solution of 2 cm thickness.

Figure 77a gives an example of an interferogram obtained under these conditions. Immediately one notices an anomaly: the central fringe does not correspond to a maximum. But it can be shown that in an interference phenomenon the maximum intensity, if it is a question of a system of interferences with a brilliant central fringe, is always obtained in the central fringe. ([43] p. 659). The explanation comes from the fact that the recorded interferogram is taken as the sum of two interferograms with opposite phases: one which comes from the emission of the chopper blades in a black box whose temperature is about 15°C while the cell is approximately at - 80°C, the temperature of dry ice. Since the chopper radiates approximately as a black body, the radiation spectrum which it emits is large. The corresponding interferogram is reduced to some fringes in the neighborhood of the zero phase difference. We recorded it one night when the sky was covered and when the emission of the night sky was therefore null (Fig. 78a). The corresponding spectrum (Fig. 78b) is cut on the long wave side by glass which becomes absorbent. In order to attenuate this signal strongly in phase opposition, it is sufficient to place before the cell an interference filter which cuts off beyond 2 μ and lets pass the radiations near 1,6 μ. With such a filter, the interferogram is returned to nearly normal with a much larger central fringe (Fig. 79a).

The referencing of the zero point can be done in two ways which give equivalent precision: either by taking the mean of the midpoints of the segments joining the axes of the two symmetric fringes with respect to the central fringe like ab, cd, ef, as indicated in Fig. 77a, or else by registering at zero phase difference, the interferogram of a white source with the same time constant (Fig. 80).

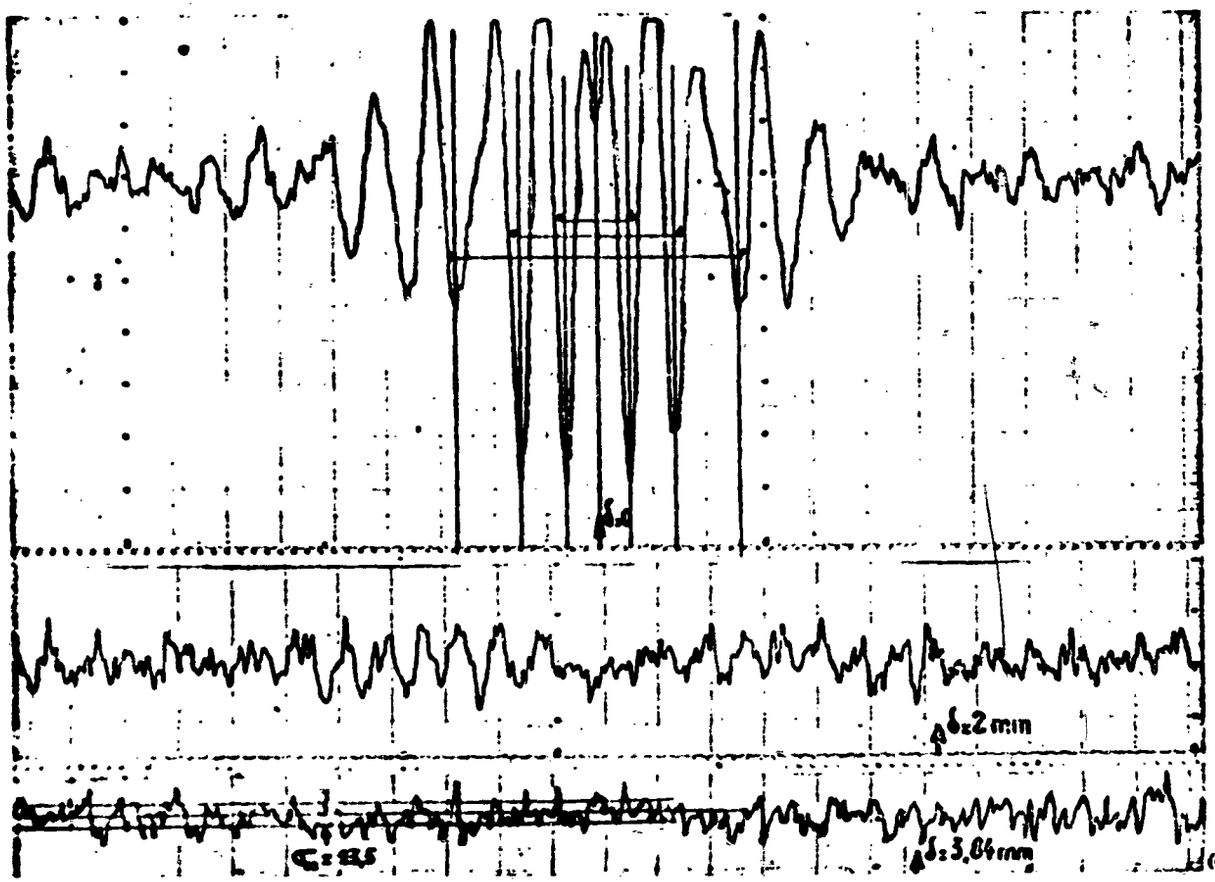

Fig. 77a. Interferogram of the Night Sky (March 8, 1959), Lead Sulfide Cell Without a Filter;

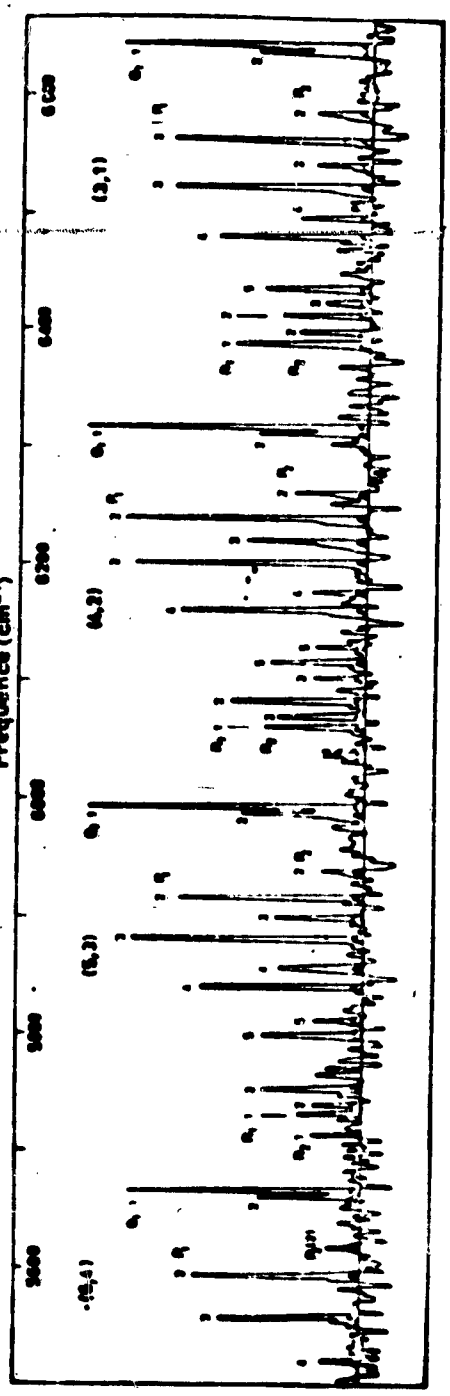

Fig. 77b. Spectrum of the Night Sky. [Bruit = noise]

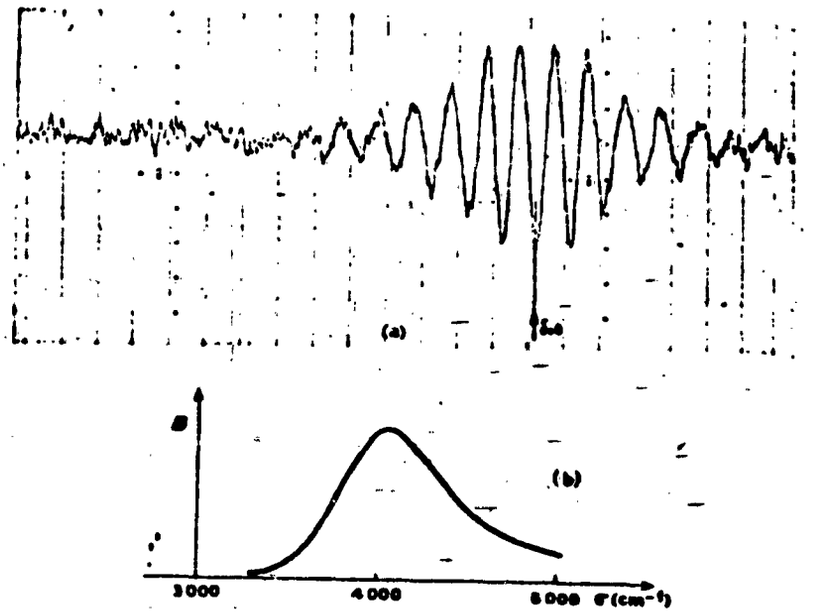

Fig. 78. (a) Interferogram of the Radiation Emitted by the Modulator; (b) Spectrum of the Radiation Emitted by the Modulator.

We give below three spectra obtained at resolutions 900 (Fig. 81 and 79b) and 2,000 (Fig. 77b).

Spectrum of Fig. 81. Effective resolution, 900. Time for recording the interferogram, 2 hrs.

Figure 81 gives a comparison between two spectra: one at resolution 900 obtained through a Fourier transformation and one at resolution 150 obtained with a grating spectrometer. This last is in fact the mean of eleven spectrums, each having been recorded during a half hour[16]. The

[16] Wallace Jones has recently obtained with a grating spectrometer a spectrum at resolution 400 by using a new germanium detector. In the two experiments compared in Fig. 81, the detector was a Kodak cell.

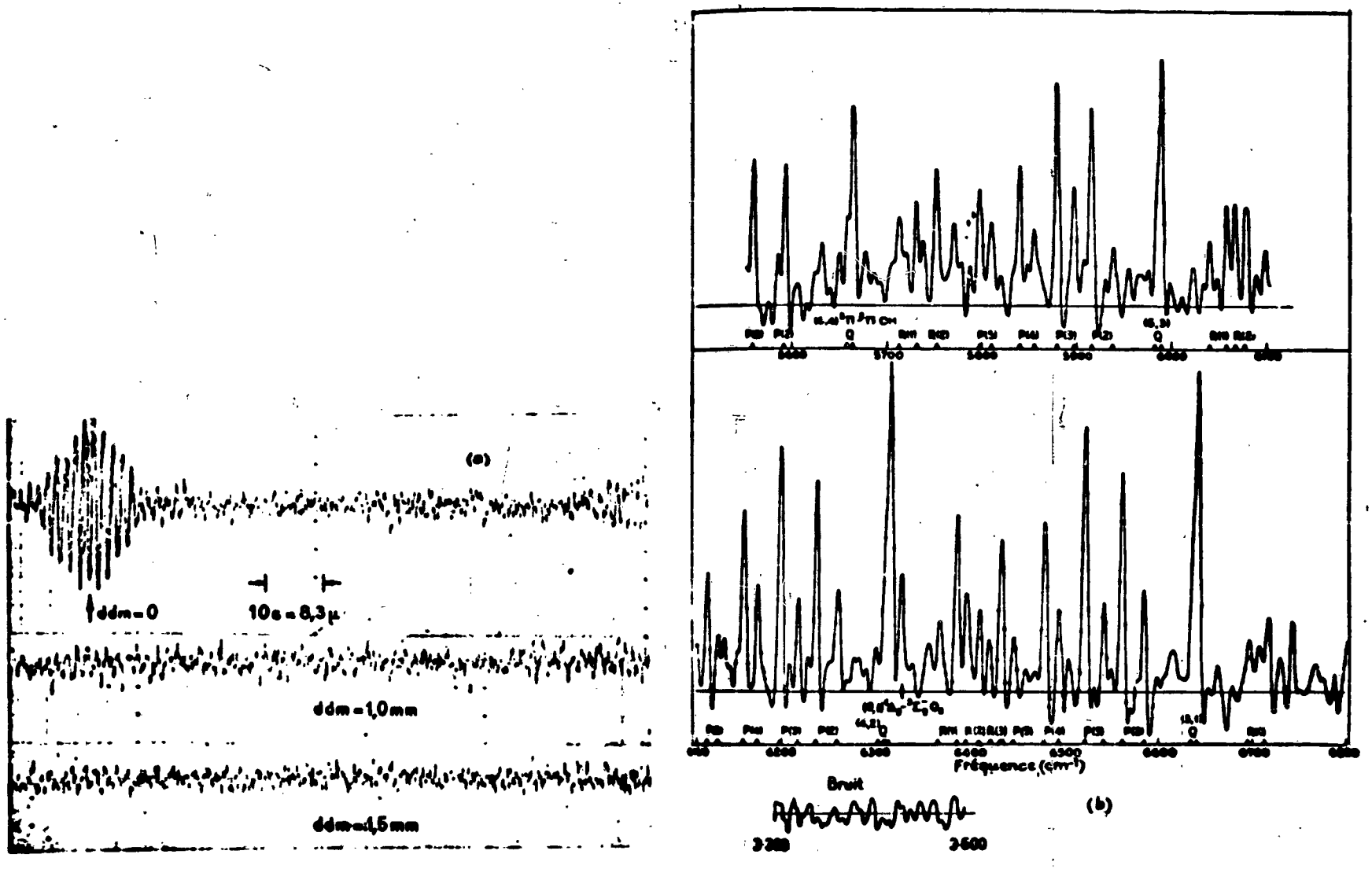

Fig. 79. (a) Interferogram of the Night Sky (February 28, 1959), Lead Sulfide Cell With Interference Filter; (b) Spectrum of the Night Sky.

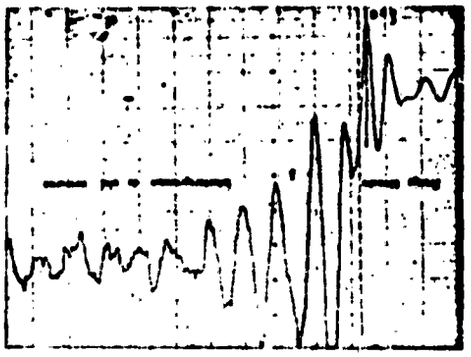

Fig. 80. Interferogram of the Night Sky and White Source Recorded With the Same Time Constant.

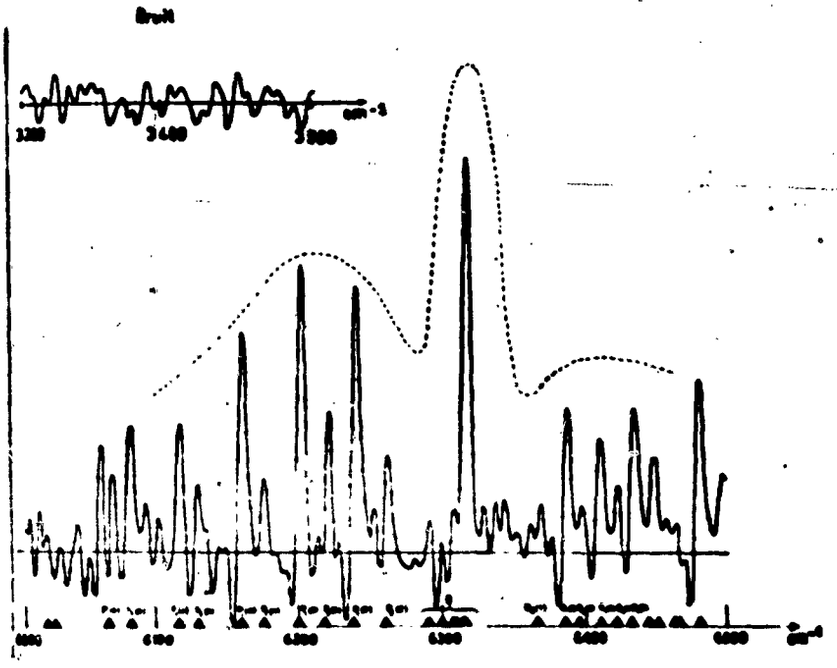

Fig. 81. Spectrum of the Night Sky: ----- R = 150, —— R = 900. [Bruit = noise]

negative maxima that one sees on the low wave number side of each ray which has a strong intensity show that there has been an error in determining the zero point of the interferogram.

Spectrum of Fig. 79b. Using the interferogram of Fig. 79a recorded at twilight the following have been calculated:

Maximum phase difference obtained, 1.96mm;

calculated limit of resolution taking into account the width of the beam, 6.25 cm^{-1};

measured limit of resolution, 6.3 cm^{-1};

spectral domain studied, 1,250 cm^{-1} between 5,550 and 6,800 cm^{-1}; number of spectral elements, 210;

recording time, 40 min.

We were limited in the choice of the recording speed by the response time of the recording pen which took 0.8 sec to go from one extremity of the scale to the other. The limit speed of the pen hence is 30 mm/sec. With the recording frequencies chosen, i.e., 0.5 cps in the middle of the spectrum, and the maximum amplitude of the fringes, i.e., 150mm for zero phase difference, the maximum speed of the pen was only 150 mm/sec. It is very much lower everywhere else in the interferogram and, under these conditions, the recording function can be considered as perfectly linear.

The time constant used was $\tau = 0.125$ sec.

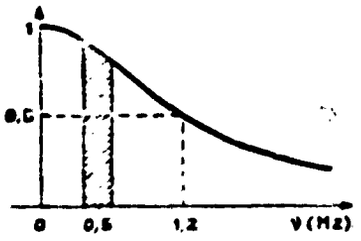

Fig. 82. Relative Position of the Noise Spectrum and of the Spectrum of Fourier Frequencies.

Figure 82 shows the relative position of the spectrum of the Fourier frequencies and of the noise spectrum.

Conditions under which the F.T. was taken: numerical F.T. with an interval $h = 0.36$ sec (the distance separating two points corresponds to a variation of a phase difference of a half wave length of the red

cadmium line). Under these conditions $h/\tau = 3$ and, according to Fig. 57, the signal/noise ratio is weakened by a factor 0.7.

The total number of points taken: 6,120.

Number of calculated points: 840, i.e., 4 per spectral element.

Calculation time on the IBM 704: 1 hr, 20 min.

Mean square error of the fluctuations of the interferogram $\sigma_x = 7.6$ u. This error has been calculated by taking the square root of the mean of the squares of the ordinates picked off the interferogram by choosing 4 points per noise correlation radius. The portion of the interferogram chosen corresponds to $\delta = \delta_{max}$. One is certain that for this phase difference, the signal in the interferogram is zero. Actually the diameter of the hole has been chosen such that the product ΔR be maximum (III.2). Under these conditions at the maximum phase difference, the modulation fell to zero.

The predicted mean square error of the fluctuations in the spectrum (see IV.23b),

$$\sigma_X = \frac{1}{0.7}\left(0.9 \times 4 \times 0.406 \times \frac{2,400}{8} \times 57\right)^{1/2} = 211 \text{ u sec.}$$

Mean square error measured in the spectrum: 212 u sec.

The calculation was made in the neighborhood of 3,500 cm^{-1} because in this region the glass is absorbent and one is certain that the signal there is zero.

Such good agreement must be considered fortuitous.

Spectrum of Fig. 77b. Using the interferogram of Fig. 77a recorded without a filter, it was calculated:

maximum phase difference obtained, L = 3.84 mm;
theoretical limit of resolution, $\delta\sigma_0 = 3$ cm^{-1};
measured limit of resolution, 3 cm^{-1};
number of spectral elements studied, 400;
recording time, 2 hrs, 30 min;
time constant, $\tau = 0.25$ sec;

h = 0.72 sec, whence h/τ = 3;
number of points chosen, 11,928;
number of output points, 1,500;
calculation time on the IBM 650, 150 hrs[17]

If this calculation had been made on the IBM 704, one could have been able to make a numerical filtering to isolate the interesting region of width $\Delta\sigma$ = 1,100 cm^{-1} between 5,550 and 6,650 cm^{-1}. In this case the calculation of the convolution would have been made using 11,928 input points, but the interval h' chosen in order to make the F.T. would have been only of the order of 1,000.

Mean square error of the fluctuations of the interferogram: σ_x = 13.5 u.

Mean square error of the fluctuations of the spectrum:

$$\sigma_\chi = \frac{1}{0.7}\left(0.9 \times 4 \times 0.406 \times \frac{9,000}{4} \times 180.8\right)^{1/2} = 1,000 \text{ u sec.}$$

Measured mean square error: 1,012 u sec.

(2) Study of the Region Around 1 μ

The detector is a Lallemand photomultiplier chilled with dry ice. Hence for the maximum noise reduction (here it is photon noise) it is necessary to isolate the region to be studied by a filter. For this result we have used a combination of a colored filter which cuts all the visible up to 8,000 Å and of an interference filter whose transmission curve is given by Fig. 83. On the long wave length side, the spectrum is limited by the region of sensitivity of the cell. The interferograms are of the type represented by Fig. 84a. We calculated two spectra using the same interferogram, one using

[17] This calculation was made at the University of Toronto's IBM-650 calculator which has magnetic drum and fast access memories.

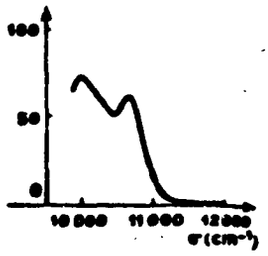

Fig. 83. Transmission Curve of the Interference Filter Centered on 1 μ; as Ordinate, Transmission Factor in Percent.

an almost triple length of the interferogram: 1.22 mm. Total recording time: 2 hrs.

The resolutions obtained are respectively of the order of 350 and 1,000 (Fig. 84b). A nearly identical spectrum had been obtained with a grating spectrograph for an exposure of 48 hr.

(3) Resumé of the Results Obtained in the Study of the Spectrum of the Emission of the Night Sky

The conclusions that can be drawn from the study of the spectra have been discussed elsewhere [62]; here we shall give only a resumé:

all the observed lines can be attributed to the radical OH;

the rotational structure of the bands (3.1), (4.2), (5.3) and (6.4) is completely determined;

one has been able to set up a table of observed frequencies for the vibration-rotation lines of the radical OH, a task which is difficult to do based on experiments performed in the laboratory because of the difficulty of constructing suitable sources;

the attempt to determine a rotation temperature using the intensities of the lines shows that agreement cannot be obtained between the calculated temperatures using branches P, Q and R simultaneously. A possible explanation is that the transmission probabilities calculated by Benedict, Plyler & Humphreys [63] and used in the determination of temperature

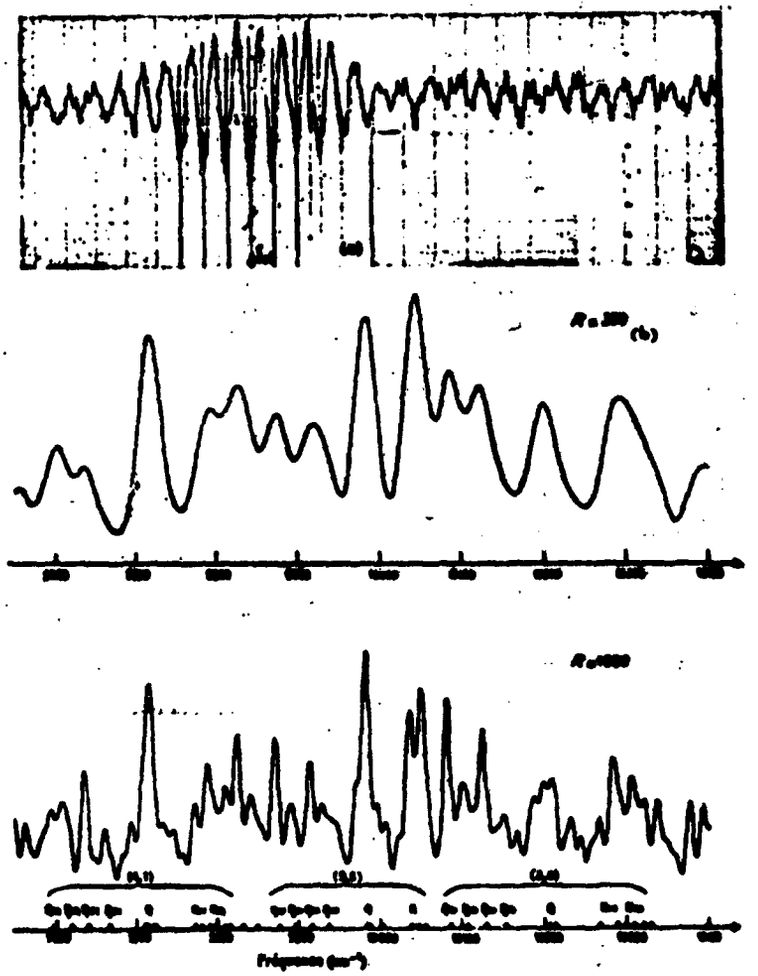

Fig. 84. (a) Interferogram of the Night Sky, Photomultiplier; (b) Spectrum of the Night Sky.

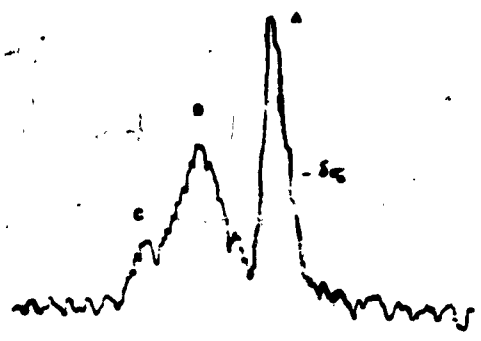

Fig. 85. Spectrum of Recombination Radiation Recorded by a Grating Spectrometer, R_0 = 1,400.

based on the intensities of the lines are false. Besides, the authors had predicted this possibility because they neglected the vibration-rotation interaction.

3. STUDY OF THE RE-EMISSION RADIATION OF GERMANIUM

We have also studied by this method the intrinsic recombination radiation in germanium. A complete study of the results obtained will be the subject of a thesis by O. Parodi. Here we shall confine ourselves to presenting the first spectra obtained.

A first study was made by C. Benoit à la Guillaume & O. Parodi who had studied with a grating spectrometer (Fig. 85) the recombination radiation emitted by a germanium crystal in which an excess of minority carriers had been created by optical injection. At the temperature of liquid helium, they discovered three lines. Lines A and C are due to the annihilation of an indirect exciton with simultaneous emission of a longitudinal acoustic photon (A) or optical tranverse photon (C). The origin of the line B which appears only below 2°K was not exactly determined. We have been able to prove that it was a line due to recombination at centers associated with dislocations. Its intensity varies with the point where the optical injection was made in the crystal; it disappeared when the sample was placed in a magnetic field.

The theoretical limit of resolution of the grating spectrometer $\delta\sigma_0$ was 4 cm^{-1}. The width of line A measured in the spectrum in Fig. 85 equals 14 cm^{-1}.

One could hope for several advantages of the F.T. method:

a. To explore a more extended spectral domain between 5,600 and 6,100 cm^{-1} without increasing the measurement time. In fact the question of this time is of first importance in this experiment because lighting the crystal heats it and the consumption of helium necessary to keep the temperature below 2°K increases rapidly.

b. To increase the signal/noise ratio which is necessary for two reasons:

1°. The recordings with a grating spectrometer did not allow sufficient precision in deducing the law of variation of the displacement of the line A as a function of the magnetic field in which the crystal is placed;

2°. One could hope to disclose the eventual presence of lines around 5,950 cm^{-1} whose existence had been suspected by Haynes [59];

c. To increase the resolution in order eventually to determine the structure of the line A.

Even though this problem may not be a problem with a great number of spectral elements, like that of the night sky, it appeared desirable to approach it with this method.

We tried several ways of recording the interferogram.

(1) Recording at a Constant Speed

Since the spectrum studied is much simpler than that of the night sky, the interferogram is very different (Fig. 86a). It has the appearance of a sine wave whose amplitude is slowly modulated:

maximum phase difference, L = 2.1mm;
theoretical limit of resolution, $\delta\sigma_0$ = 5.7 cm^{-1};
measurement time, 40 min.

In this case again, the recording speed is limited by the maximum speed of the recording pen

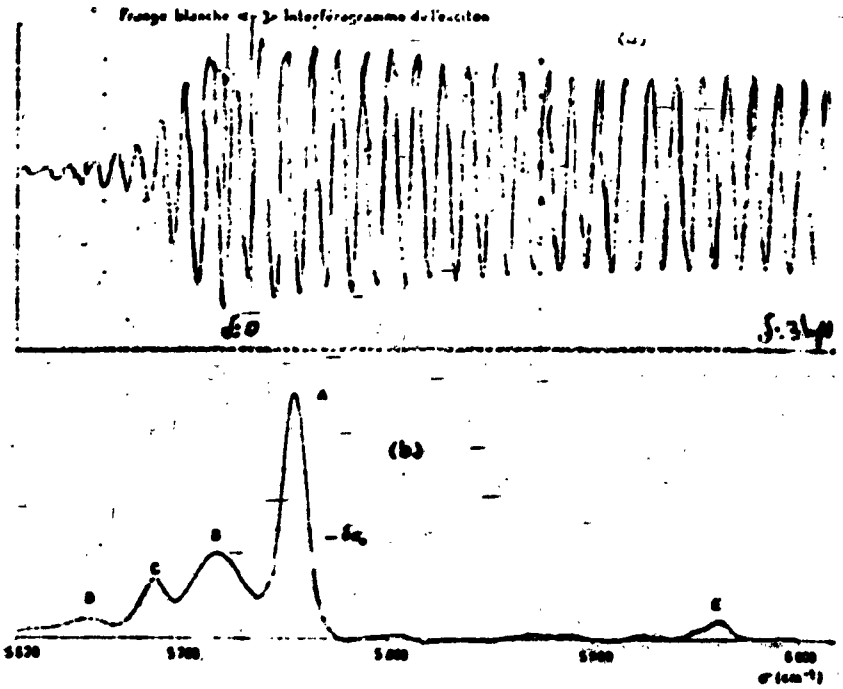

Fig. 86. (a) Interferogram Recorded at Constant Speed, R_0 = 1,000; (b) Spectrum Obtained From This Interferogram.

The spectrum calculated numerically from this interferogram is shown in Fig. 86b:

width at mid-height of the line, 14 cm^{-1};

signal/noise ratio for line A, of the order of 100.

Again one finds the lines A, B, C.

Furthermore the presence of a line D is disclosed around 5,655 cm^{-1} which can also be interpreted as a dislocation line (it appears only below 2°K and disappears in the field) and of a line E around 5,960 cm^{-1} whose origin is not explained and which apparently is double. In order to make sure, it is necessary to increase the resolution, hence the maximum phase difference obtained. It cannot be a question of making a recording at a constant speed because:

1°. The measurement time would be much too large with the recorder we used;

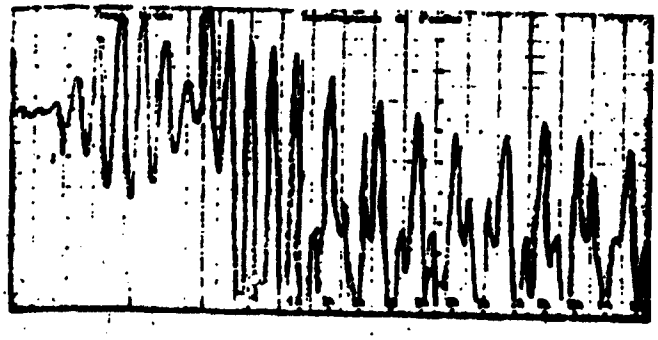

Fig. 87.

2°. The number of points to pick from the interferogram would be too large.

Two solutions can be considered: recording at a variable speed, the method of changing the frequency.

(2) Recording at Variable Speed

We have already explained in the preceding chapter that this system had been tried, had correctly functioned (Fig. 87) but that, being given the characteristics of our mechanical setup, the useable time was not a sufficient fraction of the total time and the s/n ratio was insufficient.

(3) Method of Changing the Frequency

This procedure allows the recording of lower electrical frequencies (hence an exploration speed which can be considerably increased and a measurement time very diminished) and at the same time the bringing into better coincidence the noise spectrum with the spectrum of the Fourier frequencies (hence a smaller number of points to choose).

The spectral domain occupied is $\Delta\sigma$ = 500 cm^{-1} between 5,600 and 6,100 cm^{-1}. If one chooses the heterodyne wave number σ_0 = 6,100 cm^{-1}, the spectrum to be studied after changing frequency is found between 0 and 500 cm^{-1} and can be obtained by a simple cosine transform of the new interferogram

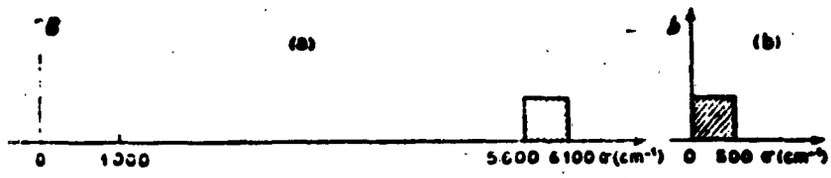

Fig. 88. Spectral Domain Occupied Before and After Changing the Frequency.

(Fig. 88). For the same speed of the moving carriage the maximum frequency of the signal to be studied will then be divided by 12.

Recall that, being given the irregularities in the carriage drive and frequency instabilities which result from it, there is no question of using an electrical signal furnished by a low-frequency oscillator in order to make a change of frequency. It must be furnished by the interferometer itself under the same conditions as the signal to be studied. We have not used the signal coming out of an optical line of wave number 6,100 cm^{-1} but, noticing that the wave number of the green mercury line is 18,312 cm^{-1} and that 18,312 $cm^{-1}/3$ = 6,104 cm^{-1}, one finds that it is sufficient to use the third harmonic frequency corresponding to the green mercury line.

SOME DETAILS OF THE EXPERIMENT. The diagram of the set-up is shown in Fig. 89, the apparatus itself in Fig. 90.

Reference Line. As reference line we have used the green mercury line. The signal furnished by the photomultiplier is sent on the one hand to a set of multivibrators which divide its frequency by 3, on the other hand to the writing relay of the recorder. Moreover this relay can write either a square pulse for each reference fringe or a signal having a frequency three times smaller.

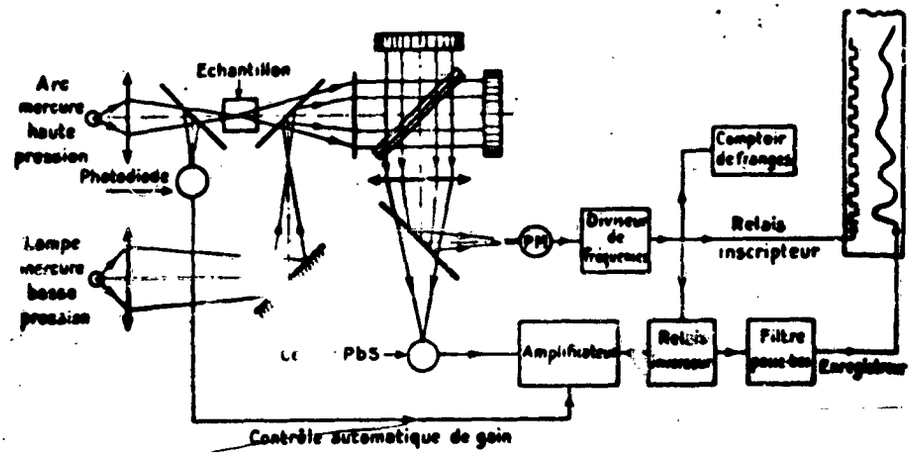

Fig. 89. Schematic Diagram for the Application of the Method of Changing Frequency. [High (low) pressure mercury arc (lamp), chopper, photomultiplier, frequency divider, fringe counter, writing relay; lead sulphide cell, automatic gain control, amplifier, inverting relay, low pass filter, recorder]

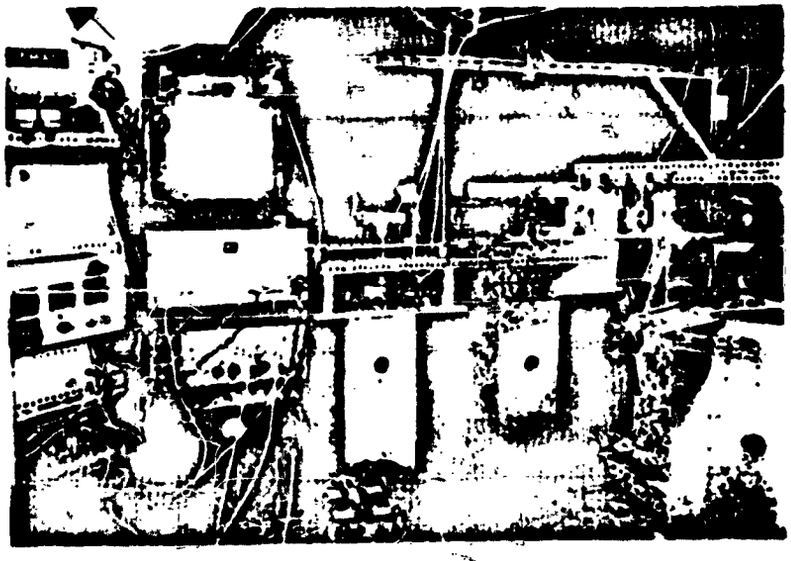

Fig. 90.

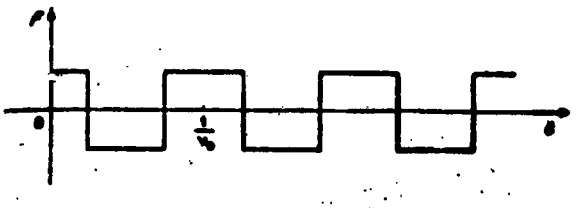

Fig. 91. Square-Pulse Function F(t) of Period $1/\nu_0$.

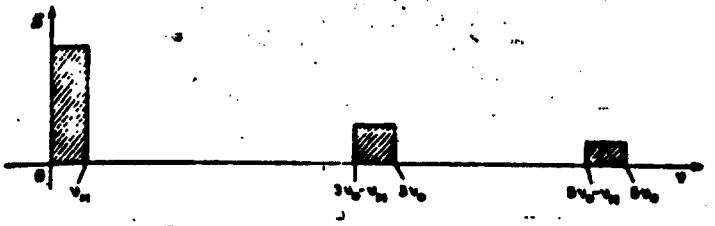

Fig. 92. Spectrum Obtained by the Cosine Transform of the Product I(t) F(t).

Change of Frequency. We have not multiplied the initial interferogram by a sinusoidal signal $\cos 2\pi\nu_0 t$, but by a square pulse function F(t) (Fig. 91) which one can put in the form

$$F(t) = \cos 2\pi\nu_0 t + \frac{1}{3}\cos 2\pi\, 3\nu_0 t + \frac{1}{5}\cos 2\pi\, 5\nu_0 t + \ldots ,$$

which is much easier to generate because all one has to do is invert the signal at equal time intervals[18].

Hence after multiplication, the frequencies to be analyzed occupy the intervals 0, ν_M (ν_M being the maximum frequency corresponding to $\sigma_M = 500$); $3\nu_0 - \nu_M$, $3\nu_0$; $5\nu_0 - \nu_M$, $5\nu_0$ (Fig. 9

[18] The inversion of the signal would take place at equal intervals of time if the advance of the carriage were perfect; practically it is done at time intervals corresponding to the passing of 1.5 fringes of the mercury line.

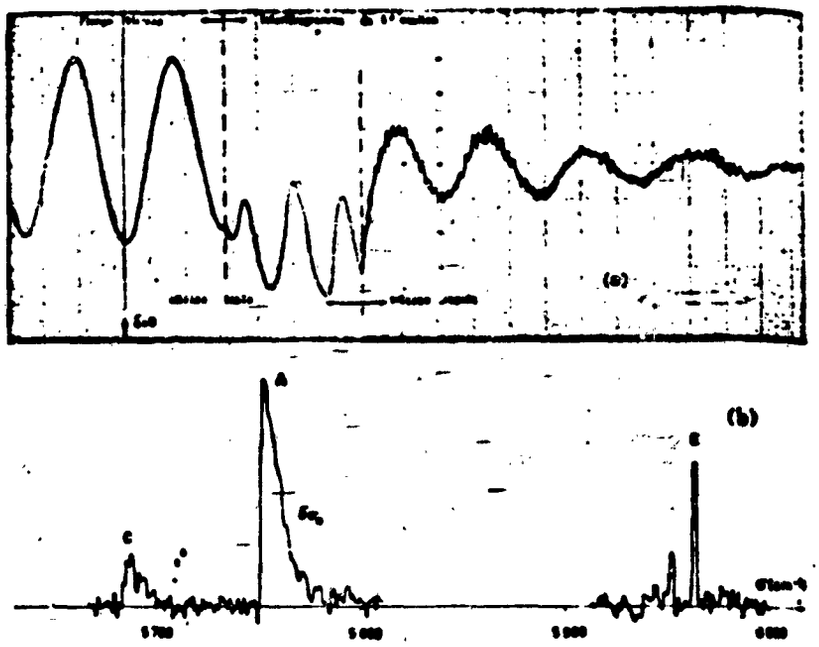

Fig. 93. (a) Interferogram Obtained by the Method of Changing Frequency; (b) Spectrum Deduced From This Interferogram, $R_0 = 6{,}000$.
[vitesse lente (rapide) = slow (fast) speed]

It is necessary to take into account the parasite spectra in the choice of the interval h. Their frequency is higher than that of the terms in $\nu_0 + \nu_M$ which, as we explained in the preceding chapter, are filtered by a low-pass filter. Moreover we shall make a numerical filtering which completely annuls their effect.

Suppression of the Mean Level. The signal furnished by the lead sulfide cell includes the modulated part, which we call the interferogram and with which we have been concerned up until now, and a constant component which after changing the frequency, gives an important signal at the frequency ν_0. Hence it is necessary to eliminate this constant signal by adding to it an equal signal in the opposite sense. A residue of the mean signal on the interferogram gives rapid oscillations which are superposed on the slow fringes of the new interferogram (Fig. 93a). This signal at the frequency ν_0 is moreover

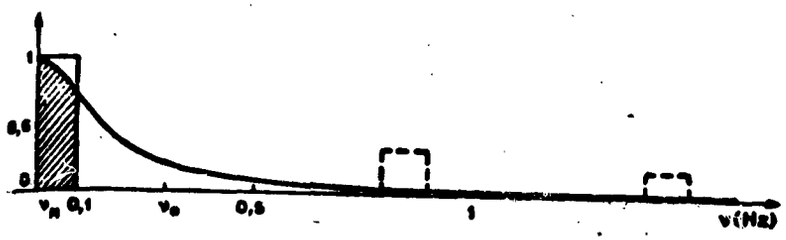

Fig. 94. Relative Position of the Noise Spectrum and of the Fourier Frequency Spectrum, τ = 1 sec.

strongly attenuated by the low-pass filter which is supposed to eliminate completely the terms of frequency $\nu_0 + \nu_M$.

Locating the Zero. In order that the marking be done with sufficient precision in the neighborhood of zero, the speed is 16 times smaller than the normal recording speed; at the passage of the white fringe furnished by a continuous source, one releases a counter which counts the fringes of the mercury line. Its indications set off the frequency multiplication; the same movement divides by 3 the frequency of the writing relay of the reference fringe. A last operation provides that at any instant whatever one may pass to a speed 16 times larger.

Recorded Interferogram (Fig. 93a). It has not been recorded under the best conditions:

maximum phase difference attained, L = 11.7mm;

theoretical limit of resolution, $\delta\sigma_\theta$ = 1 cm^{-1};

recording time, 1 hr, 30 min;

electrical frequencies of the signal to be studied taken between 0 and 0.1 cps (Fig. 94);

time constant τ = 1 sec.

Spectrum of Fig. 93b. Figure 93b shows the spectrum obtained from the interferogram of Fig. 93a:

value of the interval h, 0.5 sec, where h/τ = 0.5 and the s/n ratio in the spectrum is practically the same as if one had used all the points of the interferogram;

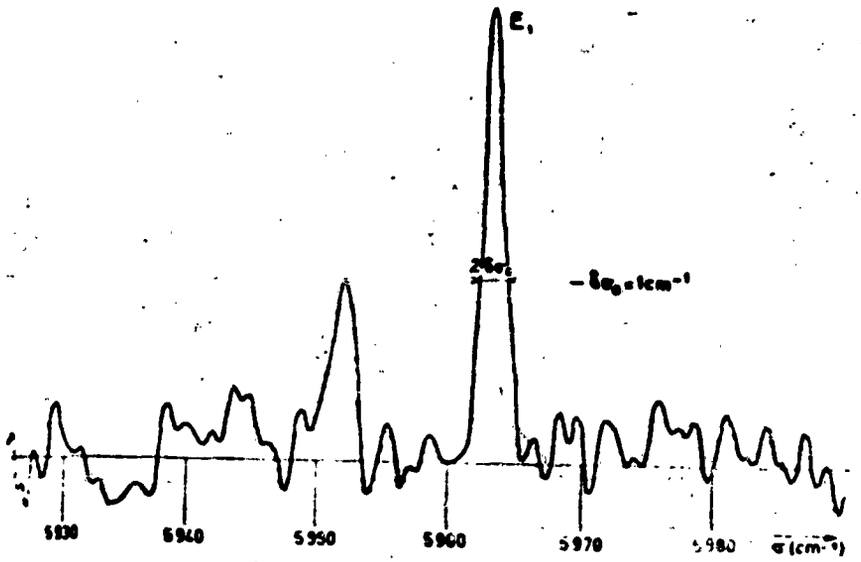

Fig. 95. Intrinsic Recombination Radiation in Germanium, R_0 = 6,000.

number of points chosen, 12,672;

number of calculated points, 401.

A numerical filtering (width of the filter was chosen equal to 500 cm^{-1}) resulted in the reduction of the number of points used for making the F.T.

The calculation was made only in the regions of the lines A, C and E. Calculation time: 22 min.

An examination of the spectrum shows two interesting results:

the line A is distinctly asymmetric;

the line E is divided into two lines at 5,952 and 5,963 cm^{-1};

detailed examination of the line E_1 (Fig. 95) shows that its width is of the order of 2 cm^{-1}; thus it has been studied with an excessive resolution. Also in later experiments whose results are not given here, we contented ourselves with a resolution of the order of 4,000. Since the noise in the spectrum of Fig. 93b appeared to us to be due in a great part to the fluctuations of the mean level of the interferogram,

we stabilized the mercury arc and reduced the potential of the lead sulfide cell as is indicated in Fig. 89.

4. CONCLUSION

The use of the Fourier transformation method allowed us to go from a resolution of 150 to a resolution of 2,000 in the study of the radiation emitted by the night sky. In the case of the recombination radiation in germanium, a problem with a small number of spectral elements, the results are less spectacular. However, we have been able to demonstrate the asymmetry of the line due to the annhiliation of an exciton with emission of a longitudinal acoustic photon and the presence of two lines around 5,960 cm^{-1} whose origin is not accounted for yet.

VII. COMPARISON OF DIFFERENT SPECTROSCOPIC METHODS

The Fourier transformation spectroscopic method that we have just treated requires very different techniques from those of classical methods. However there are no fundamental differences among all the methods. Whatever method is used, the reproduced spectrum is always the cosine transform of the even part $\Gamma(\delta)$, of the autocorrelation function $C(\delta)$ of the incident luminous vibration. It is this function $\Gamma(\delta)$ that up till now we have called "interferogram".

We are going to show how, in classical methods (prism, grating, or Fabry-Perot spectrometer) the flux that one measures at the exit of the instrument is the F.T. of $\Gamma(\delta)$, obtained, for each frequency, as the sum of a particular series of n equidistant discrete values of $\Gamma(\delta)$, n being the number of interfering beams. In the Fourier transformation method, n - 2; the flux that one measures for the value h of the phase difference is the sum of only two particular values of $\Gamma(\delta)$: $\Gamma(0)$ and $\Gamma(h)$ and it is necessary to make the Fourier transformation a posteriori.

One particularly rapid way of making a synthesis of different spectroscopic methods consists in applying to the treatment of the luminous vibration by a spectrometer, some of the more elementary results relative to the determination of the spectrum of fluctuating magnitudes. Indeed the electromagnetic field at a point in space is a random function of time. Fellgett [14,15], Gebbie [20] and Mertz [64] have already briefly indicated this way of treating spectroscopic instruments. The theoretical problems relative to the random magnitudes and to their spectra have been treated in a satisfactory way for the first time by Wiener and Lévy in a study of Brownian

movement. Since then, these studies have been pushed very far from a purely mathematical point of view and the results have been applied to the theory of turbulence and to the treatment of background noise in the theory of communications.

Before developing the particular case of optical spectroscopy we are going to recall some definitions and theorems concerning the spectral analysis of a random variable.

1. ROLE OF A LINEAR, HOMOGENEOUS FILTER IN SPECTRAL ANALYSIS

One can associate with a variable $X(t)$ [deterministic or random function of time] a power spectrum only if the mean power $E\{|X(t)|^2\}$, defined as the arithmetic mean of the quantity $|X(t)|^2$ measured at the same instant t for an infinity of trials macroscopically identical, is independent of time. Then for each frequency component ν obtained using $X(t)$ in a Fourier decomposition:

$$X(t) = \int_{-\infty}^{+\infty} b(\nu)\, e^{2i\pi\nu t}\, d\nu ,$$

it will be possible to assign a definite $B(\nu)$.

The mean power is the sum

$$E\left\{|X(t)|^2\right\} = \int_{-\infty}^{+\infty} B(\nu)\, d\nu . \qquad \text{(VII.1)}$$

We are interested only in random functions fulfilling these conditions; these are the functions one meets in optics. They are functions with stationary covariance and their study rests for a large part on the theorem of Khinchin according to which the F.T. of the correlation function $C_X(\tau) = E\{X(t)\, X^*(t-\tau)\}$ is precisely $B(\nu)$:

$$B(\nu) = \int_{-\infty}^{+\infty} C_X(\tau)\, e^{-2i\pi\nu\tau}\, d\tau . \qquad \text{(VII.2)}$$

A spectral analysis is made with the aid of a filter. We shall call the linear filter $\widehat{d}$ ([48] p. 347) a linear, homogeneous transformation with respect to time which makes Y(t) correspond to the variable X(t) in such a way that

$$(VII.3) \quad Y(t) = X(t) * P(t) = \int_{-\infty}^{+\infty} X(\theta)\, P(t-\theta)\, d\theta ,$$

P(t) being the percussional response of the filter, i.e., its response to the Dirac impulse[19].

The complex quantity $G(\nu)$ with modulus $g(\nu)$ which is called filter gain is the F.T. of P(t)

$$(VII.4) \quad G(\nu) = \int_{-\infty}^{+\infty} P(t)\, e^{-2i\pi\nu t}\, dt .$$

Two classical calculations lead to putting the mean power, after filtering, in one or the other of two fundamental forms:

$$(VII.5) \quad E\left\{|Y(t)|^2\right\} = \int_{-\infty}^{+\infty} B(\nu)\, |G(\nu)|^2\, d\nu ,$$

[19] In the electromagnetic theory of light [65] a light impulse is a train of very short waves, which gets shorter when its distribution into given frequencies given by a Fourier expansion gets larger (Fig. 96).

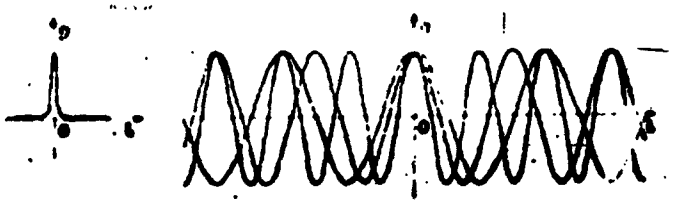

Fig. 96. Light Impulse and its Fourier Decomposition.

(VII.6) $$E\left\{|Y(t)|^2\right\} = \int_{-\infty}^{+\infty} C_\chi(\tau)\, C_p(\tau)\, d\tau ,$$

$C_p(\tau)$ being the autocorrelation function of P(t).

These two equations are equivalent; moreover one can pass from one to the other by Parseval's relation, after noticing that the F.T. of $C_\chi(\tau)$ is the spectral decomposition $B(\nu)$ looked for and that the F.T. of $C_p(\tau)$ is the square of the modulus of the gain of the filter $\mathcal{F}$.

Moreover we can notice that when the function P(t) is real, it is simply the real part $\mathrm{Re}[C_\chi(\tau)] = \mathcal{C}_\chi(\tau)$ which enters into Eq. (VII.6); it then becomes[(*8)]

(VII.7) $$E\left\{|Y(t)|^2\right\} = \int_{-\infty}^{+\infty} \mathrm{Re}\left[C_\chi(\tau)\right] C_p(\tau)\, d\tau .$$

The real part of a correlation function being even, its F.T. is also an even function and the relation (VII.5) then takes

---

(*8) In fact

$$E\left\{|Y(t)|^2\right\} = E\left\{Y(t)Y^*(t)\right\} = E\left\{\frac{1}{2}\left[Y(t)Y^*(t) + Y^*(t)Y(t)\right]\right\}$$

$$= E\left\{\frac{1}{2}\iint \chi(\theta)P(t-\theta)d\theta\chi^*(\theta')P^*(t-\theta')d\theta' + \right.$$

$$\left. + \frac{1}{2}\iint \chi^*(\theta)P^*(t-\theta)d\theta\chi(\theta')P(t-\theta')d\theta'\right\}.$$

In the case where P(t) is a real function, $P(t-\theta) \equiv P^*(t-\theta)$ and one can group terms:

$$E\left\{|Y(t)|^2\right\} = \iint\left[\frac{1}{2}E\left\{\chi(\theta)\chi^*(\theta')\right\} + \frac{1}{2}E\left\{\chi^*(\theta)\chi(\theta')\right\}\right]$$

$$P(t-\theta)P(t-\theta')d\theta d\theta' = \int_{-\infty}^{+\infty}\frac{1}{2}\left[C_\chi(\tau)+C_\chi^*(-\tau)\right]C_p(\tau)d\tau =$$

$$= \int_{-\infty}^{+\infty} \mathrm{Re}\left[C_\chi(\tau)\right] C_p(\tau)\, d\tau .$$

the form

$$\text{(VII.8)} \qquad E\left\{|Y(t)|^2\right\} = \int_{-\infty}^{+\infty} B_p(\nu)\,|G(\nu)|^2\,d\nu\ ,$$

$B_p(\nu)$ being the even part of the spectrum $B(\nu)$ as was defined in Chapter II.

Formula (VII.8) shows that the mean power is the chopped energy in the spectrum times the energy transmission curve of the filter $|G(\nu)|^2$. If $\mathcal{J}$ is a rectangular band-pass filter, one has $|G(\nu)|^2 = 1$ where ν is taken between ν_1 and ν_2 and $G(\nu) = 0$ elsewhere. The ideal filter for making the spectral analysis will have zero width but, if ν_1 and ν_2 are very close together, one can say that the measured power is proportional to the spectral density corresponding to a frequency ν_0 taken between ν_1 and ν_2. Then,

$$\text{(VII.9)} \qquad E\left\{|Y(t)|^2\right\} = B(\nu_0)\,\Delta\nu\ .$$

One explores the spectrum by varying the band-pass of the filter.

2. GENERALITIES ABOUT THE SPECTROMETERS CONSIDERED AS FILTERS

A classical spectrometer (prism, grating, Fabry-Perot) or a two-beam interferometer used as a spectrometer is composed of an optical part which at every instant receives luminous radiations and transmits a certain proportion of them to a detector-amplifier-measuring setup, which is provided with a time constant and measures the mean power carried by the transmitted radiations. Let us first consider the case of the spectrometer used with infinitely thin entrance and exit diaphragms, the useful practical case being easily deduced from this (Fig. 97a). Let $X(t)$ be the value of the electric field in the interior of the entrance diaphragm (point source) and

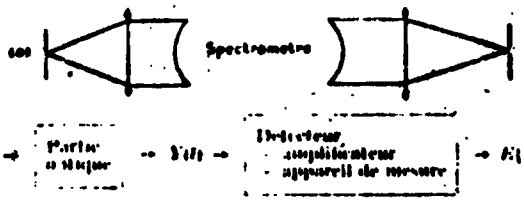

Fig. 97. (a) Schematic Diagram of the Optical Part of a Spectrometer; (b) Schematic Diagram of the Operation of a Spectrometer.

Y(t) the value of the electric field in the interior of the exit diaphragm where the detector is placed (Fig. 97b). The signal furnished by the latter is amplified then transmitted to a recorder, the ensemble having a time constant τ so that one measures approximately the quantity

$$\int_t^{t+\tau} |Y(t)|^2 \, dt .$$

We shall suppose that in what follows that the time τ is big enough so that we need not distinguish between $\int_t^{t+\tau} |Y(t)|^2 \, dt$ and the mean power $\overline{|Y(t)|^2}$ (which will be rigorous only if $\tau \to \infty$). This approximation completely neglects noise, which we do not consider in this chapter. The Laplacian stationary character of X(t) being given, $\overline{|Y(t)|^2}$ has the same value as $E\{|Y(t)|^2\}$.

The problem is to determine with what approximation $E\{|Y(t)|^2\}$, which we shall henceforth call Φ, the flux measured by the detector[81] is the spectrum of X(t) such as we have

[81] In the theoretical case considered here, the diaphragms are infinitely thin and Φ is a line. In all practical cases, the beam will have width U and one will measure a flux.

defined it in paragraph VII.1, i.e., to what approximation the instrument takes the F.T. of the autocorrelation function of X(t).

(1) Expression for the Flux Φ

The spectrometer breaks up the incident radiation into different components (spatially in the case of grating or prism spectrometer, amplitudinally in the case of the Fabry-Perot spectrometer) which it transmits with optical delays in arithmetic progression and different attenuations before combining them in such a way that Y(t) can be put in the form

$$\text{(VII.10)} \quad Y(t) = \rho_1 X(t) + \rho_2 X(t-\tau_1) + \rho_3 X(t-2\tau_1) + \ldots + \rho_n X[t-(n-1)\tau_1] ,$$

where $k\tau_1$ is the delay of the (k+1) beam and ρ_{k+1} is its transmission factor. This sum is equivalent to the integral[88]

$$\text{(VII.11)} \quad Y(t) = \int_{-\infty}^{+\infty} X(t-\tau)\rho(\tau)d\tau = \int_{-\infty}^{+\infty} X(t-\tau)P(\tau)R(\tau)d\tau ,$$

$R(\tau)$ being a Dirac distribution of periodic support of interval τ_1 and $P(\tau)$ a distribution function which takes on the particular values $\rho_1, \rho_2, \ldots, \rho_n$ for $\tau = 0, \tau_1, \ldots, (n-1)\tau_1$ and can eventually become zero for $\tau > n\tau_1$ if the number of transmitted beams before the recombination is finite. Since a convolution is commutative, (VII.11) is equivalent to

$$\text{(VII.12)} \quad Y(t) = \int_{-\infty}^{+\infty} X(\theta)\rho(t-\theta)\,d\theta .$$

In this form, the analogy with (VII.3) is complete; $\rho(t)$ is the percussional response of the spectrometer considered

[88] In the case of the prism, the number of interfering beams is infinite and the interval of the function R(τ) is zero.

as a linear filter. It is a real-valued function. Therefore one can write immediately, by comparison with (VII.8) and (VII.7),

$$\Phi = \int_{-\infty}^{+\infty} B_p(\nu)\ |G(\nu)|^2\ d\nu \quad \text{and} \quad \Phi = \int_{-\infty}^{+\infty} \mathcal{C}_X(\tau)\ C_p(\tau)\ d\tau\ .$$

Noticing that ν, t, τ and τ_1 are related to the wave number σ, to the length l measured in the wave train and to the geometric delays δ and h by the relation $\sigma = \nu/l$, $l = tc$, $\delta = \tau c$ and $h = \tau_1 c$, the two preceding equations take the form

$$\Phi = \int_{-\infty}^{+\infty} B_p(\sigma)\ |G(\sigma)|^2\ d\sigma\ , \tag{VII.13}$$

and

$$\Phi = \int_{-\infty}^{+\infty} \mathcal{C}_X(\delta)\ C_p(\delta)\ d\delta\ . \tag{VII.14}$$

These two equations have been established for a particular value of delay h between two consecutive beams; the functions $P(l)$ and $p(l)$ and the flux are functions of h. In the following we shall use the two relations (VII.13) and (VII.14) [which are in fact equivalent]. It is in considering the second relation that we shall see how the instrument makes the F.T. of $\mathcal{C}_X(\delta)$, an operation whose result is interpreted by the first relation.

The function $C_p(\delta)$ is the autocorrelation function of the product $P(l)\ R_h(l)$. Hence it is still the product of Dirac distribution of periodic support, of the same interval h, with an even function $A(\delta)$ which is the autocorrelation function of $P(l)$:

$$C_p(\delta) = A(\delta)\ R_h(\delta)\ . \tag{VII.15}$$

We shall see in what follows for each type of spectrometer, the particular form of $A(\delta)$ that we have been talking about up till now will play the same role as the weighting function introduced in the Fourier transformation method.

Replacing $C_p(\delta)$ by its value in (VII.14) we get

$$\text{(VII.16)} \qquad \Phi(k) = \int_{-\infty}^{+\infty} \mathcal{C}_\chi(\delta)\, A(\delta)\, R_k(\delta)\, d\delta \ ,$$

which is equivalent to

$$\text{(VII.17)} \qquad \Phi(k) = \mathcal{C}_0\, A_1 + 2\,\mathcal{C}_1\, A_2 + \ldots + 2\,\mathcal{C}_{n-1}\, A_n = \sum_{k=-(n-1)}^{k=n-1} \mathcal{C}_k\, A_{k+1} \ .$$

It is a finite sum of discrete values of the autocorrelation function of the incident radiation, multiplied by the weighting function $A(\delta)$ appropriate for the instrument. It is easy to show that this is a Fourier transformation. In fact, nothing changes in the value of the sum (VII.17) if one multiplies each term by the factor $\cos 2\pi\sigma_k k\delta$ in which σ_k has been chosen equal to m/δ, m being an integer, in such a way that the cosines are always equal to 1. The new sum

$$\text{(VII.18)} \qquad \Phi(k) = \sum_{k=-(n-1)}^{k=n+1} \mathcal{C}_k\, A_{k+1} \cos 2\pi\sigma_k k\delta$$

is equivalent to

$$\text{(VII.19)} \qquad \Phi(k) = \int_{-\infty}^{+\infty} \mathcal{C}_\chi(\delta)\, A(\delta)\, R_k(\delta) \cos 2\pi\sigma_k \delta\, d\delta \ .$$

This is exactly the expression (II.13) giving the value of a spectral density calculated by taking the numerical F.T. of the interferogram. By putting $F(\sigma) = T_{\cos}\,[A(\delta)\, R_k(\delta)]$, one can write (VII.19) in the form

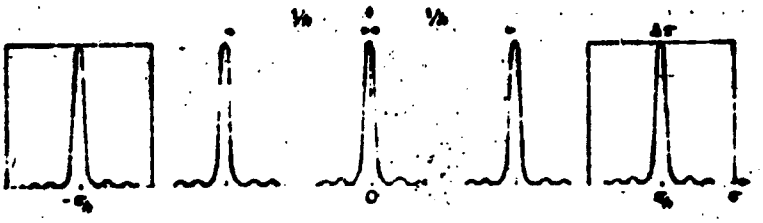

Fig. 98, Apparatus-Function.

(VII.20) $$\Phi_{(k)} \equiv B_p(\sigma_k) =$$

$$= \frac{1}{2}\int_{-\infty}^{+\infty} B_p(\sigma)\,[F(\sigma_k-\sigma) + F(\sigma_k+\sigma)]\,d\sigma\ .$$

In comparing (VII.13) and (VII.20) one sees that

(VII.21) $$|G(\sigma)|^2 = \frac{1}{2}\,[F(\sigma_k-\sigma) + F(\sigma_k+\sigma)]\ .$$

The spectral density measured for the wave number σ_k hence is the chopped energy in the spectrum multiplied by the function $|G(\sigma)|^2$ which spectroscopists call apparatus-function.

(2) Form of the Apparatus-Function

We have emphasized the analogy between the expressions (VII.19) and (II.13). Similarly the equations (VII.21) and (II.14) show that, in the classical spectrometers as in the case of the numerical F.T. of an interferogram, the apparatus-function is composed of two series of peaks separated by a distance $1/k$ and centered about σ_k and $-\sigma_k$, each one of the peaks being the F.T. of the weighting function $A(\delta)$ of the interferogram. However there are some little differences in the case where the numerical F.T. is taken as was indicated in Chapter II. In the case of a classical spectrometer since σ_k, the wave number for which the F.T. is made, is an integer multiple of $1/k$, there always is a peak centered about the origin (Fig. 98) and the

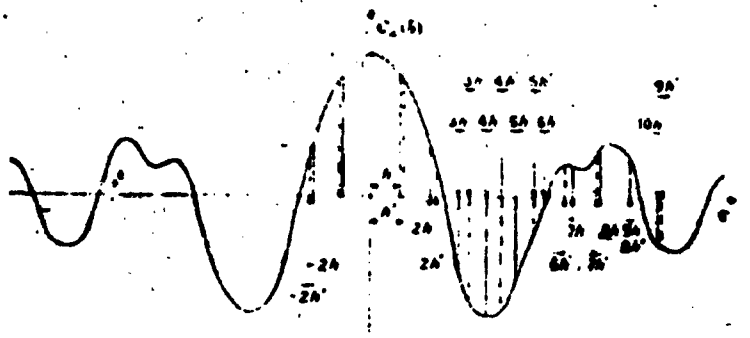

Fig. 99. Autocorrelation Function $C_\chi(\delta)$ and Grating Functions R_h of Different Intervals.

two series of peaks of the apparatus-function are mixed together in such a way that one can write

$$B_p(\sigma_k) = \int_{-\infty}^{+\infty} B_p(\sigma)\, F(\sigma_k - \sigma)\, d\sigma \,. \qquad \text{(VII.22)}$$

When one explores the spectrum, that is when one looks for the spectral density corresponding to a number σ_k, in the neighborhood of σ_k, one changes the delay between two consecutive beams which becomes h'. Hence one changes the interval of the grating function $R_h(\delta)$ which serves to pick off points in the function $\tilde{\gamma}_\chi(\delta)$ [Fig. 99]. The new value $B(\sigma_{k'})$ is therefore obtained from a new series of values of $\tilde{\gamma}_\chi(\delta)$. The new apparatus-function is not deduced from the first by two translations as is the case when one makes the numerical F.T. of an interferogram using a single series of equidistant values picked off on this interferogram as explained in Chapter II. The distance $\Delta\sigma$ between two consecutive peaks is then equal to $1/h'$, but one of the peaks remains centered about the origin (Fig. 100). Moreover, in the strictest sense, $A(\delta)$ is a function of h and the form of each maximum varies with h; of course the variations will be negligible in the spectral domain explored.

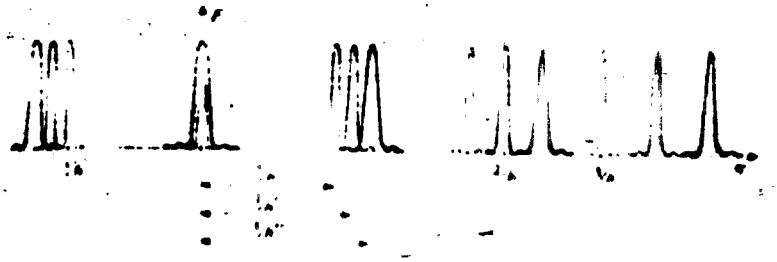

Fig. 100. Deformation of the Apparatus-Function With the Value h of the Interval; One of the maxima Remains Centered on the Zero Frequency.

We have seen that when one calculates the numerical F.T. of an interferogram, one chooses precisely the interval h in such a way that a single peak explores the spectrum. In the case of classical spectrometers, it is necessary to take the precaution eventually to limit by an optical filter the spectrum to be studied in such a way that the spectral interval occupied $\Delta\sigma$ be at most equal to $1/h$ (Fig. 98).

In general one calls the limit of resolution the width at mid-height of one of the peaks of the apparatus-function. This width will be the narrower the wider its F.T., $A(\delta)$, is, hence one will know a greater portion of its autocorrelation function.

3. FORMS OF APPARATUS-FUNCTIONS OF CLASSICAL SPECTROMETERS

It suffices to determine $p(l)$ in each type of spectrometer in order to discover immediately its theoretical apparatus function.

(1) Grating Spectrometer

Consider a grating with n slits infinitely thin and the vibrations issuing from these n slits in the direction θ' (Fig. 101a); $p(l)$ is then a Dirac distribution of interval $h = a(\sin\theta - \sin\theta')$, a being the distance between two lines of the grating, limited by a square pulse function of width $L = (n-1)\,h$ (Fig. 101b). If the grating receives an impul-

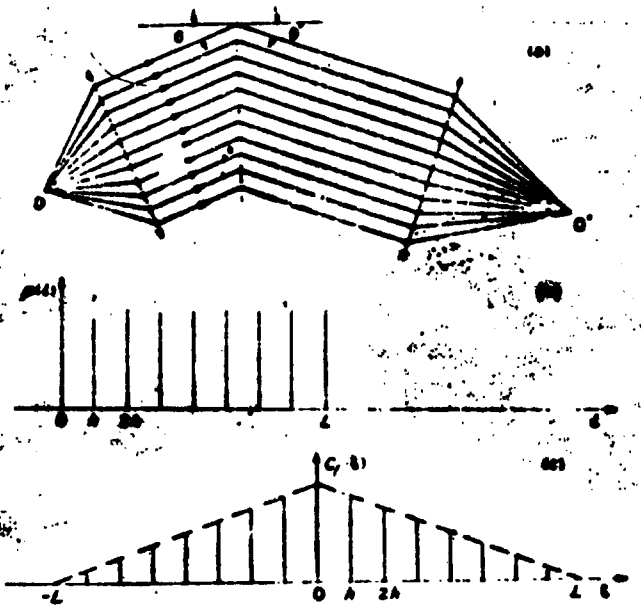

Fig. 101. (a) Schematic Diagram of a Grating Spectrometer; (b) Impulse Response of a Grating Spectrometer; (c) Autocorrelation Function of the Impulse Response of a Grating Spectrometer.

of light it transmits n impulses in the direction θ'. $C_p(\delta)$ is a Dirac distribution of interval h, modulated by a triangular function $A(\delta)$ which is zero outside the interval $-L$, $+L$ (Fig. 101c). Hence the expression of the apparatus-function

$$F(\sigma) = |G(\sigma)|^2 = T_{\cos}[C_p(\delta)] = \sum_{m=-n}^{m=+n} L^2 \left| \frac{\sin \pi L \left(\frac{m}{n} - \sigma \right)}{\pi L \left(\frac{m}{n} - \sigma \right)} \right|^2 .$$

(2) Fabry-Perot Spectrometer

Let e be the distance separating the two plates, r the amplitude reflection factor of the surfaces of the plates (Fig. 102a). In this case (Fig. 102b),

$$p(l) = r^{2\,l/h}\, R_h(l) = \exp\left(-\frac{1}{h} \operatorname{Log} \frac{1}{r^2} \right) R_h(l) ,$$

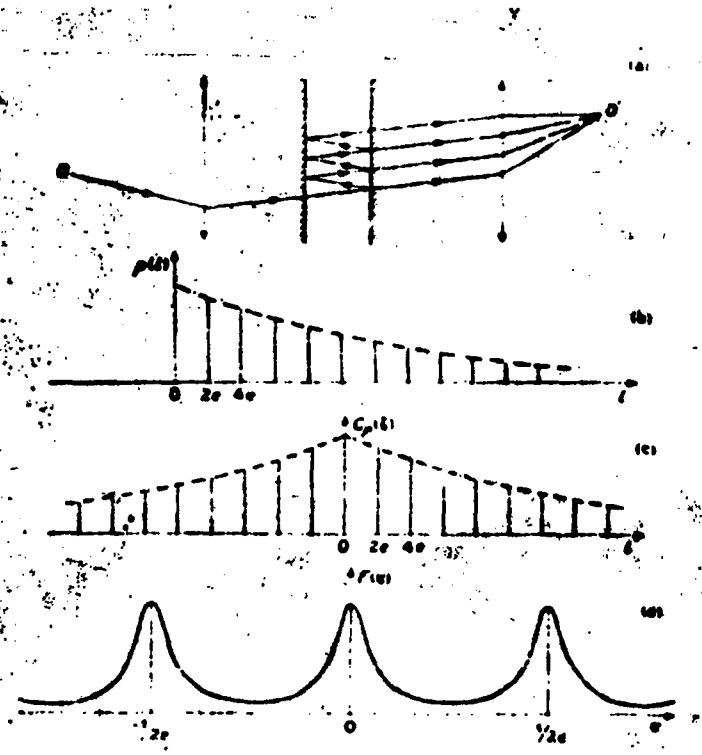

Fig. 102. (a) Schematic Diagram of a Fabry-Perot Spectrometer; (b) Impulse Response of a Fabry-Perot Spectrometer; (c) Autocorrelation Function of the Impulse Response of a Fabry-Perot Spectrometer; (d) Apparatus-Function of a Fabry-Perot Spectrometer.

where (Fig. 102c)

$$A(\delta) = \exp\left(-\left|\frac{l}{k}\right| \operatorname{Log} \frac{1}{r^2}\right)$$

and

$$F(\sigma) = |G(\sigma)|^2 = T\cos\left[\varphi(\delta)\, K_1(\delta)\right] =$$

$$= \sum_{n=-\infty}^{n=+\infty} \frac{(1/n)\operatorname{Log}(1/r^2)}{\left|\frac{1}{k}\right| \operatorname{Log}\frac{1}{r^2} + 4\pi^2\left(\frac{n}{k} - \sigma\right)^2}.$$

This is the superposition of the resonsance functions which repeat at multiples of $1/h$. This is an Airy function whose width at mid-height is $\delta\sigma = (1/h)(1-r^2)/\pi r$ (Fig. 102d).

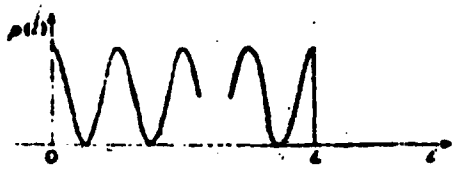

Fig. 103. Impulse Response of a Prism.

(3) Prism Spectrometer

Lord Rayleigh [66] studied the propagation of an impulse in a dispersive medium and made an application of it in the case of a prism. He showed that the percussional response of a prism in a given direction is a train of sinusoidal waves of frequency ν_1 and of length $L = e(dn/d\lambda)\,\lambda_1$ with $\lambda_1 = c/\nu_1$, if e is the length of the base of the prism (Fig. 103) and

$$F(\sigma) = |G(\sigma)|^2 = \left[\frac{\sin \pi L(\sigma_1-\sigma)}{\pi L(\sigma_1-\sigma)}\right]^2 .$$

In this case $C_p(\delta) = A(\delta)$. $A(\delta)$ is a triangular function, zero outside of the domain $-L, +L$. The function $R_h(\delta)$ has an infinitely small interval because there is an infinity of rays which interfere. The spectrum which one obtains with the prism is unique.

4. FOURIER TRANSFORMATION METHOD

In a two-wave interferometer, the incident vibration is divided into two vibrations of equal amplitude. If the instrument receives an impulse, it transmits two staggered impulses in the time $\tau_1 = h/c$ (Fig. 104a); $C_p(\delta)$ has a particularly simple form. It is composed of three verticals: two at $\delta = \pm h$ of height 1 and another of double height at $\delta = 0$ (Fig. 104b) in such a way that

$$\Phi(h) = \int_{-\infty}^{+\infty} \mathcal{F}_X(\delta)\, C_p(\delta)\, d\delta = 2\,\mathcal{F}_X(0) + 2\,\mathcal{F}_X(h) .$$

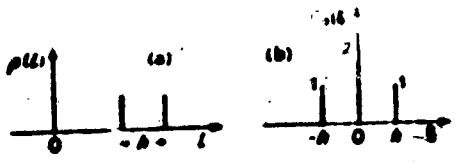

Fig. 104. (a) Impulse Response of a Michelson Interferometer; (b) Autocorrelation Function of the Impulse Response of a Michelson Interferometer.

Here $\Phi(h)$ is the sum of two particular values of $\mathcal{C}_\chi(\delta)$. This is not enough to make a Fourier transformation. In fact, $\Phi(h)$ is composed of a constant part $\mathcal{C}_\chi(0)$ of a variable part which gives precisely $\mathcal{C}_\chi(\delta)$ when one varies h linearly as a function of time.

To reconstruct the spectrum from the interferogram, one should be able to treat the interferogram exactly as the classical spectrometers do, by forming for the calculation of the spectral density corresponding to each wave number the sum of a particular series of discrete and equidistant values of the interferogram. One should be able, of course, to choose $A(\delta)$ at will in such a way that one could obtain exactly the same theoretical apparatus-function as with a classic spectrometer, with the two series of peaks mixed together and a peak constantly centered on the zero frequency. But practically, it is much simpler to choose a single series of values of $\mathcal{C}_\chi(\delta)$ and numerically to take the Fourier transformation by varying the cosines as explained in Chapter II.

5. CONCLUSION

All spectrometers take the F.T. of the even part $\mathcal{C}_\chi(\delta)$ of the autocorrelation function of the luminous vibration. The resolution is limited because $\mathcal{C}_\chi(\delta)$ is known only between 0 and L, the maximum phase difference between the interfering beams. When the disperser is a prism, the F.T. of $\mathcal{C}_\chi(\delta)$ is made by using a continuous sequence of values between 0 and L, and the spectrum obtained is unique. In the other classical spectrometers the F.T. is obtained as the sum of discrete equidistant values of $\mathcal{C}_\chi(\delta)$; the apparatus-function is therefore

composed of a series of peaks, each one of them being the F.T. of the weighting function A(δ) appropriate for the instrument which multiplies $\sigma_\chi(\delta)$. In the Fourier transformation method it is $\sigma_\chi(\delta)$ which is measured. One can either make the F.T. by using a continuous sequence of values of $\sigma_\chi(\delta)$ as for the prism, in which case the spectrum obtained is unique; or numerically calculate the F.T. using discrete equidistant values of $\sigma_\chi(\delta)$. If one uses a different series of values for each wave number, since one can choose A(δ) at will, one can obtain exactly the same apparatus-function as with any classical spectrometer. When the Fourier transformation is made based on a single series of values of $\sigma_\chi(\delta)$, the apparatus-function is composed of two series of peaks which are displaced in opposite directions during the exploration and the limit of resolution is fixed from one extremity of the spectrum to the other.

VIII. CONCLUSION

In conclusion, it seems to us that the spectrometric method using Fourier transformations is, in the infrared, the most powerful of the spectrometric methods. Indeed it unites the fundamental advantage of the classical interferometric methods, namely the large useable solid angle, and that of the "multiplex" methods, in which the whole measuring time is used for the determination of each spectral element. Its superiority over the other methods increases with the number of spectral elements to be studied. It permits us to treat in the near infrared two problems at least one of which would have been impossible to resolve by other methods. In both cases, the gain which can be attained is expressed as a considerable increase in resolution.

But its use, as soon as the desired resolutions pass several thousands, poses some problems which are not yet resolved: obtaining a large phase difference without putting the interferometer out of order and calculating the F.T. of the interferogram. In order to perform this last operation, at the present time two devices are used: harmonic analyzers which do not allow one to exceed resolutions of the order of 100 and digital computers.

The calculation time for a spectrum by a numerical Fourier transformation is proportional to the number N of input points. In the absence of noise, N will be of the order of the number M of spectral elements in the spectrum to be studied. The study of the factors upon which noise in the calculated spectrum depends shows that in order to obtain the maximum signal/noise ratio in the spectrum, if the interferogram has been recorded through a low-pass filter, N can be very much larger than M. Several ways of recording the

interferogram or of calculating / llow one to obtain the spectrum under the best conditions and at the same time to use a number N near 1' to make the Fourier transform: static recording, method of changing the frequency, numerical filtering. Whatever method is used when treating a problem with a great number of spectral elements by Fourier transformation, one meets two difficulties: the first which deals with the need to pick off a great number of points from the interferogram can be mitigated by using a converter system which records directly on punched cards the necessary values of the interferogram. But the second which is concerned with the long calculation time and the delay which occurs between recording the interferogram and obtaining the spectrum is inevitable. The regular use of this method for problems at even medium resolution, hence appears difficult as long as one does not have a high-speed calculator available for Fourier transforms which allows one to obtain the spectrum very rapidly after recording the interferogram.

In concluding I must express my appreciation to Professor Jacquinot who started me on this research.

I thank P. Connes, my fellow research workers H. Gush and O. Parodi for the part they have taken in the experimental work and for numerous and fruitful discussions, P. Giacomo for the help he gave me at the time of the construction of the interferometer, R. Chabbal, all the technicians and workers of the Aimé Cotton Laboratories, and J. Arsac for the advice he gave me in the study of questions concerning noise.

Equally I thank the Committee of the European Scientific Computing Center and Mr. Wattson, Director of the Computing Center of the University of Toronto, for granting hours of free computing time on the IBM 704 and 650.

REFERENCES

[1] P. Jacquinot, 17e Congrés du G.A.M.S., p. 25 (1954).

[2] A. Couder, J. phys. radium, 8, 99 (1937).

[3] R. Chabbal, Rev. Opt., 37, 49, 336, 501, 608 (1958).

[4] P. Connes, Rev. Opt., 38, 157, 416 (1959) and 39, 402 (1960).

[5] A. Michelson, Phil. Mag, 31, 256 (1891).

[6] A. Michelson, Phil. Mag, 34, 280 (1892).

[7] Lord Rayleigh, Phil. Mag, 34, 407 (1892).

[8] A. Keith Pierce, J. Opt. Soc. Am., 47, 6 (1957).

[9] D. A. Jackson, Proc. Royal Soc, 165, 303 (1958).

[10] D. A. Jackson, private communication.

[11] J. Terrien, J. phys. radium, 19, 390 (1958).

[12] J. Terrien, Teddington Symposium (1959).

[13] P. Felgett, Private communication to M. J. E. Golay, J. Opt. Soc. Am., 39, 437 (1949).

[14] P. Felgett, Thesis, Cambridge University (1951).

[15] P. Felgett, J. phys. radium, 19, 187 (1958).

[16] P. Felgett, J. phys. radium, 19, 237 (1958).

[17] J. Strong, J. Opt. Soc. Am., 47, 354 (1957).

[18] H. A. Gebbie & G. A. Vanasse, Nature, 178, 432 (1956).

[19] H. A. Gebbie, Phys. Rev., 107, 1194 (1957).

[20] H. A. Gebbie, J. phys. radium, 19, 230, (1958).

[21] L. W. Mertz, J. phys. radium, 19, 233 (1958).

[22] N. G. Bakhshiev, Optika i Spektroskopiya, 2, 816 (1957).

[23] J. D. Strong & G. A. Vanasse, J. phys radium, 19, 192 (1958).

[24] J. D. Strong & G. A. Vanasse, J. Opt. Soc. Am., 49, 845 (1959).

[25] A. Michelson, Studies of optics, University Press, Chicago.

[26] Mlle. B. Dossier, Rev. opt, 33, 57, 147, 267, 552 (1954).

[27] J. Arsac, Optica Act (Paris), 3, 55 (1956).

[28] C. Shannon, Bell System Tech. J., 3, 47, 379 (1948).

[29] M. Woodward, Probability & information theory, Pergamon Press, London (1955), p. 21.

[30] A. Kohlenberg, J. Appl. Phy., 24, 1432 (1953).

[31] C. Shannon & S. Weaver, The mathematical theory of communication, University of Illinois Press (1949), p. 53.

[32] L. W. Mertz, private communication.

[33] E. R. Peck, J. Opt. Soc. Am., 45, 961 (1955).

[34] J. O. Harrison & C. W. Stroke, J. Opt. Soc. Am., 45, 116 (1955).

[35] G. W. Stroke, Bul. Research Council Israel, 5, 339 (1957).

[36] P. Jacquinot & C. Dufour, J. recherches centre nat. recherche sci., Lab. Bellevue (Paris), 2, 91 (1948).

[37] P. Jacquinot, J. Opt. Soc. Am., 44, 761 (1954).

[38] Mme. J. Connes, J. phys. radium, 19, 197 (1958).

[39] P. Connes, Rev. opt., 35, 37 (1956).

[40] G. W. Stroke, J. Opt. Soc. Am., 47, 1097 (1957).

[41] E. R. Peck, J. Opt. Soc. Am., 38, 1015 (1948).

[42] H. A. Gebbie, Teddington Symposium (1959).

[43] A. Angot, Complements de mathematiques, edit. Rev. Opt., Paris (1957).

[44] Mlle. A. -M. Camus, M. Francon, E. Ingelstam & A. Maréchal, Rev. opt., 30, 123 (1951).

[45] R. W. Wood, Phys. Rev., 40, 1048 (1932).

[46] L. W. Mertz, Opt. Soc. Am. Meeting (1960).

[47] P. Grivet & A. Blaquière, Le bruit de fond, Masson Paris (1958).

[48] A. Blanc-Lapierre & R. Fortet, Théorie des fonctions aléatories, Masson, Paris (1953).

[49] J. Gauchois, Ann. Radioélec., 11, 308 (1956).

[50] P. Jacquinot, J. phys. radium, 19, 79 (1958).

[51] P. Jacquinot, Stockholm Symposium (1959).

[52] P. M. Duffieux, L'intégrale de Fourier et ses applications à l'optique, copies may be obtained from the author, Univ. Besancon, p. 109.

[53] J. C. Braithwaite & J. Brooks, Opt. Soc. Am. meeting (1960).

[54] L. W. Mertz, Stockholm Symp
[55] M. Vinokur, Thesis, Paris (
[56] Mme. J. Connes & V. Nozal, (to appear).
[57] H. P. Gush & A. Vallance J Terres. Phys., 7, 285 (195
[58] O. Parodi & C. Benoit a la and Control, 6, 356 (1959
[59] J. R. Haynes, M. Lax & W. Solids, 8, 392 (1959).
[60] D. E. Williamson, J. Opt.
[61] Mme. J. Connes & H. P. G. (1959).
[62] Mme. J. Connes & H. P. C
[63] W. S. Benedict, E. K. Pl Phys, 21, 398 (1953).
[64] L. W. Mertz, private co
[65] R. Longhurst, Geometric Green & Co., London (19
[66] Lord Rayleigh, Scientif

ACKNOWLEDGME

The translator wishes to thank Revue D'Optique for permission to t circulate it within the U. S. Depar

It is a pleasure to express ap Robert J. Stirton for considerable to Henry N. Browne, Jr. for reviewi fait fulness to the original.